

The role of q -spin singlet pairs of physical spins in the dynamical properties of the spin-1/2 Heisenberg-Ising XXZ chain

José M. P. Carmelo^{1,2,3} and Pedro D. Sacramento⁴

¹*Center of Physics of University of Minho and University of Porto, P-4169-007 Oporto, Portugal*

²*Department of Physics, University of Minho, Campus Gualtar, P-4710-057 Braga, Portugal*

³*Boston University, Department of Physics, 590 Commonwealth Ave, Boston, MA 02215, USA*

⁴*CeFEMA, Instituto Superior Técnico, Universidade de Lisboa, Av. Rovisco Pais, P-1049-001 Lisboa, Portugal*

(Dated: 31 July 2021)

Dynamical correlation functions contain important physical information on correlated spin models. Here a dynamical theory suitable to the $\Delta = 1$ isotropic spin-1/2 Heisenberg chain in a longitudinal magnetic field is extended to anisotropy $\Delta > 1$. The aim of this paper is the study of the (k, ω) -plane line shape of the spin dynamical structure factor components $S^{+-}(k, \omega)$, $S^{-+}(k, \omega)$, and $S^{zz}(k, \omega)$ of the $\Delta > 1$ spin-1/2 Heisenberg-Ising chain in a longitudinal magnetic field near their (k, ω) -plane sharp peaks. However, the extension of the theory to anisotropy $\Delta > 1$ requires as a first step the clarification of the nature of a specific type of elementary magnetic configurations in terms of physical spins 1/2. To reach that goal, that the spin $SU(2)$ symmetry of the isotropic $\Delta = 1$ point is in the case of anisotropy $\Delta > 1$ replaced by a continuous quantum group deformed q -spin $SU_q(2)$ symmetry plays a key role. For $\Delta > 1$, spin projection S^z remains a good quantum number whereas spin S is not, being replaced by the q -spin S_q in the eigenvalue of the Casimir generator of the continuous $SU_q(2)$ symmetry. Based on the isomorphism between the irreducible representations of the $\Delta = 1$ spin $SU(2)$ symmetry and $\Delta > 1$ continuous $SU_q(2)$ symmetry and on their relation to the occupancy configurations of the Bethe-ansatz quantum numbers one finds that the elementary magnetic configurations under study are q -spin neutral. This determines the form of S matrices on which the extended dynamical theory relies. They are found in this paper to describe the scattering of n -particles whose relation to configurations of physical spins 1/2 is established. Specifically, their internal degrees of freedom refer to unbound q -spin singlet pairs of physical spins 1/2 described by $n = 1$ real single Bethe rapidities and to $n = 2, 3, \dots$ bound such q -spin singlet pairs described by Bethe n -strings for $n > 1$. There is a relationship between the negativity and the length of the momentum k interval of the k dependent exponents that control the power-law line shape of the spin dynamical structure factor components near the lower threshold of a given (k, ω) -plane continuum and the amount of spectral weight over the latter. Using such a relationship, one finds that in the thermodynamic limit the significant spectral weight contributions from Bethe n -strings at a finite longitudinal magnetic field refer to specific two-parametric (k, ω) -plane gapped continua in the spectra of the spin dynamical structure factor components $S^{+-}(k, \omega)$ and $S^{zz}(k, \omega)$. In contrast to the $\Delta = 1$ isotropic chain, excited energy eigenstates including up to $n = 3$ Bethe n -strings lead to finite spectral-weight contributions to $S^{+-}(k, \omega)$. Most spectral weight stems though from excited energy eigenstates whose q -spin singlet $S^z = S_q = 0$ pairs of physical spins 1/2 are all unbound. It is associated with (k, ω) -plane continua in the spectra of the spin dynamical structure factor components that are gapless at some specific momentum values. We derive analytical expressions for the line shapes of $S^{+-}(k, \omega)$, $S^{-+}(k, \omega)$, and $S^{zz}(k, \omega)$ valid in the vicinity of (k, ω) -plane lines of sharp peaks. Those are mostly located at and just above lower thresholds of (k, ω) -plane continua associated with both states with only unbound q -spin singlet pairs and states populated by such pairs and a single $n = 2$ or $n = 3$ n -particle. Our results provide physically interesting and important information on the microscopic processes that determine the dynamical properties of the non-perturbative spin-1/2 Heisenberg-Ising chain in a longitudinal magnetic field.

PACS numbers:

I. INTRODUCTION

The spin-1/2 Heisenberg chain XXZ is a physically interesting quantum problem whose integrability was shown by R. Orbach [1]. The ground-state and the simplest excited states were studied by J. des Cloizeaux and M. Gaudin [2]. In a series of three papers, C.N. Yang and C.P. Yang exhaustively discussed the ground-state properties of the model [3].

Dynamical correlation functions contain important physical information on correlated spin models. In the case of the spin-1/2 Heisenberg chain XXZ , most previous studies on dynamical properties referred to anisotropy $\Delta < 1$ [4–9]. Therefore, here we consider the spin-1/2 Heisenberg chain [10–14] with anisotropy $\Delta > 1$ [11, 14], the so called spin-1/2 Heisenberg-Ising chain. That model has a gapped spin-insulating quantum phase at magnetic field $h = 0$

and spin density $m = 0$. Previous studies on its dynamical correlation functions refer mostly to that quantum phase [15].

More recently, there has been a study on the dynamical properties of the model for $\Delta > 1$ at finite magnetic fields by a finite-size method that relied on the algebraic Bethe ansatz formalism [16]. The dynamical theory used in the studies of this paper rather refers to the thermodynamic limit and provides analytical expressions for the dynamical correlation functions valid in that limit. In spite of some technical similarities of the $\Delta < 1$ and $\Delta > 1$ Bethe-ansatz solutions, that dynamical theory has a different specific form for each of them.

The dynamical structure factor components $S^{xx}(k, \omega)$, $S^{yy}(k, \omega)$ e $S^{zz}(k, \omega)$ are given by,

$$\begin{aligned} S^{aa}(k, \omega) &= \sum_{j=1}^N e^{-ikj} \int_{-\infty}^{\infty} dt e^{-i\omega t} \langle GS | \hat{S}_j^a(t) \hat{S}_j^a(0) | GS \rangle \\ &= \sum_{\nu} |\langle \nu | \hat{S}_k^a | GS \rangle|^2 \delta(\omega - \omega_{\nu}^{aa}(k)) \quad \text{for } a = x, y, z. \end{aligned} \quad (1)$$

Here and in this paper we use the notation k for the excitation momentum of energy eigenstates relative to a reference ground state. In Eq. (1), the spectra read $\omega_{\nu}^{aa}(k) = (E_{\nu}^{aa} - E_{GS})$, E_{ν}^{aa} refers to the energies of the excited energy eigenstates that contribute to the dynamical structure factors components $aa = xx, yy, zz$, \sum_{ν} is the sum over such states, E_{GS} is the initial ground state energy, and \hat{S}_k^a are for $a = x, y, z$ the Fourier transforms of the usual local $a = x, y, z$ spin operators \hat{S}_j^a , respectively.

The components $S^{+-}(k, \omega)$ and $S^{-+}(k, \omega)$ of the spin dynamical structure factor are directly related to the two transverse components $S^{xx}(k, \omega)$ and $S^{yy}(k, \omega)$, Eq. (1) for $aa = xx, yy$, which are identical, $S^{xx}(k, \omega) = S^{yy}(k, \omega)$, as follows,

$$S^{xx}(k, \omega) = S^{yy}(k, \omega) = \frac{1}{4} (S^{+-}(k, \omega) + S^{-+}(k, \omega)). \quad (2)$$

One can then address the properties of $S^{xx}(k, \omega) = S^{yy}(k, \omega)$ in terms of those of $S^{+-}(k, \omega)$ and $S^{-+}(k, \omega)$. The main goal of this paper is the study of the power-law line shape of the spin dynamical structure factor components $S^{+-}(k, \omega)$, $S^{-+}(k, \omega)$, and $S^{zz}(k, \omega)$ of the $\Delta > 1$ spin-1/2 Heisenberg-Ising chain in a longitudinal magnetic field near their (k, ω) -plane lines of sharp peaks.

The dynamical theory used in Refs. 17, 18 for the isotropic point, $\Delta = 1$, refers to the thermodynamic limit. It provides analytical expressions for the momentum dependent exponents that control the power-law line shape of such spin dynamical structure factor components near their sharp peaks. In the isotropic case, a necessary condition for the validity of that theory is that the S matrices associated with the scattering of n -particles are dimension-one scalars of a particular form given below in Sec. V. At $\Delta = 1$ a n -particle internal degrees of freedom refer to a single unbound singlet pair of physical spins 1/2 for $n = 1$ and to a number n of bound such pairs for $n > 1$ [19, 20]. The phase shifts in the the S matrices expressions can be extracted from the exact Bethe-ansatz solution. The momentum dependent exponents that control the power-law line shape of the spin dynamical structure factor components under consideration near their sharp peaks are simple combinations of such phase shifts [17, 18].

The form of the dimension-one scalar S matrices under consideration follows in the isotropic case from the *spin-neutral* nature of both the unbound singlet pairs of physical spins 1/2 described by $n = 1$ real single Bethe rapidities and $n > 1$ bound such pairs described by n -stings associated with complex Bethe-ansatz rapidities [19, 20]. The extension of the dynamical theory of Refs. 17, 18 to $\Delta > 1$ requires that the corresponding S matrices have a similar form, which for $\Delta > 1$ remains an unsolved problem.

The Hamiltonian of the spin-1/2 Heisenberg-Ising chain describes $N = \sum_{\sigma=\uparrow, \downarrow} N_{\sigma}$ physical spins 1/2 of projection $\sigma = \uparrow, \downarrow$. For anisotropy parameter range $\Delta = \cosh \eta \geq 1$ and thus $\eta \geq 0$, spin densities $m = (N_{\uparrow} - N_{\downarrow})/N \in [0, 1]$, exchange integral J , and length $L \rightarrow \infty$ for finite N/L , that Hamiltonian in a longitudinal magnetic field h reads,

$$\hat{H} = \hat{H}_{\Delta} + g\mu_B h \sum_{j=1}^N \hat{S}_j^z \quad \text{where} \quad \hat{H}_{\Delta} = J \sum_{j=1}^N \left(\hat{S}_j^x \hat{S}_{j+1}^x + \hat{S}_j^y \hat{S}_{j+1}^y + \Delta \hat{S}_j^z \hat{S}_{j+1}^z \right). \quad (3)$$

In such expressions, \hat{S}_j is the spin-1/2 operator at site $j = 1, \dots, N$ with components $\hat{S}_j^{x,y,z}$, g is the Landé factor, and μ_B is the Bohr magneton. The present study uses natural units of lattice spacing and Planck constant one.

It is well known that the Hamiltonian \hat{H}_{Δ} in Eq. (3) has spin $SU(2)$ symmetry at $\Delta = \cosh \eta = 1$ and thus $\eta = 0$. For $\Delta > 1$ and $\eta > 0$ it has a related continuous quantum group deformed symmetry $SU_q(2)$ associated with the q -spin S_q in the eigenvalue of the Casimir generator [21, 22]. In either case, the 2^N irreducible representations of the corresponding symmetry refer to the 2^N energy eigenstates of the Hamiltonian $\hat{H} = \hat{H}_{\Delta} + g\mu_B h \sum_{j=1}^N \hat{S}_j^z$, Eq. (3).

For $\eta > 0$, spin projection S^z remains a good quantum number whereas spin is not, spin S being replaced by the q -spin S_q . Inside the $\eta > 0$ many-particle system, each of the N physical spins $1/2$ have q -spin $S_q = 1/2$ and spin projection $S^z = \pm 1/2$. Hence the present designation *physical spin* $1/2$ refers to $S = 1/2$ and $S_q = 1/2$ for $\eta = 0$ and $\eta > 0$, respectively.

A first step of the extension of the dynamical theory used in Refs. 17, 18 for the isotropic case to anisotropy $\Delta > 1$ refers to showing that for the corresponding spin- $1/2$ XXZ chain, the $n = 1$ real single Bethe rapidities and the $n > 1$ Bethe n -strings describe unbound q -spin singlet $S^z = S_q = 0$ pairs of physical spins $1/2$ and bound states of a number $n > 1$ of such q -spin singlet pairs, respectively. This ensures that the S matrices associated with the scattering of the corresponding n -particles introduced in this paper are for $\eta > 0$ dimension-one scalars whose form is similar to that for the $\eta = 0$ isotropic case. The phase shifts associated with the S matrices are indeed found to differ from those of the isotropic case only in their dependence on η .

A key step of our study to reach the results for $\eta > 0$ is made possible by explicitly accounting for the isomorphism of the $\eta = 0$ spin $SU(2)$ and $\eta > 0$ q -spin $SU_q(2)$ symmetries's irreducible representations. Due to such an isomorphism, q -spin S_q has exactly the same values as spin S . Specifically, accounting for the one-to-one correspondence between the configurations of the N physical spins $1/2$ described by the Hamiltonian, Eq. (3), that generate such representations and the occupancy configurations of the quantum numbers of the exact Bethe-ansatz solution that generate the corresponding energy eigenstates.

The confirmation that the dimension-one scalar S matrices under consideration have for $\Delta > 1$ the same form as for the isotropic $\Delta = 1$ case, renders the extension to anisotropy $\Delta > 1$ of the dynamical theory suitable to $\Delta = 1$ a straightforward procedure. The use of that dynamical theory provides useful information on the (k, ω) -plane spectral-weight distributions of $S^{+-}(k, \omega)$, $S^{xx}(k, \omega)$, and $S^{zz}(k, \omega)$. Most of such spectral weight stems from specific classes of excited energy eigenstates whose spectra are associated with that distribution.

Analytical expressions for these dynamical correlation function components valid at and just above their (k, ω) -plane lines of sharp peaks are derived. Our results provide interesting and important information on the non-perturbative microscopic processes that control the physics of the spin- $1/2$ Heisenberg-Ising chain in a longitudinal magnetic field.

II. A SUITABLE REPRESENTATION FOR THE SPIN-1/2 HEISENBERG-ISING CHAIN IN TERMS OF PHYSICAL SPINS $1/2$ CONFIGURATIONS

A. General representation for the whole Hilbert space

The structure of the Bethe n -strings depends on the system size. The thermodynamic limit in which that structure simplifies [10, 11, 14] is that more relevant for the description of physical spin systems. The $n = 1$ real single Bethe rapidities and the Bethe n -strings are defined for $\eta \geq 0$ in terms of general Bethe-ansatz rapidities whose form in that limit is given by,

$$\Lambda_j^{n,l} = \Lambda_j^n + i(n+1-2l) \quad \text{where} \quad l = 1, \dots, n. \quad (4)$$

Here $j = 1, \dots, L_n$, $n = 1, \dots, \infty$, and we have used the notation of Ref. 10, whose relation to the $\eta > 0$ rapidities $\varphi_{n,j}$ of Ref. 11 is $\Lambda_j^n = -\varphi_{n,j}/\eta$. The real numbers Λ_j^n on the right-hand side of Eq. (4) are defined by a number $n = 1, \dots, \infty$ of coupled Bethe-ansatz equations [10, 11, 14]. Those are given in Eq. (A3) of Appendix A in a useful functional form.

For $n = 1$, the rapidity $\Lambda_j^{n,l}$ is real and otherwise its imaginary part is finite, except at $l = (n+1)/2$ when l is odd. A n -string is a group of $n > 1$ rapidities with the same real part Λ_j^n . Below in Sec. III it is confirmed that a $n = 1$ real single Bethe rapidity and a $n > 1$ Bethe n -string describe one unbound q -spin singlet $S^z = S_q = 0$ pair of physical spins $1/2$ and $n > 1$ bound such pairs, respectively.

One associates a *Bethe-ansatz n -band* with each $n = 1, \dots, \infty$ value. It contains $L_n = N_n + N_n^h$ discrete momentum values $q_j \in [q_n^-, q_n^+]$ with spacing $q_{j+1} - q_j = 2\pi/L$ where $j = 1, \dots, L_n$. In this paper we use the notation q for the momentum values of such n -bands whereas, as reported above in Sec. I, k refers to the excitation momentum of an energy eigenstate relative to a reference ground state.

In Appendix A it is found that the n -band limiting momentum values read $q_n^\pm = \pm \frac{\pi}{L}(L_n - 1 \mp \delta L_n^\eta)$. Here L_n and δL_n^η are independent and dependent on η , respectively. In that Appendix the former numbers are found to read,

$$L_n = N_n + N_n^h \quad \text{where} \quad N_n^h = 2S_q + \sum_{n'=n+1}^{\infty} 2(n' - n)N_{n'} \quad \text{for} \quad n = 1, \dots, \infty, \quad (5)$$

whereas δL_n^η is given below.

The Bethe-ansatz quantum numbers I_j^n are the n -band momentum values $q_j = \frac{2\pi}{L} I_j^n$ in units of $\frac{2\pi}{L}$. They are given by $I_j^n = 0, \pm 1, \dots, \pm \frac{L_n-1}{2}$ for L_n odd and $I_j^n = \pm 1/2, \pm 3/2, \dots, \pm \frac{L_n-1}{2}$ for L_n even. Such numbers and thus the set of n -band discrete momentum values $\{q_j\}$ have a Pauli-like occupancy of zero and one, respectively.

The corresponding numbers N_n and N_n^h are those of occupied and unoccupied n -band discrete momentum values q_j , respectively, of an energy eigenstate. Such a state n -band momentum distribution thus reads $N_n(q_j) = 1$ and $N_n(q_j) = 0$ for the N_n and N_n^h momentum values q_j that are occupied and unoccupied, respectively. Hence $\sum_{j=1}^{L_n} N_n(q_j) = N_n$ and $\sum_{j=1}^{L_n} N_n^h(q_j) = N_n^h$ where $N_n^h(q_j) = 1 - N_n(q_j)$. The solution of Bethe-ansatz equations for the Hamiltonian, Eq. (3), given in functional form in Eq. (A3) of Appendix A, provides the real part, $\Lambda_j^n = \Lambda^n(q_j)$, of the $n = 1, 2, \dots$ rapidities, Eq. (4). We call them $n = 1, 2, \dots$ rapidity functions $\Lambda^n(q_j)$ of an energy eigenstate.

Each such a state is uniquely defined by the set of n -band momentum distributions $\{N_n(q_j)\}$ for $n = 1, 2, \dots$ and $j = 1, \dots, L_n$. The Bethe-ansatz solution refers to subspaces spanned by energy eigenstates for which $S^z = -S_q$. As confirmed below in Sec. IIIB, the remaining $S_q > 0$ energy eigenstates for which $S^z = -S_q + n_z$ where $n_z = 1, \dots, 2S_q$ are also accounted for by the present general representation.

Consistently with the q_j 's being momentum values, the momentum eigenvalues are in functional form given by,

$$P = \pi \sum_{n=1}^{\infty} N_n + \sum_{n=1}^{\infty} \sum_{j=1}^{L_n} N_n(q_j) q_j. \quad (6)$$

Importantly, both the numbers L_n , Eq. (5), and the momentum eigenvalues are independent of the anisotropy parameter $\Delta = \cosh \eta$. In contrast, the energy eigenvalues and the numbers δL_n^η in $q_n^\pm = \pm \frac{\pi}{L} (L_n - 1 \mp \delta L_n^\eta)$ depend on η and on the n -band momentum values q_j through the rapidity functions $\Lambda^n(q_j)$. Within the present functional representation the former read,

$$E = - \sum_{n=1}^{\infty} \sum_{j=1}^{L_n} N_n(q_j) \frac{J}{n} \left(\frac{\sinh^2(n\eta)}{\cosh(n\eta) - \cos(\Lambda^n(q_j)\eta)} - C_n(\eta) \right) + g\mu_B h S^z. \quad (7)$$

Here the constant $C_n(\eta)$ is given by,

$$C_n(\eta) = \left(1 - \frac{n \sinh(\eta)}{\sinh(n\eta)} \right) (1 + \cosh(n\eta)). \quad (8)$$

It suitably defines the zero-energy level of the related n -band energy dispersions given in Appendix B. The magnetic field $h = h(m)$ in Eq. (7) is at $m = 0$ and for $m \in [0, 1]$ given by [13],

$$\begin{aligned} h(0) &\in [0, h_{c1}] \quad \text{and} \\ h(m) &= \frac{1}{g\mu_B} \frac{J \sinh(\eta) 2\pi\sigma_1(B)}{\xi_{11}} \in [h_{c1}, h_{c2}], \end{aligned} \quad (9)$$

respectively. Here $2\pi\sigma_1(B)$ is the distribution $2\pi\sigma_1(\varphi)$, Eq. (B6) of Appendix B, the parameter B is given in Eq. (B3) of that Appendix, and the parameter ξ_{11} is defined in Eq. (C17) of Appendix C. The critical magnetic fields read [13],

$$h_{c1} = \frac{2J}{\pi g\mu_B} \sinh(\eta) K(u_\eta) \sqrt{1 - u_\eta^2} \quad \text{and} \quad h_{c2} = \frac{J(\Delta + 1)}{g\mu_B} = \frac{J(\cosh \eta + 1)}{g\mu_B}. \quad (10)$$

The critical field h_{c1} refers to the transition from the $m = 0$ spin-insulating quantum phase to the $0 < m < 1$ spin-conducting quantum phase and h_{c2} refers to that from the latter phase to the fully-polarized ferromagnetic quantum phase. The complete elliptic integral $K(u_\eta)$ appearing in the h_{c1} expression is defined as,

$$K(u_\eta) = \int_0^{\frac{\pi}{2}} d\theta \frac{1}{\sqrt{1 - u_\eta^2 \sin^2 \theta}} \quad \text{and} \quad \eta = \pi \frac{K(u'_\eta)}{K(u_\eta)} = \pi \left(\frac{\int_0^{\frac{\pi}{2}} d\theta \frac{1}{\sqrt{1 - (1 - u_\eta^2) \sin^2 \theta}}}{\int_0^{\frac{\pi}{2}} d\theta \frac{1}{\sqrt{1 - u_\eta^2 \sin^2 \theta}}} \right). \quad (11)$$

The η -dependent function $u_\eta = u_\eta(\eta)$ has been defined in this equation by the corresponding inverse function.

The critical field h_{c1} has limiting behaviors $h_{c1} \rightarrow 0$ for $\eta \rightarrow 0$ and $h_{c1} \approx J(\Delta - 2)/(g\mu_B)$ for $\eta \gg 1$. That $h_{c1} \rightarrow 0$ as $\eta \rightarrow 0$ is imposed by the emergence of the isotropic point's spin $SU(2)$ symmetry. It follows that the field interval

$h \in [-h_{c1}, h_{c1}]$ of the $\Delta > 1$ spin-insulating quantum phase shrinks to $h = 0$ at $\Delta = 1$. In this paper we consider magnetic fields $h \geq 0$ for which $N_\uparrow \geq N_\downarrow$, so that such a $\eta > 0$ quantum phase occurs for $h \in [0, h_{c1}]$.

In Appendix A the functional representation of the numbers δL_n^η in $q_n^\pm = \pm \frac{\pi}{L}(L_n - 1 \mp \delta L_n^\eta)$ is found to read,

$$\delta L_n^\eta = \sum_{n'=1}^{\infty} F_{n,n'}(\eta) \sum_{j=1}^{L_{n'}} N_{n'}(q_j) \left(\frac{\eta \Lambda^{n'}(q_j)}{\pi} \right) = - \sum_{n'=1}^{\infty} F_{n,n'}(\eta) \sum_{j=1}^{L_{n'}} N_{n'}(q_j) \left(\frac{\varphi_{n'}(q_j)}{\pi} \right). \quad (12)$$

Here $F_{n,n'}(\eta)$ has a long expression not needed for our studies whose limiting behaviors are,

$$\begin{aligned} F_{n,n'}(\eta) &= n n' \eta \quad \text{for } \eta \ll 1 \\ &= n + n' - |n - n'| - \delta_{n',n} \quad \text{for } \eta \gg 1. \end{aligned} \quad (13)$$

Since $\Lambda^{n'}(q_j) = \Lambda_j^{n'} \in [-\pi/\eta, \pi/\eta]$ and $\varphi_{n'}(q_j) = \varphi_{n',j} \in [-\pi, \pi]$, one has in Eq. (12) that $\eta \Lambda^{n'}(q_j)/\pi = \varphi_{n'}(q_j)/\pi \in [-1, 1]$. For $\eta > 0$ ground states and excited energy eigenstates contributing to the dynamical properties studied in this paper, the numbers δL_n^η either vanish or are of order $1/L$ and also vanish in the thermodynamic limit.

Within our representation in terms of the N physical spins $1/2$ described by the Hamiltonian, Eq. (3), the designation *n-particles* refers both to *1-particles* and *n-string-particles* for $n > 1$:

- The internal degrees of freedom of a 1-particle correspond to a single $n = 1$ unbound pair of physical spins $1/2$ whose neutral q -spin nature is confirmed in Sec. III. Its translational degrees of freedom refer to the 1-band momentum $q_j \in [q_1^-, q_1^+]$ carried by each of the N_1 1-particles of an energy eigenstate;
- The internal degrees of freedom of a n -string-particle refer to the $n > 1$ physical spins $1/2$ pairs bound within a configuration described by the corresponding n -string whose neutral q -spin nature is confirmed in Sec. III to be the same as that of unbound pairs. Its translational degrees of freedom correspond to the $n > 1$ n -band momentum $q_j \in [q_n^-, q_n^+]$ carried by each of the N_n n -string-particles of an energy eigenstate for which $N_n > 0$.

B. Representation for the subspaces of interest for the dynamical properties

For ground states and their excited energy eigenstates associated with a significant amount of spin dynamical structure factor spectral weight, one has in the thermodynamic limit and except for corrections of $1/L$ order that the limiting n -band numbers $q_n^\pm = \pm \frac{\pi}{L}(L_n - 1 \mp \delta L_n^\eta)$ simplify to $q_1^\pm = \pm k_{F\uparrow}$ for $n = 1$ and to $q_n^\pm = \pm(k_{F\uparrow} - k_{F\downarrow})$ for $n > 1$. Here $k_{F\uparrow} = \frac{\pi}{2}(1 + m)$ and $k_{F\downarrow} = \frac{\pi}{2}(1 - m)$. Ground states refer in that limit and again neglecting corrections of $1/L$ order to a 1-band Fermi sea $q_j \in [-k_{F\downarrow}, k_{F\downarrow}]$ and empty n -bands for $n > 1$. In the thermodynamic limit, the n -band discrete momentum values q_j such that $q_{j+1} - q_j = 2\pi/L$ are often replaced by a continuous variable q .

The following ground-state analysis is consistent with both the unbound pair in each 1-particle corresponding to a q -spin singlet $S^z = S_q = 0$ configuration and the occurrence of *unpaired physical spins* $1/2$ in some energy eigenstates, as confirmed below in Sec. III. (Ground states are not populated by $n > 1$ n -string-particles.)

In the spin-insulating quantum phase that for $\eta > 0$ occurs for spin density $m = 0$ and magnetic fields $h \in [0, h_{c1}]$, the 1-band is full in the ground state, $q \in [-\pi/2, \pi/2]$. For N even all N physical spins $1/2$ are paired within a number $N/2$ of 1-particles each containing a single pair. This is a gapped quantum phase for $0 \leq h < h_{c1}$.

The magnetic field range $h \in [h_{c1}, h_{c2}]$ refers to a spin-conducting quantum phase in which the 1-band is occupied in the ground state for $q \in [-k_{F\downarrow}, k_{F\downarrow}]$ and unoccupied for $|q| \in [k_{F\downarrow}, k_{F\uparrow}]$. The ground state contains a number $N_1 = N_\downarrow$ of 1-particles each referring to a pair of physical spins $1/2$ of opposite projection. The remaining $N - 2N_\downarrow = N_\uparrow - N_\downarrow$ physical spins $1/2$ are unpaired.

Finally, in the fully-polarized ferromagnetic quantum phase occurring for $h > h_{c2}$, there are no n -particles in the ground state both for $n = 1$ and $n > 1$. Indeed, in that state all N physical spins $1/2$ are unpaired and have the same spin projection.

The n -particle energy dispersions $\varepsilon_n(q)$ defined by Eqs. (B13)-(B18) of Appendix B play an important role in our study. The 1-particle energy dispersion refers to the energy $\varepsilon_1(q)$ associated with creation onto a ground state of one 1-particle at a 1-band momentum in the interval $|q| \in [k_{F\downarrow}, k_{F\uparrow}]$. That dispersion also corresponds to the energy $-\varepsilon_1(q)$ associated with creation onto such a state of one 1-hole at a 1-band momentum in the interval $q \in [-k_{F\downarrow}, k_{F\downarrow}]$. The $n > 1$ n -string-particle energy dispersion refers to the energy $\varepsilon_n(q)$ associated with creation onto a ground state of one n -particle at a n -band momentum in the interval $q \in [-(k_{F\uparrow} - k_{F\downarrow}), (k_{F\uparrow} - k_{F\downarrow})]$.

The 1-particle, 2-string-particle, and 3-string-particle energy dispersions are plotted in units of J in Figs. 1, 2, and 3, respectively, as a function of the corresponding band momentum q for spin densities $m = 0.2$, $m = 0.5$, and $m = 0.8$ and several anisotropy Δ values. Their simple limiting analytical expressions for $h \in [0, h_{c1}]$ and $m = 0$ and

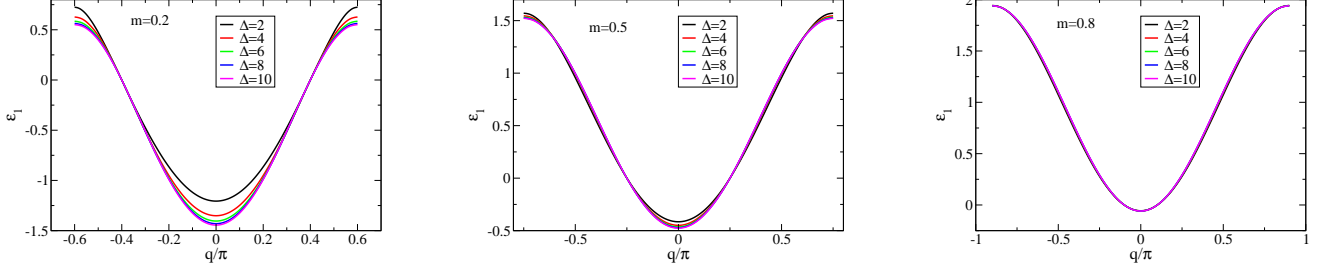


Figure 1: The 1-particle energy dispersion $\varepsilon_1(q)$ in units of J defined by Eqs. (B13) and (B14) of Appendix B plotted as a function of the 1-band momentum $q \in [-k_{F\uparrow}, k_{F\uparrow}]$ for spin densities $m = 0.2$, $m = 0.5$, and $m = 0.8$ and several anisotropy Δ values.

for $h = h_{c2}$ and $m = 1$ are in Appendix B found to read,

$$\begin{aligned}
 \varepsilon_1(q) &= -\frac{J}{\pi} \sinh(\eta) K(u_\eta) \sqrt{1 - u_\eta^2 \sin^2 q} + \frac{1}{2} g \mu_B h \quad \text{for } q \in [-\pi/2, \pi/2] \quad \text{and } h \in [0, h_{c1}] \\
 &= -\frac{J}{\pi} \sinh(\eta) K(u_\eta) \left(\sqrt{1 - u_\eta^2 \sin^2 q} - \sqrt{1 - u_\eta^2} \right) \quad \text{for } q \in [-\pi/2, \pi/2] \quad \text{and } h = h_{c1} \\
 \varepsilon_1(q) &= J(1 - \cos q) \quad \text{for } q \in [-\pi, \pi] \quad \text{and } h = h_{c2},
 \end{aligned} \tag{14}$$

and

$$\begin{aligned}
 \varepsilon_n(0) &= (n-1) g \mu_B h \quad \text{for } q = 0 \quad \text{and } h \in [0, h_{c1}] \\
 &= \frac{2(n-1)J}{\pi} \sinh(\eta) K(u_\eta) \sqrt{1 - u_\eta^2} \quad \text{for } q = 0 \quad \text{and } h = h_{c1} \\
 \varepsilon_n(q) &= \frac{J}{n} (1 - \cos q) + n J (1 + \cosh(\eta)) \\
 &\quad - J \frac{\sinh(\eta)}{\sinh(n\eta)} (1 + \cosh(n\eta)) \quad \text{for } q \in [-\pi, \pi] \quad \text{and } h = h_{c2}.
 \end{aligned} \tag{15}$$

The excitation energies $\delta E = E_\nu - E_{GS}$ where E_ν and E_{GS} are the energy eigenvalues of the excited state and ground state, respectively, considered below in Sec. IV are expressed in terms of simple combinations of such 1-particle and n -string-particle energy dispersions.

In the literature, fractionalized particles such as one-dimensional spin waves [23] usually called spinons [24] at $m = 0$ and psinons and antipspinons for $m > 0$ [25, 26] are often used. However, their transformation laws under both the spin operators in the Hamiltonian expression, Eq. (3), and the generators of the $\eta = 0$ $SU(2)$ symmetry and $\eta > 0$ continuous $SU_q(2)$ symmetry given below in Sec. III A remain unknown. In contrast, the present n -particle representation refers to 1-particles and n -string-particles whose relation to configurations of physical spins 1/2 is confirmed below in Sec. III to be more direct. Importantly, the dynamical properties of the spin-1/2 Heisenberg-Ising chain with anisotropy $\Delta > 1$ in a longitudinal magnetic field studied below in Sec. V are naturally and directly described by the scattering of such n -particles.

Spinons, psinons, and antipspinons are well defined in subspaces with no n -strings or with a vanishing density of n -strings in the thermodynamic limit. Spinons are 1-band holes within excited energy eigenstates of the $m = 0$ ground state. Psinons and antipspinons are 1-holes that emerge or are moved to inside the 1-band Fermi sea and 1-particles that emerge or are moved to outside that sea, respectively, in excited energy eigenstates of ground states corresponding to the $\eta > 0$ spin-conducting quantum phase that occurs for $h_{c1} < h < h_{c2}$.

III. THE NATURE OF THE BOUND AND UNBOUND ELEMENTARY MAGNETIC CONFIGURATIONS IN TERMS OF PHYSICAL SPINS 1/2

The results of this section refer to the quantum problem defined by the Hamiltonian \hat{H} , Eq. (3), acting on its whole Hilbert space.

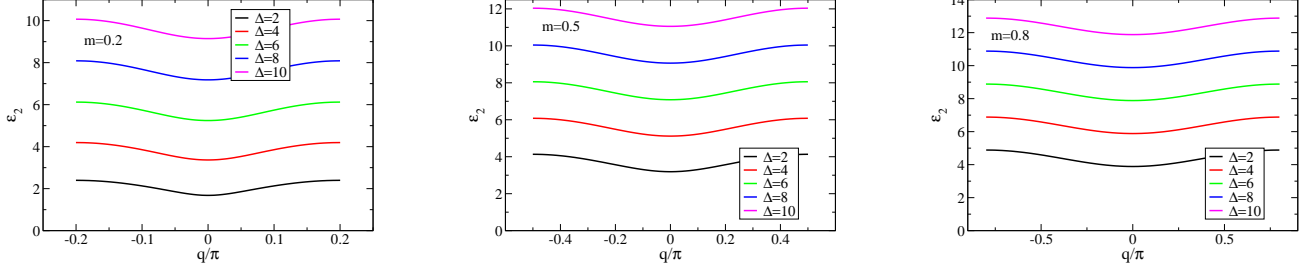


Figure 2: The 2-string-particle energy dispersion $\varepsilon_2(q)$ in units of J defined by Eqs. (B15) and (B16) of Appendix B for $n = 2$ plotted as a function of the 2-band momentum $q \in [-(k_{F\uparrow} - k_{F\downarrow}), (k_{F\uparrow} - k_{F\downarrow})]$ for spin densities $m = 0.2$, $m = 0.5$, and $m = 0.8$ and several anisotropy Δ values.

A. The isomorphism of the $SU(2)$ and $SU_q(2)$ symmetries irreducible representations

Since the Hilbert space of the present quantum problem is the same for $\eta = 0$ and $\eta > 0$, there is a uniquely defined unitary transformation that relates the two sets of 2^N $\eta = 0$ and $\eta > 0$ energy eigenstates, $\{|l_r, S, S^z, 0\rangle\}$ and $\{|l_r, S_q, S^z, \eta\rangle\}$, respectively. Indeed, both of them refer to sets of complete and orthonormal energy eigenstates for the same Hilbert space of dimension 2^N . In such a state notation, l_r stands for all quantum numbers other than spin S for $\eta = 0$, q -spin S_q for $\eta > 0$, S^z for $\eta \geq 0$, and η itself needed to specify $|l_r, S_q, S^z, \eta\rangle$ for *any* fixed $\eta \geq 0$ value. In Appendix A it is shown that the quantum numbers described by l_r are independent of η .

That unitary transformation defines a one-to-one relation between the 2^N $\eta = 0$ and 2^N $\eta > 0$ energy eigenstates, respectively, of the Hamiltonian, Eq. (3). It is associated with unitary operators \hat{U}_η^\pm such that,

$$|l_r, S_q, S^z, \eta\rangle = \hat{U}_\eta^+ |l_r, S, S^z, 0\rangle \quad \text{and} \quad |l_r, S, S^z, 0\rangle = \hat{U}_\eta^- |l_r, S_q, S^z, \eta\rangle. \quad (16)$$

Fortunately, the specific involved form of the unitary operators \hat{U}_η^\pm is not needed for our studies. Only that they are uniquely defined and the transformations they generate, Eq. (16), are needed.

As discussed below in Sec. IIIB, in Appendix A it is confirmed that the values of l_r , S_q , and S^z in $|l_r, S_q, S^z, \eta\rangle$ actually remain invariant under \hat{U}_η^\pm , yet only at $\eta = 0$ the number S_q is the spin S . That invariance implies that for any two $\eta > 0$ and $\eta = 0$ energy eigenstates, respectively, related as in Eq. (16), the q -spin S_q has for $\eta > 0$ exactly the same values as the spin S at $\eta = 0$. (N is even and odd when the states S_q is an integer and half-odd integer number, respectively.)

That the irreducible representations of the $\eta > 0$ continuous $SU_q(2)$ symmetry [21, 22] are isomorphic to those of the $\eta = 0$ $SU(2)$ symmetry, requires that,

$$\begin{aligned} \hat{S}_\eta^\pm |l_r, S_q, S^z, \eta\rangle &\propto \hat{U}_\eta^+ \hat{S}^\pm \hat{U}_\eta^- |l_r, S_q, S^z, \eta\rangle \\ (\hat{S}_\eta)^2 |l_r, S_q, S^z, \eta\rangle &\propto \hat{U}_\eta^+ (\hat{S})^2 \hat{U}_\eta^- |l_r, S_q, S^z, \eta\rangle. \end{aligned} \quad (17)$$

To confirm that this requirement is fulfilled, the generators of the continuous $SU_q(2)$ symmetry are in the following expressed in terms of those of the spin symmetry $SU(2)$ symmetry. Besides transformations generated by the unitary operators \hat{U}_η^\pm in Eqs. (16) and (17), this includes state summations,

$$\sum_{l_r, S_q, S^z} = \sum_{l_r} \sum_{S_q=0 \text{ or } 1/2}^{N/2} \sum_{S^z=-S_q}^{S_q}. \quad (18)$$

Here (i) $\sum_{S_q=0}^{N/2}$ and (ii) $\sum_{S_q=1/2}^{N/2}$ refers to (i) N even and S_q integer and (ii) N odd and S_q half integer, respectively. The summation \sum_{l_r} gives the number of fixed- S_q energy eigenstates that is found below to equal the number $\mathcal{N}_{\text{singlet}}(S_q)$ of corresponding q -spin singlet configurations at fixed S_q .

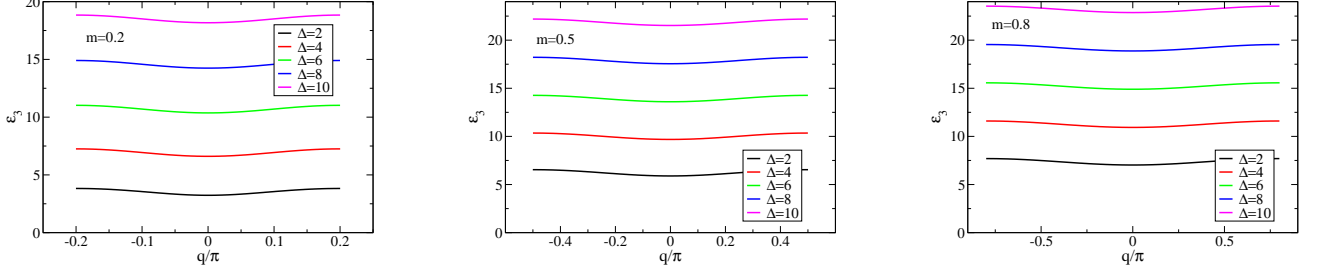


Figure 3: The same as in Fig. 2 for the 3-string-particle energy dispersion $\varepsilon_3(q)$.

The following expressions refer to the required exact relations,

$$\begin{aligned} \hat{S}_\eta^\pm &= \sum_{l_r, S_q} \sum_{S^z = -S_q + \frac{(1 \pm 1)}{2}}^{S_q - \frac{(1 \pm 1)}{2}} \sqrt{\frac{\sinh^2(\eta(S_q + 1/2)) - \sinh^2(\eta(S^z \pm 1/2))}{((S_q + 1/2)^2 - (S^z \pm 1/2)^2) \sinh^2 \eta}} \\ &\times \langle l_r, S_q, S^z \pm 1, \eta | \hat{U}_\eta^+ \hat{S}^\pm \hat{U}_\eta^- | l_r, S_q, S^z, \eta \rangle | l_r, S_q, S^z \pm 1, \eta \rangle \langle l_r, S_q, S^z, \eta |, \end{aligned} \quad (19)$$

and

$$\begin{aligned} (\hat{\tilde{S}}_\eta)^2 &= \sum_{l_r, S_q, S^z} \frac{\sinh^2(\eta(S_q + 1/2)) - \sinh^2(\eta/2)}{((S_q + 1/2)^2 - 1/4) \sinh^2 \eta} \\ &\times \langle l_r, S_q, S^z, \eta | \hat{U}_\eta^+ (\hat{\tilde{S}})^2 \hat{U}_\eta^- | l_r, S_q, S^z, \eta \rangle | l_r, S_q, S^z, \eta \rangle \langle l_r, S_q, S^z, \eta |, \end{aligned} \quad (20)$$

respectively. Combining this latter summation over the operators $|l_r, S_q, S^z\rangle \langle l_r, S_q, S^z|$ with the expression of $\hat{S}_\eta^+ \hat{S}_\eta^-$ obtained from the use of Eq. (19), straightforwardly leads to the known $(\hat{\tilde{S}}_\eta)^2$'s expression [21, 22],

$$(\hat{\tilde{S}}_\eta)^2 = \hat{S}_\eta^+ \hat{S}_\eta^- - \frac{\sinh^2(\eta/2)}{\sinh^2 \eta} + \frac{\sinh^2(\eta(\hat{S}^z + 1/2))}{\sinh^2 \eta}. \quad (21)$$

That of the commutator $[\hat{S}_\eta^+, \hat{S}_\eta^-]$ in terms of the operator $\hat{U}_\eta^+ [\hat{S}^+, \hat{S}^-] \hat{U}_\eta^-$ is thus given by,

$$\begin{aligned} [\hat{S}_\eta^+, \hat{S}_\eta^-] &= \sum_{l_r, S_q, S^z} \frac{\sinh(\eta 2S^z)}{2S^z \sinh \eta} \langle l_r, S_q, S^z, \eta | \hat{U}_\eta^+ [\hat{S}^+, \hat{S}^-] \hat{U}_\eta^- | l_r, S_q, S^z, \eta \rangle | l_r, S_q, S^z, \eta \rangle \langle l_r, S_q, S^z, \eta | \\ &= \frac{\sinh(\eta 2\hat{S}^z)}{\sinh \eta}. \end{aligned} \quad (22)$$

Important symmetries are associated with the following commutations involving the momentum operator and \hat{S}^z ,

$$[\hat{P}, \hat{U}_\eta^\pm] = 0; \quad [\hat{S}^z, \hat{U}_\eta^\pm] = 0. \quad (23)$$

It follows that both the momentum eigenvalues P , Eq. (6), and spin projection S^z are good quantum numbers independent of η for the whole $\eta \geq 0$ range. Consistently, the commutator $[\hat{S}^z, \hat{S}_\eta^\pm]$ has the known simple form,

$$[\hat{S}^z, \hat{S}_\eta^\pm] = \pm \hat{S}_\eta^\pm. \quad (24)$$

The expressions of the q -spin $SU_q(2)$ symmetry generators, Eqs. (19) and (20), continuously evolve into those of the spin $SU(2)$ symmetry as η is continuously decreased to zero. And the $SU_q(2)$ symmetry itself also continuously evolves into the $SU(2)$ symmetry as η is adiabatically turned off to zero.

That the irreducible representations of the $\eta > 0$ continuous $SU_q(2)$ symmetry are isomorphic to those of the $\eta = 0$ $SU(2)$ symmetry, with the spin S being replaced by the q -spin S_q , refers to an important symmetry. It is behind the use of the unified notation $|l_r, S_q, S^z, \eta\rangle$ of the energy eigenstates for $\eta \geq 0$. Within it, one has that $S_q = S$ at $\eta = 0$. The whole analysis reported in the following also applies to the isotropic point under the replacement of q -spin S_q by spin S .

B. Confirmation of the $n = 1$ unbound pairs and $n > 1$ bound pairs q -spin neutral nature

For $\eta > 0$, a singlet means a $S_q = 0$ configuration of physical spins $1/2$. Standard counting of spin $SU(2)$ symmetry irreducible representations also applies to those of the continuous q -spin $SU_q(2)$ symmetry. One then finds from the use of the two isomorphic algebras that $\sum_{l_r} \mathcal{N}_{\text{singlet}}(S_q)$ for the model in each fixed- S_q subspace. Here,

$$\mathcal{N}_{\text{singlet}}(S_q) = \binom{N}{N/2 - S_q} - \binom{N}{N/2 - S_q - 1}, \quad (25)$$

is that subspace number of independent singlet configurations of physical spins $1/2$. Including multiplet configurations when $S_q > 0$, the dimension is larger and given by $\mathcal{N}(S_q) = (2S_q + 1) \mathcal{N}_{\text{singlet}}(S_q)$. Consistently,

$$\sum_{S_q} \mathcal{N}(S_q) = 2^N, \quad (26)$$

gives the total number of both irreducible representations and energy and momentum eigenstates.

For $S_q > 0$, one finds from the use of the $SU(2)$ and $SU_q(2)$ symmetries algebras that each energy eigenstate is populated by physical spins $1/2$ in two types of configurations. A set of $M = 2S_q$ physical spins $1/2$ participate in a multiplet configuration. A complementary set of even number $2\Pi = N - 2S_q$ physical spins $1/2$ participate in singlet configurations. All the states with the same S_q value whose number is $\mathcal{N}(S_q) = (2S_q + 1) \mathcal{N}_{\text{singlet}}(S_q)$ have the same Casimir operator's eigenvalue, $[\sinh^2(\eta(S_q + 1/2)) - \sinh^2(\eta/2)] / \sinh^2 \eta$.

It follows that the energy eigenstates are superpositions of such configuration terms. In them, each term is characterized by a different partition of N physical spins $1/2$. $M = 2S_q$ such spins participate in a $2S_q + 1$ multiplet. A product of singlets involves the remaining even number $2\Pi = N - 2S_q$ of physical spins $1/2$. Those form a tensor product of singlet states.

The *unpaired spins* $1/2$ and *paired spins* $1/2$ are the members of such two sets of $M = 2S_q$ and $2\Pi = N - 2S_q$ physical spins $1/2$, respectively.

The $SU_q(2)$ symmetry quantum number S_q naturally emerges within the Bethe-ansatz solution through the $n = 1, 2, \dots$ numbers $N_n^h = 2S_q + \sum_{n'=n+1}^{\infty} 2(n' - n)N_{n'}$, Eq. (5). In the following it is confirmed that the dimension of each subspace spanned by q -spin lowest-weight-states (LWSs) with fixed values of S_q is in terms of Bethe-ansatz quantum numbers occupancy configurations also given by $\mathcal{N}_{\text{singlet}}(S_q)$, Eq. (25). This is a needed major step towards showing that n -strings and $n = 1$ real single Bethe rapidities describe bound states of a number $n = 2, \dots, \infty$ of $S^z = S_q$ or 0 physical spins $1/2$ pairs and a single unbound such a pair, respectively.

The Bethe-ansatz solution refers to subspaces spanned by $SU_q(2)$ symmetry LWSs $|l_r, S_q, -S_q, \eta\rangle$. For such states, all the $M = 2S_q$ unpaired physical spins $1/2$ have the same spin projection, $S^z = -S_q$. (For the highest-weight-states (HWSs) of the $SU_q(2)$ symmetry algebra, $S^z = S_q$.) Similarly to the bare ladder spin operators \hat{S}^\pm , the action of the ladder operators \hat{S}_η^\pm , Eq. (19), onto $S_q > 0$ energy eigenstates flips a physical spin $1/2$ projection. A number $2S_q$ of $SU_q(2)$ symmetry non-LWSs outside the Bethe-ansatz solution are generated from the corresponding $n_z = S_q + S^z = 0$ LWS $|l_r, S_q, -S_q, \eta\rangle$ as,

$$|l_r, S_q, S^z, \eta\rangle = \frac{1}{\sqrt{C_\eta}} (\hat{S}_\eta^+)^{n_z} |l_r, S_q, -S_q, \eta\rangle. \quad (27)$$

Here $n_z \equiv S_q + S^z = 1, \dots, 2S_q$ so that $S^z = -S_q + n_z$ and,

$$C_\eta = \prod_{l=1}^{n_z} \frac{\sinh^2(\eta(S_q + 1/2)) - \sinh^2(\eta(l - S_q - 1/2))}{\sinh^2 \eta} \quad \text{for } n_z = 1, \dots, 2S_q. \quad (28)$$

One has for LWSs of the Bethe-ansatz solution that $-2S^z = 2S_q = N - \sum_{n'=1}^{\infty} 2n' N_{n'}$. For the set of non-LWSs of the same tower, the value of $S^z = -S_q + n_z$ changes upon varying that of the number $n_z = 1, \dots, 2S_q$. However, the values of both $N - \sum_{n'=1}^{\infty} 2n' N_{n'}$ and $2S_q$ remain unchanged for all such non-LWSs. It then follows from the boundary-condition relation, $2S_q = N - \sum_{n'=1}^{\infty} 2n' N_{n'}$ at $S^z = -S_q$, that it remains valid for the whole tower of $2S_q + 1$ states.

According to the $SU(2)$ and $SU_q(2)$ symmetries algebras, $M = 2S_q$ and $2\Pi = N - 2S_q$ are the numbers of unpaired physical spins $1/2$ and paired physical spins $1/2$, respectively. The exact relation $2S_q = N - \sum_{n=1}^{\infty} 2n N_n$ then implies that the number of paired physical spins $1/2$ within an energy eigenstate with $\Pi = \sum_{n=1}^{\infty} n N_n$ singlet pairs is given by $2\Pi = \sum_{n=1}^{\infty} 2n N_n$.

It is due to the isomorphism between the irreducible representations of the $SU(2)$ and $SU_q(2)$ symmetries, that the numbers L_n , Eq. (5), are independent of η . As justified in Appendix A, that independence ensures that the set of quantum numbers described by l_r that label the energy eigenstates, Eq. (16), are independent of that anisotropy parameter. This is a needed confirmation for the set of quantum numbers described by l_r that label such states being exactly the same for the two $\eta > 0$ and $\eta = 0$ energy eigenstates related as $|l_r, S_q, S^z, \eta\rangle = \hat{U}_\eta^+ |l_r, S, S^z, 0\rangle$, Eq. (16).

The exact relation, $2S_q = N - \sum_{n=1}^{\infty} 2n N_n$, reveals that for each subspace with fixed S_q value, the allowed numbers N_n can be given by zero and *all* positive integers that obey the exact sum rule, $\sum_{n=1}^{\infty} 2n N_n = N - 2S_q = 2\Pi$. Such a sum rule is a necessary condition for the validity of statement (i), that n -strings describe bound states of $n > 1$ out of the $\Pi = N/2 - S_q$ physical spins 1/2 singlet pairs of an energy eigenstate; and for the validity of statement (ii), that 1-particles refer to one unbound pair out of such $\Pi = N/2 - S_q$ pairs.

Importantly, the independence of η of the numbers L_n , Eq. (5), implies that an exact relation proved in Appendix A of Ref. 10 for $S = -S^z$ LWSs of the $\eta = 0$ spin chain holds for all 2^N energy eigenstates of the $\eta \geq 0$ chain provided that N_\downarrow (denoted by M in that reference, which here rather denotes the number of unpaired physical spins 1/2 of an energy eigenstate, $M = 2S_q$) is replaced in it by $N/2 - S$ for $\eta = 0$ and by $N/2 - S_q$ for $\eta > 0$. In the following we introduce the corresponding general *exact relation* that confirms the validity of statements (i) and (ii).

The occupancy configurations of 1-particles and $n > 1$ n -string-particles of a LWS and of the non-LWSs of the same tower are *exactly the same*. Indeed, such $2S_q + 1$ states only differ in the projections of the $M = 2S_q$ unpaired physical spins 1/2. Due to the Pauli-like occupancy of the n -bands, for a subspace with fixed S_q and $\{N_n\}$ values, there is in each n -band with finite occupancy $N_n > 0$ a number $\binom{L_n}{N_n}$ of such occupancy configurations. Each of them is associated with a different LWS and corresponding tower of non-LWSs.

For a larger fixed- S_q subspace containing several subspaces with a different set of fixed $\{N_n\}$ values, this holds for each such a set that obeys the exact sum rule, $\sum_{n=1}^{\infty} 2n N_n = N - 2S_q = 2\Pi$. We recall that the dimension $\mathcal{N}(S_q) = (2S_q + 1)\mathcal{N}_{\text{singlet}}(S_q)$ of such a larger fixed- S_q subspace corresponds to $2S_q + 1$ multiplet configurations and a number $\mathcal{N}_{\text{singlet}}(S_q)$ of singlet configurations given in Eq. (25). Indeed, for the non-LWSs generated from the LWSs as given in Eq. (27), the value of $2S_q = N - \sum_{n=1}^{\infty} 2n N_n$ remains unchanged, which is equivalent to the sum rule $\sum_{n=1}^{\infty} 2n N_n = N - 2S_q = 2\Pi$.

From the relation under consideration given in Appendix A of Ref. 10, one then straightforwardly finds the following more general *exact relation*,

$$\binom{N}{N/2 - S_q} - \binom{N}{N/2 - S_q - 1} = \sum_{\{N_n\}} \prod_{n=1}^{\infty} \binom{L_n}{N_n}. \quad (29)$$

The left-hand side of this equation is the subspace singlet dimension $\mathcal{N}_{\text{singlet}}(S_q)$ in $\mathcal{N}(S_q) = (2S_q + 1)\mathcal{N}_{\text{singlet}}(S_q)$, Eq. (25), in terms of physical spins 1/2 independent configurations. On its right-hand side, $\sum_{\{N_n\}}$ is a sum over all sets $\{N_n\}$ obeying the two equivalent exact Bethe-ansatz sum rules $2S_q = N - \sum_{n=1}^{\infty} 2n N_n$ and $2\Pi = \sum_{n=1}^{\infty} 2n N_n = N - 2S_q$. It follows that in each fixed- S_q subspace, the number of independent configurations of the 1-particles and n -string-particles for $n > 1$ associated with the set of $\Pi = \sum_{n=1}^{\infty} n N_n = N/2 - S_q$ singlet pairs of physical spins 1/2 exactly equals that of physical spins 1/2 singlet configurations, *i. e.* $\sum_{\{N_n\}} \prod_{n=1}^{\infty} \binom{L_n}{N_n} = \mathcal{N}_{\text{singlet}}(S_q)$.

This holds for the whole Hilbert space. It then confirms that each n -string-particle contains $n > 1$ pairs out of a number Π of singlet $S^z = S_q = 0$ pairs associated with the $2\Pi = N - 2S_q$ paired physical spins 1/2 of an energy eigenstate and each 1-particle contains one of such Π pairs.

This is consistent with the transformation, Eq. (27), of the $S_q > 0$ energy eigenstates $|l_r, S_q, S^z, \eta\rangle$ under the ladder operators \hat{S}_η^\pm . Indeed, the operator \hat{S}_η^+ in Eq. (27) only flips the $n_z = 1, \dots, 2S_q = M$ unpaired physical spins 1/2. It leaves invariant the singlet configuration of the $2\Pi = N - 2S_q$ paired physical spins 1/2. That all $2\Pi = N - 2S_q$ paired physical spins 1/2 of an energy eigenstate participate only in singlet configurations is also confirmed by the transformation laws of the $S_q = 0$ energy eigenstates $|l_r, 0, 0, \eta\rangle$ with no unpaired physical spins 1/2 that are populated by $2\Pi = N$ paired physical spins 1/2. Those transform as $\hat{S}_\eta^\pm |l_r, 0, 0, \eta\rangle = 0$.

The $n > 1$ pairs of physical spins 1/2 bound within a configuration described by a n -string that corresponds to the internal degrees of freedom of one n -string-particle and the unbound pair of physical spins 1/2 that refers to the internal degrees of freedom of one 1-particle only exist within the many-body system. Our results show that for $\eta = 0$ and $\eta > 0$ such pairs have $S^z = S = 0$ and $S^z = S_q = 0$, respectively. Hence as was known for the isotropic case [19, 20], at $\eta = 0$ they have zero spin. On the other hand, for $\eta > 0$ spin *is not* a good quantum number and thus cannot be used to label such pairs. We have found they have zero q -spin S_q under the generators of the continuous $SU_q(2)$ symmetry algebra.

The result of this section that $n = 1$ real single Bethe rapidities describe unbound singlet $S^z = S_q = 0$ pairs of physical spins 1/2 and $n > 1$ Bethe n -strings describe a number $n = 2, 3, \dots$ of bound such pairs renders the extension of the $\Delta = 1$ dynamical theory used in the studies of Refs. 17, 18 to $\Delta > 1$ a simple and direct procedure.

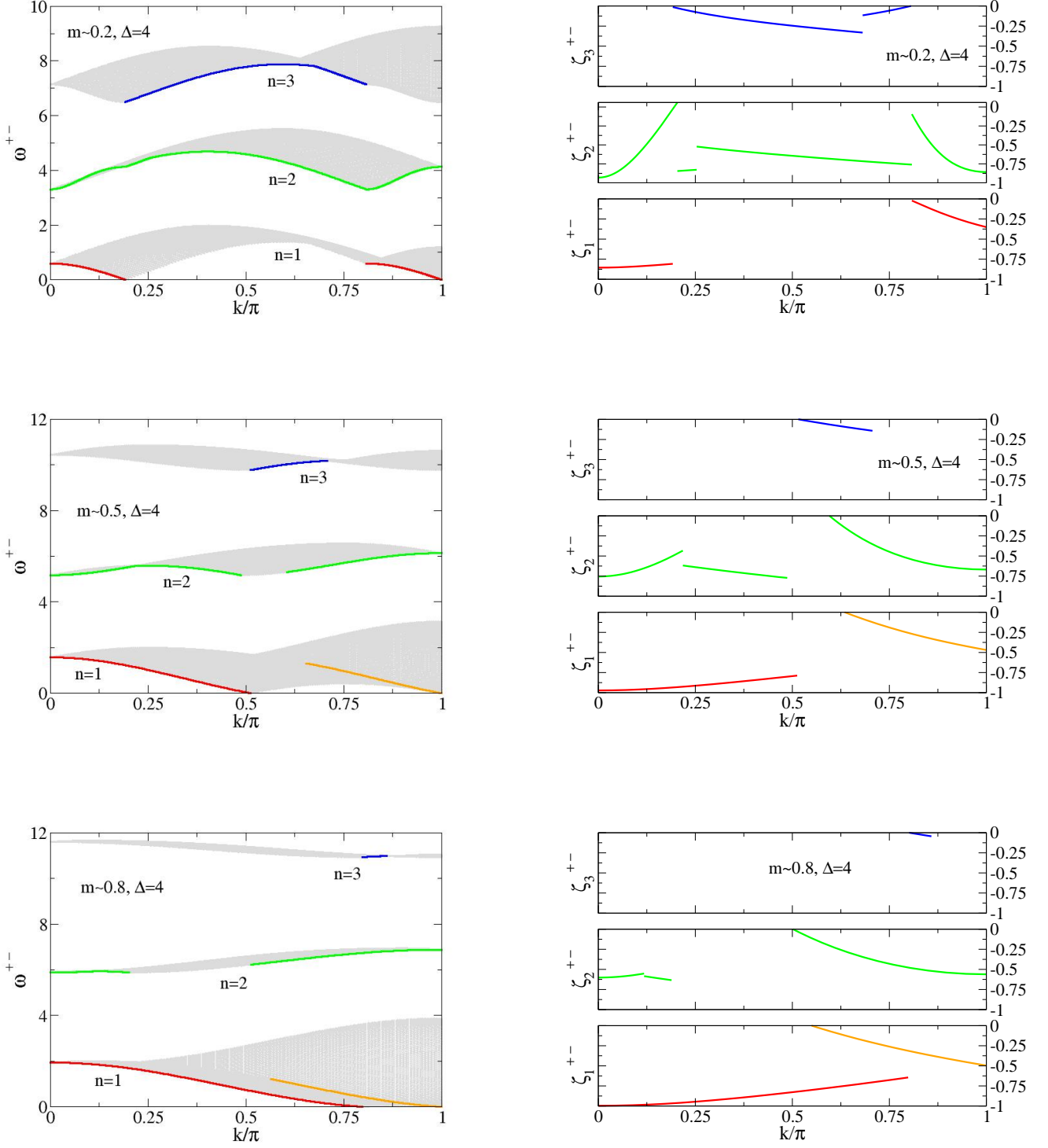


Figure 4: The (k, ω) -plane continua where there is more spectral weight in $S^{+-}(k, \omega)$ at $\Delta = 4$ for $m = 0.1920 \approx 0.2$, $m = 0.5125 \approx 0.5$, and $m = 0.7985 \approx 0.8$ (left) and the corresponding negative k dependent exponents that control the line shape $S^{+-}(k, \omega) \propto (\omega - \omega_n^{+-}(k))^{\zeta_n^{+-}(k)}$ in the k intervals near the lower thresholds of the $n = 1$, $n = 2$, and $n = 3$ continua marked in the spectra (right.) In them $S^{+-}(k, \omega)$ displays sharp peaks.

Finally, that the results reported in this section refer to the thermodynamic limit is consistent with the use of the ideal n -strings of form, Eq. (4), considered in Refs. 10 and 11. Deformations from the ideal n -strings that occur in large finite-size systems [27], such as the collapse of narrow pairs, preserve the total number $\Pi = N/2 - S_q$ of singlet $S^z = S_q = 0$ pairs of physical spins $1/2$. They only lead to a different distribution of such pairs within the exact sum rule, $\sum_{n=1}^{\infty} n N_n = \Pi$. Such finite-size deformations do not affect our results as the equalities in Eq. (29) remain unchanged.

Before addressing the above mentioned dynamical theory extension and the use of the corresponding extended dynamical theory for $\Delta > 1$, in the following the issue where in the Bethe-ansatz solution is stored the information on the unpaired physical spins $1/2$ is shortly discussed.

C. Where in the Bethe-ansatz solution are the unpaired physical spins $1/2$?

Out of the $2\Pi = \sum_{n=1}^{\infty} 2n N_n = N - 2S_q$ paired physical spins $1/2$ of an energy eigenstate, two are contained in each of its N_1 1-particles described by the $n = 1$ real single Bethe rapidities and $2n$ in each of its N_n n -string-particles are for $n > 1$ described by the Bethe n -strings. In the case of $S_q > 0$ energy eigenstates, the question is then where in the Bethe-ansatz solution's quantities is stored the information on the $M = 2S_q$ unpaired physical spins $1/2$ leftover?

The clarification of this issue involves a squeezed space construction [28]. Each Bethe-ansatz n -band is found to correspond in the thermodynamic limit to a n -squeezed lattice with $L_n = N_n + N_n^h$ sites. A number N_n^h of such sites are not occupied by 1-particles for $n = 1$ and by n -string-particles for $n > 1$. Hence they are the n -squeezed lattice unoccupied sites.

Out of the N sites of the original lattice, the occupancies of $2S_q$ such sites by the $M = 2S_q$ unpaired physical spins $1/2$ remain invariant under the squeezed space construction. This important symmetry refers to each of the local configurations whose superposition generates an energy eigenstate.

Information on the $M = 2S_q$ unpaired physical spins $1/2$ is then found to be stored by the Bethe-ansatz solution in the n -squeezed lattice's N_n^h unoccupied sites. Those are directly related to the N_n^h n -holes. Out of the $N_n^h = 2S_q + \sum_{n'=n+1}^{\infty} 2(n' - n)N_{n'}$, Eq. (5), unoccupied sites of each n -squeezed lattice, a number $2S_q$ of such sites is in the original lattice singly occupied by unpaired physical spins $1/2$.

For energy eigenstates without n -strings, one has that $N_1^h = 2S_q$. In that case all $N_1^h = 2S_q$ 1-holes describe the translational degrees of freedom of the $M = 2S_q$ unpaired physical spins $1/2$. Such 1-holes are often in the literature identified with spinons, our results clarifying their relation to the unpaired physical spins $1/2$.

IV. EXCITATION SPECTRA OF THE DYNAMICAL STRUCTURE FACTOR COMPONENTS

The results of this paper reported in this section and in Sec. V refer to the spin-conducting quantum phase for magnetic fields $h_{c1} < h < h_{c2}$. The spectra and the dynamical properties are qualitatively different in the spin-insulating quantum phase associated with magnetic fields $0 \leq h < h_{c1}$. The latter problem was studied previously in the literature [15] and is not addressed in this paper. However, the limiting behaviors for $0 \leq h < h_{c1}$ and $h = h_{c2}$ of several important quantities are given in Appendix B.

A. Classes of excited states that lead to most (k, ω) -plane spectral weight for $m > 0$

A consequence of the singlet $S^z = S_q = 0$ nature of the elementary magnetic configurations under study in Sec. III, is that the general dimension-one scalar S matrices whose expression is given below in Sec. V have for the spin-conducting phase at fields $h_{c1} < h < h_{c2}$ the same form as for the isotropic case for $0 < h < h_{c2}$. Such S matrices refer to the scattering of the q -spin neutral 1-particles and q -spin neutral n -string-particles that controls the line shape near the sharp peaks in $S^{+-}(k, \omega)$, $S^{-+}(k, \omega)$, and $S^{zz}(k, \omega)$.

To properly identify the (k, ω) -plane lines of sharp peaks under study in Sec. V, in this section we provide the expressions in the thermodynamic limit of the spectra of the classes of excited states that contribute to a significant amount of spin dynamical structure factor's spectral weight. As justified in that section, the spectra of the corresponding selected classes of excited states lead to the (k, ω) -plane continua shown in Figs. 4,5,6,7,8,9. For technical reasons, such figures refer to spin densities $m = 0.1920 \approx 0.2$, $m = 0.5125 \approx 0.5$, and $m = 0.7985 \approx 0.8$ for anisotropy $\Delta = 4$ and spin densities $m = 0.2056 \approx 0.2$, $m = 0.4918 \approx 0.5$, and $m = 0.7997 \approx 0.8$ for anisotropy $\Delta = 8$.

All $n = 1$ continua in these figures refer to spectra of excited energy eigenstates for which $N_1 = N_{\downarrow}$ and $N_n = 0$ for $n > 1$ where the number N_{\downarrow} of down physical spins refers here and for all other continua to the excited states under consideration. The $n = 2$ continua in Figs. 4,5,8,9 correspond to spectra of excited energy eigenstates for which

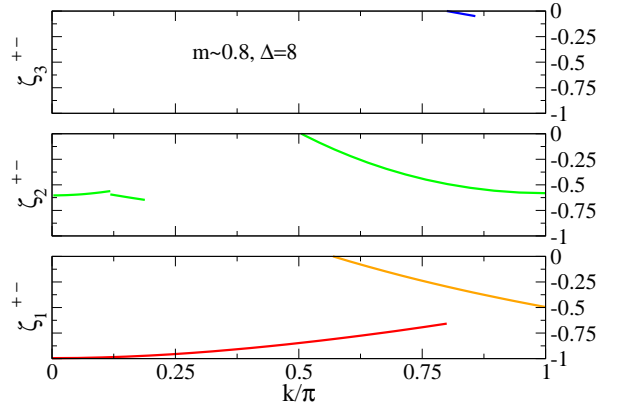
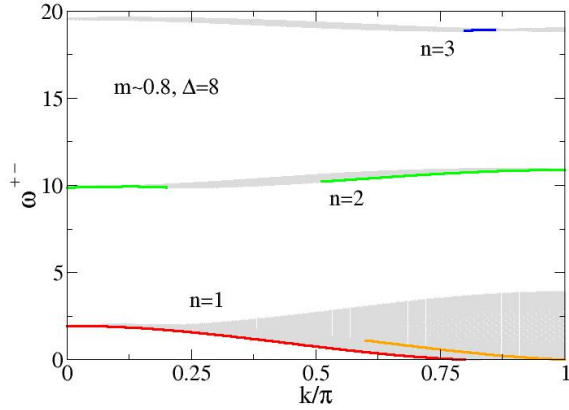
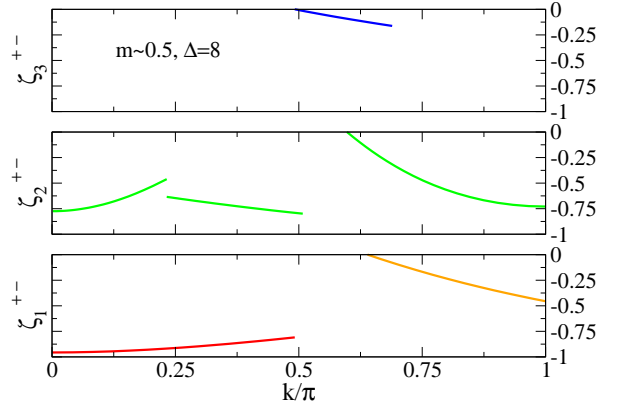
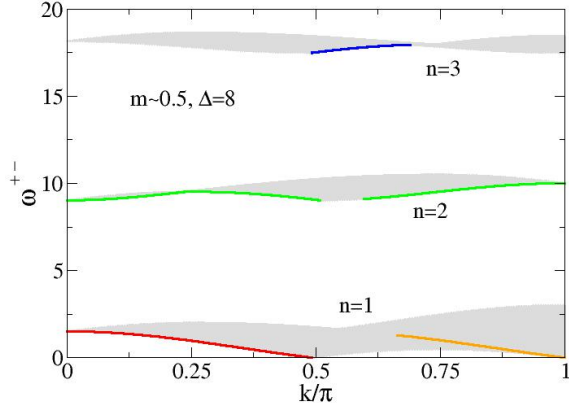
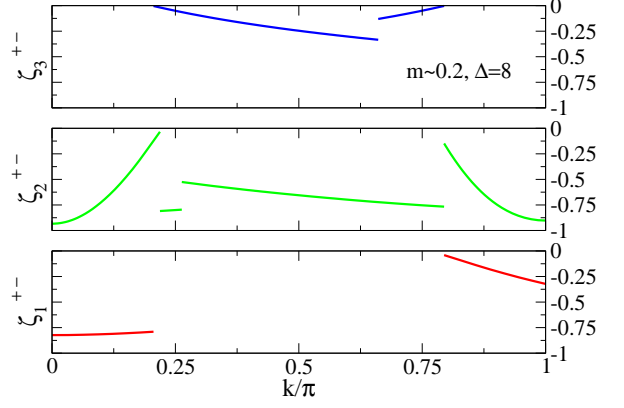
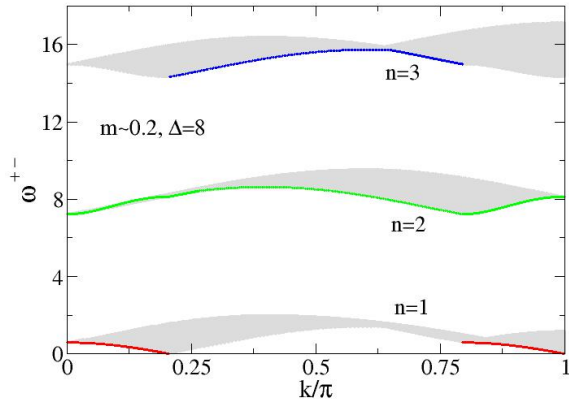


Figure 5: The same as in Fig. 4 for spin densities $m = 0.2056 \approx 0.2$, $m = 0.4918 \approx 0.5$, and $m = 0.7997 \approx 0.8$ and anisotropy $\Delta = 8$.

$N_1 = N_\downarrow - 2$, $N_2 = 1$, and $N_n = 0$ for $n > 2$. Finally, the $n = 3$ continua in Figs. 4,5 refer to spectra of excited energy eigenstates for which $N_1 = N_\downarrow - 3$, $N_2 = 0$, $N_3 = 1$, and $N_n = 0$ for $n > 3$. Hence, as justified in Sec. V, the n -string states that contribute to a significant amount of spectral weight are populated only by either a single 2-string-particle or a single 3-string-particle.

In the present thermodynamic limit, the spectra of the classes of selected excited states have simple expressions in terms of the 1-particle energy dispersion $\varepsilon_1(q)$ plotted in Fig. 1 and $n = 2$ and $n = 3$ n -string-particle energy dispersions $\varepsilon_n(q)$ plotted in Figs. 2 and 3, respectively.

B. The excitation spectra with most spectral weight for $m > 0$

The expressions of the two-parametric spectra given in the following refer to a k extended zone scheme. However, in Figs. 4,5,6,7,8,9 they have been brought to the first Brillouin zone for positive momentum values $k > 0$. In the case of $S^{+-}(k, \omega)$, the spectrum associated with the lower (k, ω) -plane $n = 1$ continuum shown in Figs. 4,5 is the superposition of the following two spectra,

$$\begin{aligned} \omega_1^{+-}(k) &= \omega_{1A}^{+-}(k) + \omega_{1B}^{+-}(k) \quad \text{where} \\ \omega_{1A}^{+-}(k) &= \varepsilon_1(q) - \varepsilon_1(q') \quad \text{with} \quad k = \iota\pi + q - q' \quad \text{for} \\ &\quad |q| \in [k_{F\downarrow}, k_{F\uparrow}], \quad q' \in [-k_{F\downarrow}, k_{F\downarrow}] \quad \text{and} \quad \iota = \pm 1 \\ \omega_{1B}^{+-}(k) &= \varepsilon_1(q) + \varepsilon_1(q') \quad \text{with} \quad k = \iota\pi + q + q' \quad \text{for} \\ &\quad q \in [k_{F\downarrow}, k_{F\uparrow}], \quad q' \in [-k_{F\uparrow}, -k_{F\downarrow}] \quad \text{and} \quad \iota = \pm 1. \end{aligned} \quad (30)$$

The spectrum of that dynamical structure factor component associated with the gapped middle (k, ω) -plane $n = 2$ continuum shown in such figures reads,

$$\begin{aligned} \omega_2^{+-}(k) &= -\varepsilon_1(q) + \varepsilon_2(q') \quad \text{with} \quad k = \iota k_{F\downarrow} - q + q' \quad \text{for} \\ &\quad q \in [-k_{F\downarrow}, k_{F\downarrow}], \quad q' \in [0, (k_{F\uparrow} - k_{F\downarrow})] \quad \text{and} \quad \iota = 1 \\ &\quad q \in [-k_{F\downarrow}, k_{F\downarrow}], \quad q' \in [-(k_{F\uparrow} - k_{F\downarrow}), 0] \quad \text{and} \quad \iota = -1. \end{aligned} \quad (31)$$

The $S^{+-}(k, \omega)$ spectrum associated with the gapped upper (k, ω) -plane $n = 3$ continuum also shown in Figs. 4,5 is the superposition of the following two spectra,

$$\begin{aligned} \omega_3^{+-}(k) &= \omega_{3A}^{+-}(k) + \omega_{3B}^{+-}(k) \quad \text{where} \\ \omega_{3A}^{+-}(k) &= -\varepsilon_1(q) + \varepsilon_3(q') \quad \text{with} \quad k = \iota k_{F\uparrow} - q + q' \quad \text{for} \\ &\quad q \in [-k_{F\downarrow}, k_{F\downarrow}], \quad q' \in [-(k_{F\uparrow} - k_{F\downarrow}), 0] \quad \text{and} \quad \iota = 1 \\ &\quad q \in [-k_{F\downarrow}, k_{F\downarrow}], \quad q' \in [0, (k_{F\uparrow} - k_{F\downarrow})] \quad \text{and} \quad \iota = -1 \\ \omega_{3B}^{+-}(k) &= -\varepsilon_1(q) - \varepsilon_1(q') + \varepsilon_3(0) \quad \text{with} \quad k = \iota\pi - q - q' \quad \text{for} \\ &\quad q \in [0, k_{F\downarrow}], \quad q' \in [-k_{F\downarrow}, 0] \quad \text{and} \quad \iota = \pm 1. \end{aligned} \quad (32)$$

As justified in Sec. V, in the case of $S^{-+}(k, \omega)$ only the (k, ω) -plane $n = 1$ continuum has a significant amount of spectral weight. It is shown in Figs. 6,7. The corresponding spectrum reads,

$$\begin{aligned} \omega_1^{-+}(k) &= -\varepsilon_1(q) - \varepsilon_1(q') \quad \text{where} \quad k = \iota\pi - q - q' \quad \text{for} \\ &\quad q \in [-k_{F\downarrow}, k_{F\downarrow}], \quad q' \in [-k_{F\downarrow}, k_{F\downarrow}] \quad \text{and} \quad \iota = \pm 1. \end{aligned} \quad (33)$$

The $S^{zz}(k, \omega)$ spectrum associated with the lower (k, ω) -plane $n = 1$ continuum shown in Figs. 8,9 is given by,

$$\begin{aligned} \omega_1^{zz}(k) &= \varepsilon_1(q) - \varepsilon_1(q') \quad \text{with} \quad k = q - q' \quad \text{for} \\ &\quad |q| \in [k_{F\downarrow}, k_{F\uparrow}], \quad q' \in [-k_{F\downarrow}, k_{F\downarrow}]. \end{aligned} \quad (34)$$

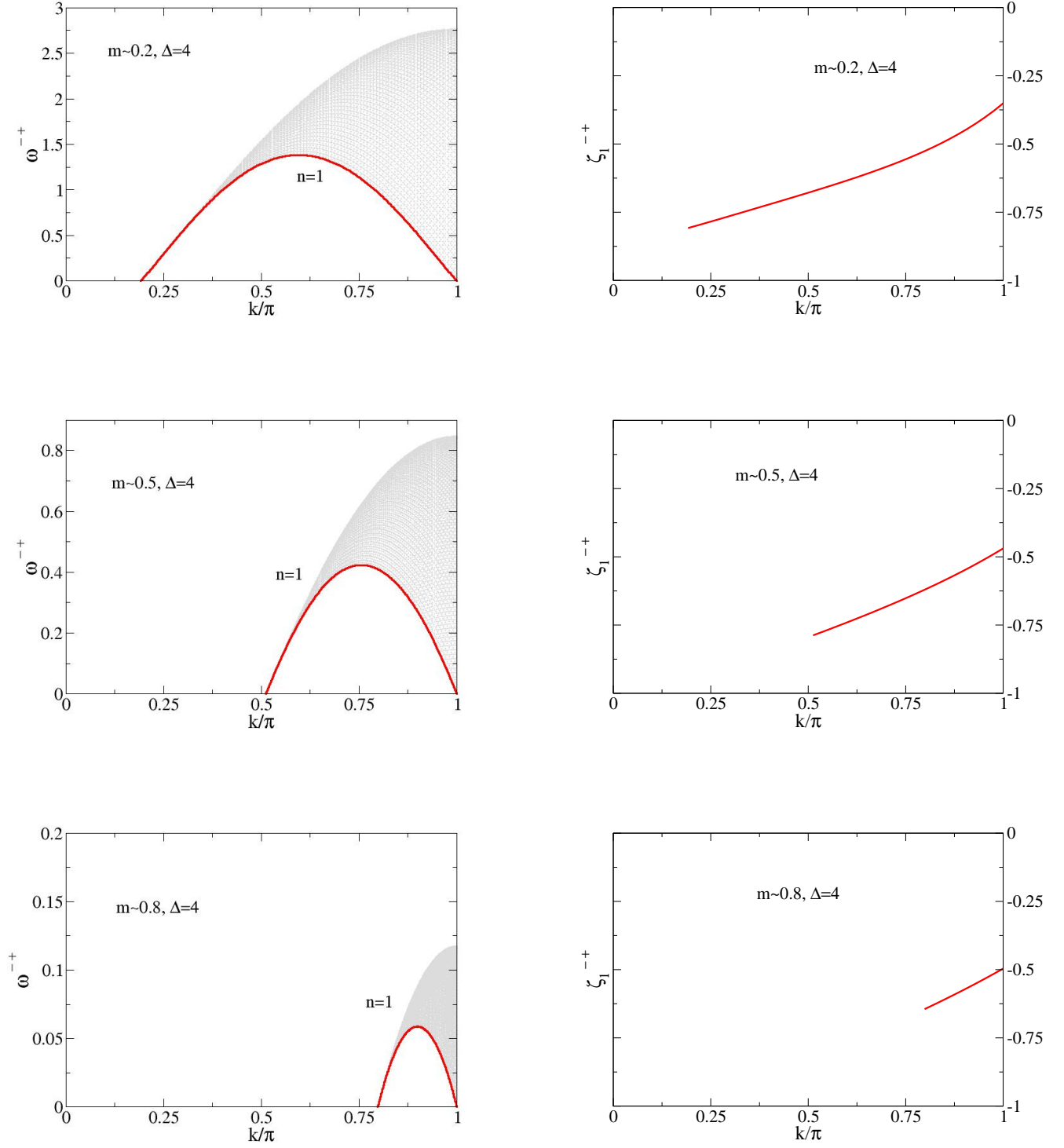


Figure 6: The (k, ω) -plane continuum where there is more spectral weight in $S^{--}(k, \omega)$ at $\Delta = 4$ for $m = 0.1920 \approx 0.2$, $m = 0.5125 \approx 0.5$, and $m = 0.7985 \approx 0.8$ (left) and the negative k dependent exponents that control the line shape $S^{--}(k, \omega) \propto (\omega - \omega_1^{--}(k))^{\zeta_1^{--}(k)}$ in the marked k intervals near the lower threshold of that continuum (right).

The gapped $n = 2$ continuum shown in these figures is the superposition of the following two spectra,

$$\begin{aligned}
\omega_2^{zz}(k) &= \omega_2^{zz}(k) + \omega_2^{zz}(k) \quad \text{where} \\
\omega_2^{zz}(k) &= -\varepsilon_1(q) + \varepsilon_2(q') \quad \text{with} \quad k = \iota k_{F\uparrow} - q + q' \quad \text{for} \\
q &\in [-k_{F\downarrow}, k_{F\downarrow}], \quad q' \in [-(k_{F\uparrow} - k_{F\downarrow}), 0] \quad \text{and} \quad \iota = 1 \\
q &\in [-k_{F\downarrow}, k_{F\downarrow}], \quad q' \in [0, (k_{F\uparrow} - k_{F\downarrow})] \quad \text{and} \quad \iota = -1 \\
\omega_2^{zz}(k) &= -\varepsilon_1(q) - \varepsilon_1(q') + \varepsilon_2(0) \\
\text{with} \quad k &= \iota\pi - q - q' \quad \text{for} \\
q &\in [0, k_{F\downarrow}], \quad q' \in [-k_{F\downarrow}, 0] \quad \text{and} \quad \iota = \pm 1.
\end{aligned} \tag{35}$$

V. THE POWER-LAW LINE SHAPE NEAR THE SHARP PEAKS CONTROLLED BY THE 1-1 AND 1- n SCATTERING OF 1-PARTICLES AND n -STRING-PARTICLES

In this section, the (k, ω) -plane power-law line shape near the sharp peaks in $S^{+-}(k, \omega)$, $S^{-+}(k, \omega)$, and $S^{zz}(k, \omega)$ is studied in the thermodynamic limit. Such sharp peaks are located in specific k intervals of the lower thresholds of the set of (k, ω) -plane continua shown in Figs. 4,5,6,7,8,9. (Below we also consider sharp peaks in the k interval of a branch line running inside the $n = 1$ (k, ω) -plane continuum of $S^{+-}(k, \omega)$.)

The results of Sec. III render the extension to anisotropy $\Delta > 1$ of the dynamical theory suitable to the isotropic point [17, 18] straightforward and direct. That some dynamical properties are different from those of the isotropic point is naturally captured by the η -dependent expressions of the dynamical structure factor components for $\eta > 0$ provided below in Sec. VB.

The general dynamical theory used for the isotropic point in Refs. 17, 18 and for anisotropy $\Delta > 1$ in the following, was introduced in Ref. 29 for the 1D Hubbard model with onsite repulsion U and transfer integral t . It is a generalization to the whole $u = U/4t > 0$ range of the approach used for the $u \rightarrow \infty$ limit in Refs. 30, 31. Momentum-dependent exponents in the expressions of dynamical correlation functions have also been obtained in Refs. 32, 33. That dynamical theory is easily generalized to several integrable problems [34], including here to the $\Delta > 1$ anisotropic spin-1/2 XXZ chain in a longitudinal magnetic field. For integrable problems, that general theory is equivalent to the mobile quantum impurity model scheme of Refs. 35 and 36, accounting for exactly the same microscopic elementary excitation processes [34, 37].

Although the general dynamical theory applies in principle to the whole (k, ω) plane, simple analytical expressions for the dynamical correlation functions are achieved near their sharp peaks. Power-law line shapes associated with positive momentum dependent exponents are also valid at and near (k, ω) -plane branch lines as defined in Ref. 18, provided there is no spectral weight or very little such a weight below them. However, the studies of this paper focus on the line shape near sharp peaks. Complementarily to the results given below in Sec. VB, in both these simplest cases, the relation of the matrix elements square $|\langle \nu | \hat{S}_k^a | GS \rangle|^2$ in Eq. (1) to the expressions of $S^{+-}(k, \omega)$, $S^{-+}(k, \omega)$, and $S^{zz}(k, \omega)$ near the corresponding power-law line shapes is an issue discussed in Appendix C.

A. The S matrices and phase shifts associated with the n -particle scattering

The dynamical theory whose expressions for the present model are given below in Sec. VB fully relies on the S matrices associated with the n -particles scattering. Such a scattering is the physically important issue discussed here. As mentioned previously, the singlet $S^z = S_q = 0$ nature of both the unbound pairs of physical spins 1/2 described by $n = 1$ real single Bethe rapidities and $n = 2, 3, \dots$ bound pairs described by Bethe n -strings ensures that the present dynamical theory applies. Indeed, the corresponding 1-particle and $n > 1$ n -string-particle S matrices are then found to have for $\eta > 0$ and magnetic fields $h \in [h_{c1}, h_{c2}]$ the following same exact scalar form as for the isotropic case,

$$S_n(q_j) = \prod_{n'=1}^{\infty} \prod_{j'=1}^{L_{n'}} S_{n,n'}(q_j, q_{j'}) \quad \text{where} \quad S_{n,n'}(q_j, q_{j'}) = e^{i \delta N_{n'}(q_{j'}) 2\pi \Phi_{n,n'}(q_j, q_{j'})}. \tag{36}$$

The quantities $2\pi \Phi_{n,n'}(q_j, q_{j'})$ in this equation are 1-particle and $n > 1$ n -string-particle phase shifts.

The technically difficult task of extending the dynamical theory to the whole (k, ω) plane would involve S matrices for all $n \geq 1$ and $n' \geq 1$ values in the quantity $S_{n,n'}(q_j, q_{j'})$ given in Eq. (36). This though leads to formal expressions containing state summations that are both analytically and numerically very difficult to be carried out.

However, for the technically simpler problem referring to our study of the power-law line shape near the sharp peaks of the dynamical structure factor components, only the 1-particle S matrix $S_1(q)$ at the 1-band Fermi points

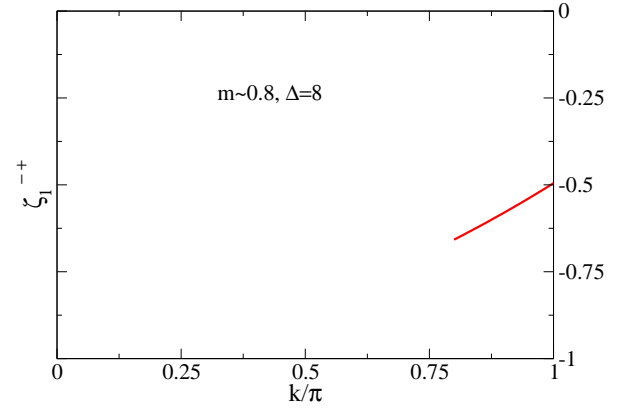
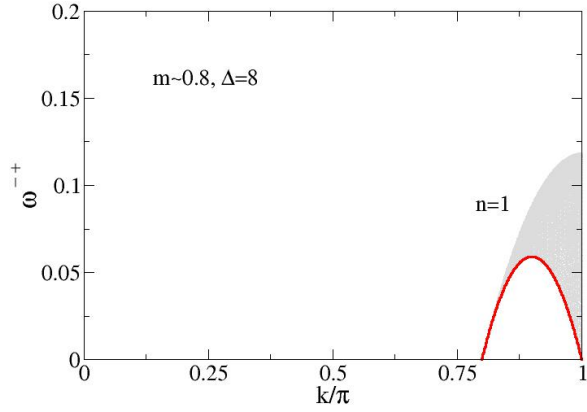
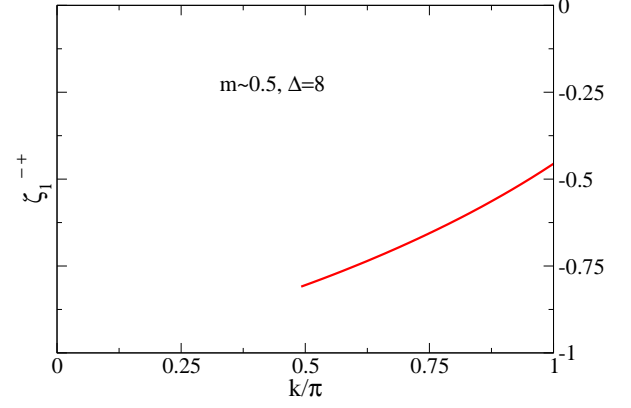
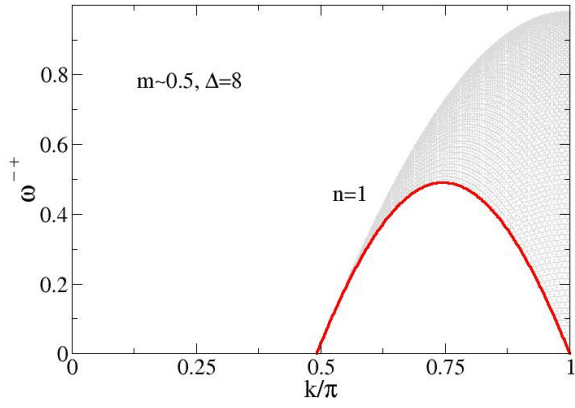
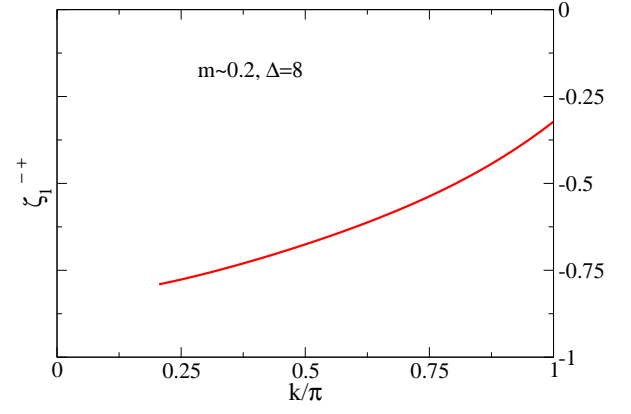
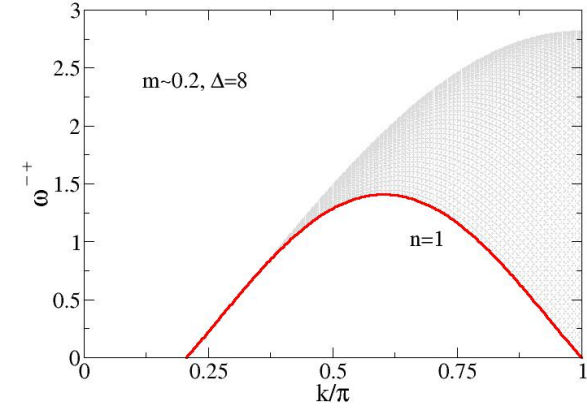


Figure 7: The same as in Fig. 6 for spin densities $m = 0.2056 \approx 0.2$, $m = 0.4918 \approx 0.5$, and $m = 0.7997 \approx 0.8$ and anisotropy $\Delta = 8$.

$q = \pm k_{F\downarrow}$ and corresponding $\eta > 0$ phase shifts $2\pi\Phi_{1,1}(\pm k_{F\downarrow}, q)$ and $2\pi\Phi_{1,n}(\pm k_{F\downarrow}, q)$ for $n > 1$ defined by Eqs. (C13)-(C16) of Appendix C play an active role. Indeed, ground states are not populated by n -string particles. Hence only the ground-state preexisting 1-particles play the role of scatterers. It follows that the corresponding 1-particle S matrix, within which the created 1-particles, 1-holes, and n -string-particles under transitions to excited states play the role of scattering centers, determines the momentum k dependence of the exponents that control the power-law line shapes near the sharp peaks in $S^{+-}(k, \omega)$, $S^{-+}(k, \omega)$, and $S^{zz}(k, \omega)$.

Physically, (i) $-2\pi\Phi_{1,1}(\pm k_{F\downarrow}, q)$ and (ii) $2\pi\Phi_{1,1}(\pm k_{F\downarrow}, q)$ are the phase shift acquired by a 1-particle of momentum $\pm k_{F\downarrow}$ upon creation (i) of one 1-hole at a 1-band momentum whose maximum interval is $q \in [-k_{F\downarrow}, k_{F\downarrow}]$ and (ii) of one 1-particle at a 1-band momentum whose maximum intervals are $q \in [-k_{F\uparrow}, -k_{F\downarrow}]$ and $q \in [k_{F\downarrow}, k_{F\uparrow}]$. On the other hand, $2\pi\Phi_{1,n}(\pm k_{F\downarrow}, q)$ is for $n = 2, 3$ the phase shift acquired by such a 1-particle of momentum $\pm k_{F\downarrow}$ upon creation of one n -string-particle at a n -band momentum whose maximum interval is $q \in [-(k_{F\uparrow} - k_{F\downarrow}), (k_{F\uparrow} - k_{F\downarrow})]$.

Hence for the present quantum problem only the dominant 1 – 1 and 1 – n scattering channels where $n = 2, 3$ contribute to the dynamical properties in what nearly the whole spectral weight is concerned. Importantly, the power-law line shape near the sharp peaks under study is *only* controlled by such dominant scattering processes. Within them, the 1-particles at and very near the 1-band Fermi points $\iota k_{F\downarrow} = \pm k_{F\downarrow}$ are the scatterers and the 1-particles or 1-holes and the 2-string-particle or 3-string-particle created under the transitions from the ground state to the excited states are the scattering centers.

Actually and as discussed in Appendix C, the 1-band momentum of the 1-particle scatterers refers to the *reference-state* $\iota = \pm 1$ Fermi points $q_{F1,\iota} = q_{F1,\iota}^0 + \frac{\pi}{L} \delta N_{1,\iota}^F$, Eq. (C1) of that Appendix. Here $q_{F1,\iota}^0$ are the initial ground-state $\iota = \pm 1$ Fermi points that in the thermodynamic limit can be written as $q_{F1,\iota}^0 = \iota k_{F\downarrow}$ and $\delta N_{1,\iota}^F$ is the deviation under the ground-state - excited state transitions in the number of 1-particles at such $\iota = \pm 1$ Fermi points. As was given in Sec. II, the quantum numbers I_j^1 in $q_j = \frac{2\pi}{L} I_j^1$ are integers or half-odd integers for L_1 odd and even, respectively. Hence, 1-band momentum shifts $\pm\pi/L$ occur when the deviations δL_1 under such transitions are odd integers. As a result, $\delta N_{1,\iota}^F$ may be an integer or a half-odd integer number.

For each ground-state - excited state transition, the relevant 1-particle S matrix is then $S_1(q_{F1,\iota})$, which for the present quantum problem involves some of the phase shifts $2\pi\Phi_{1,n}(q_{F1,\iota}, q)$ where $n = 1, 2, 3$. However, in the thermodynamic limit one can replace the reference-state $\iota = \pm 1$ Fermi points $q_{F1,\iota}$ in the argument of such a S matrix and corresponding phase shifts by the ground-state $\iota = \pm 1$ Fermi points $q_{F1,\iota}^0 = \iota k_{F\downarrow}$. The neglected contributions are irrelevant and vanish in that limit. The apparently neglected deviation $\delta N_{1,\iota}^F$ in $q_{F1,\iota} = q_{F1,\iota}^0 + \frac{\pi}{L} \delta N_{1,\iota}^F$ actually emerges in a higher order contribution that does not vanish in the thermodynamic limit.

Indeed, the momentum k dependence of the exponents considered below in Sec. VB is determined by both that deviation $\delta N_{1,\iota}^F$ and the 1-particle S matrix $S_1(q)$ at the 1-band Fermi points $q = \iota k_{F\downarrow} = \pm k_{F\downarrow}$. This occurs through an important functional of the following general form,

$$\begin{aligned} \Phi_\iota &= \iota \delta N_{1,\iota}^F - \frac{i}{2\pi} \ln S_1(\iota k_{F\downarrow}) = \iota \frac{\delta N_1^F}{2} + \delta J_1^F - \frac{i}{2\pi} \ln S_1(\iota k_{F\downarrow}) \quad \text{where} \\ S_1(\iota k_{F\downarrow}) &= \prod_{n=1}^3 \prod_{j=1}^{L_n} e^{i \delta N_n(q_j) 2\pi\Phi_{1,n}(\iota k_{F\downarrow}, q_j)} = e^{i \sum_{n=1}^3 \sum_{j=1}^{L_n} \delta N_n(q_j) 2\pi\Phi_{1,n}(\iota k_{F\downarrow}, q_j)}. \end{aligned} \quad (37)$$

Here the number deviation δN_1^F and the current-like deviation δJ_1^F in which $\delta N_{1,\iota}^F$ can be decomposed read $\delta N_1^F = \sum_{\iota=\pm 1} \delta N_{1,\iota}^F$ and $\delta J_1^F = \frac{1}{2} \sum_{\iota=\pm 1} \iota \delta N_{1,\iota}^F$, respectively. The deviations $\delta N_n(q_j)$ refer to the n -band momentum distributions.

For each specific (k, ω) -plane line of sharp peaks in the dynamical structure factor components, the functional Φ_ι , Eq. (37), refers to a form of the S matrix $S_1(\iota k_{F\downarrow})$ in that equation specific to the one-parametric spectrum $\bar{\omega}_n^{ab}(k)$ in Eq. (42) corresponding to a branch line, as defined in Ref. 18. For instance, for both the branch-line k intervals that coincide with lower threshold of the $n = 1$ continua of $S^{+-}(k, \omega)$, $S^{-+}(k, \omega)$, and $S^{zz}(k, \omega)$ and for a specific branch line considered below that for some m values runs on the $n = 1$ continuum of $S^{+-}(k, \omega)$, the functional $\Phi_\iota(k)$ is a function of the excitation momentum k that has the following simple form,

$$\Phi_\iota(k) = \iota \delta \mathcal{N}_{1,\iota}^F \pm \Phi_{1,1}(\iota k_{F\downarrow}, q) \quad \text{where} \quad k = k_1 \pm q. \quad (38)$$

Here $+$ or $-$ refers to creation of one 1-particle at a 1-band momentum q whose maximum interval is $|q| \in [k_{F\downarrow}, k_{F\uparrow}]$ or creation of one 1-hole at a 1-band momentum q whose maximum interval is $q \in [-k_{F\downarrow}, k_{F\downarrow}]$, respectively. The values of the fixed momentum value k_1 specific to the branch-line k intervals under consideration are provided in Eqs. (D4), (D5), (D18), and (D22) of Appendix D, and the renormalized $\iota = \pm 1$ number deviation $\delta \mathcal{N}_{1,\iota}^F$ is given by,

$$\delta \mathcal{N}_{1,\iota}^F = \frac{\delta N_1^F}{2\xi_{11}} + \iota \xi_{11} \delta J_1^F \quad \text{where} \quad \xi_{11} = 1 + \Phi_{1,1}(k_{F\downarrow}, k_{F\downarrow}) - \Phi_{1,1}(k_{F\downarrow}, -k_{F\downarrow}). \quad (39)$$

The 1-band q intervals for which the corresponding exponent is negative refer either to the above maximum intervals or to their well defined subintervals.

For the $n = 2, 3$ continua lower thresholds of $S^{+-}(k, \omega)$ and $n = 2$ continuum lower threshold of $S^{zz}(k, \omega)$ the functional $\Phi_\iota(k)$ has for the momentum k intervals for which the corresponding exponent is negative one of the following three simple forms,

$$\begin{aligned}\Phi_\iota(k) &= \iota \delta \mathcal{N}_{1,\iota}^F + \iota \frac{\xi_n^0}{2} - \Phi_{1,1}(\iota k_{F\downarrow}, q) \quad \text{where} \quad k = k_n - q \\ \Phi_\iota(k) &= \iota \delta \mathcal{N}_{1,\iota}^F + \xi_n^{\iota,\pm} - \Phi_{1,1}(\iota k_{F\downarrow}, q) \quad \text{where} \quad k = k_n - q \\ \Phi_\iota(k) &= \iota \delta \mathcal{N}_{1,\iota}^F + \Phi_{1,n}(\iota k_{F\downarrow}, q) \quad \text{where} \quad k = k_n + q \quad \text{for} \quad n = 2, 3.\end{aligned}\tag{40}$$

In the first two expressions of this equation, q is the 1-band momentum for creation of one 1-hole whose maximum interval is $q \in [-k_{F\downarrow}, k_{F\downarrow}]$. In the third expression, q is for $n = 2, 3$ the n -band momentum for creation of one n -string-particle whose maximum interval is $q \in [-(k_{F\uparrow} - k_{F\downarrow}), (k_{F\uparrow} - k_{F\downarrow})]$. In these expressions, the values of the fixed momentum values k_2 and k_3 specific to the branch-line k intervals under consideration are provided in Eqs. (D6)-(D9), (D23)-(D26) and Eqs. (D10)-(D13), respectively, of Appendix D. The renormalized number deviation $\delta \mathcal{N}_{1,\iota}^F$ is given in Eq. (39) and the parameters ξ_n^0 and $\xi_n^{\iota,\pm}$ for $\iota = \pm 1$ read,

$$\begin{aligned}\xi_n^0 &= 2\Phi_{1,n}(k_{F\downarrow}, 0) \quad \text{for} \quad n = 2, 3 \\ \xi_n^{\iota,\pm} &= \Phi_{1,n}(\iota k_{F\downarrow}, \pm(k_{F\uparrow} - k_{F\downarrow})) \quad \text{for} \quad n = 2, 3 \quad \text{and} \quad \iota = \pm 1.\end{aligned}\tag{41}$$

In the four types of expressions for the functional $\Phi_\iota(k)$ given in Eqs. (38) and (40), which are specific to (k, ω) -plane line shapes near branch lines of sharp peaks whose spectrum $\bar{\omega}_n^{ab}(k)$ in Eq. (42) is one-parametric, all except one of the few deviations $\delta N_n(q_j)$ that have finite values in the S matrix $S_1(\iota k_{F\downarrow})$ general expression, Eq. (37), refer to fixed n -band momentum values $q_j = q$. Those are either at the $q = \pm k_{F\downarrow}$ Fermi points for $n = 1$ or at $q = 0$ or $q = \pm(k_{F\uparrow} - k_{F\downarrow})$ for $n = 2$ or $n = 3$.

A question is to which n -band refers the only finite deviation $\delta N_n(q_j)$ whose momentum $q_j = q$ can have arbitrary values within one of the maximum intervals provided above? As given in Eq. (38), for the $n = 1$ (k, ω) -plane continua one has always that such a deviation refers to the 1-band. As revealed by inspection of the form of the expressions provided in Eq. (40), for the $n = 2$ and $n = 3$ (k, ω) -plane continua such a deviation can either refer to the 1-band or to the 2-band and 3-band, respectively.

B. The expressions of the dynamical structure factor components near sharp peaks

In all integrable problems to which the dynamical theory addressed and used here applies, one finds a direct relationship between the negativity and the length of the momentum k interval of the momentum dependent exponents that control the power-law line shape of the dynamical correlation function components near the lower threshold of a given (k, ω) -plane continuum and the amount of spectral weight over the latter. This has been confirmed for instance in the case of the present spin-1/2 chain at the isotropic point [17].

We have systematically used the present dynamical theory whose dynamical correlation functions expressions for the present model are given below to identify *all* branch lines containing sharp peaks in $S^{+-}(k, \omega)$, $S^{-+}(k, \omega)$, and $S^{zz}(k, \omega)$ for $\eta > 0$. One then finds that the corresponding (k, ω) -plane continua with a significant amount of spectral weight are those shown in Figs. 4,5,6,7,8,9. *All* (k, ω) -plane one-parametric lines of such sharp peaks emerge *only* in the two-parametric spectra, Eqs. (30)-(35), corresponding to such continua. Those refer to the classes of selected excited states that contribute to a significant amount of spectral weight. Note though that the aim of these figures is to provide the (k, ω) -plane location in the continua of the sharp peaks whose line shape is studied in the following, which refers to the marked lines in them. It is not to provide information on the relative intensities of the spectral-weight distribution over such continua.

Specifically, the found sharp peaks whose line shape is studied in the following are located in k intervals of the lower thresholds of the three $n = 1, 2, 3$ continua, one $n = 1$ continuum, and two $n = 1, 2$ continua. They are shown in Figs. 4,5 for $S^{+-}(k, \omega)$, Figs. 6,7 for $S^{-+}(k, \omega)$, and Figs. 8,9 for $S^{zz}(k, \omega)$, respectively. We denote by $\bar{\omega}_n^{ab}(k)$ where $n = 1, 2, 3$ for $ab = +- , n = 1$ for $ab = -+ ,$ and $n = 1, 2$ for $ab = zz$ the corresponding one-parametric spectra of the lower thresholds of the continua containing nearly the whole spectral weight in the components $S^{ab}(k, \omega)$. The corresponding two-parametric spectra $\omega_n^{ab}(k)$ associated with such continua are given for $m > 0$ in Eqs. (30)-(35).

The expressions of the $n = 1, 2, 3$ one-parametric spectra $\bar{\omega}_n^{+-}(k)$ are provided in Eqs. (D4), (D6)-(D9), and (D10)-(D13), respectively, of Appendix D. That of $\bar{\omega}_1^{-+}(k)$ is given in Eq. (D18) of that Appendix. The expressions of the $n = 1, 2$ spectra $\bar{\omega}_n^{zz}(k)$ are given in Eqs. (D22) and (D23)-(D26), respectively, of the same Appendix. (The

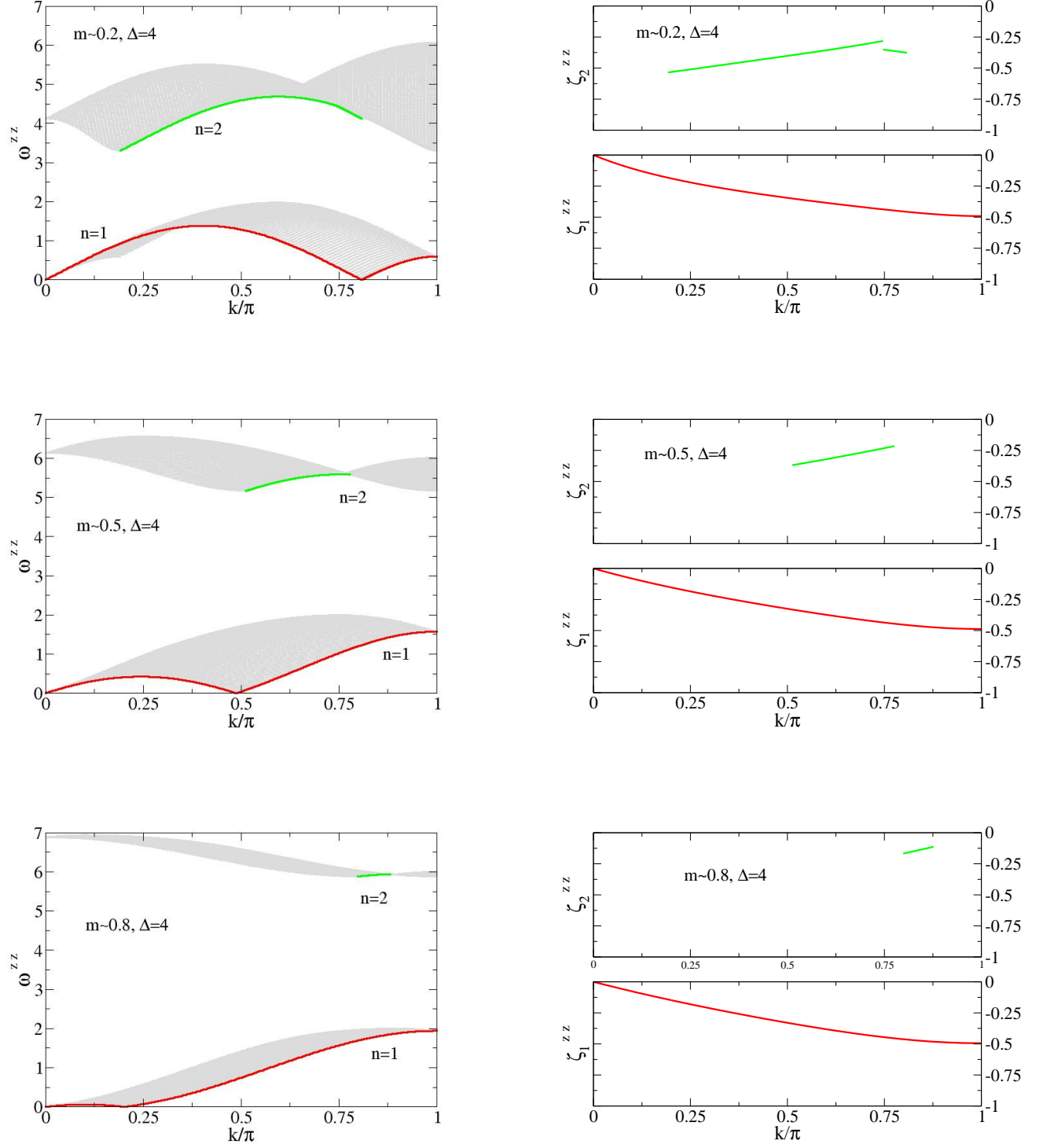


Figure 8: The (k, ω) -plane continua where there is more spectral weight in $S^{zz}(k, \omega)$ at $\Delta = 4$ for $m = 0.1920 \approx 0.2$, $m = 0.5125 \approx 0.5$, and $m = 0.7985 \approx 0.8$ (left) and the negative k dependent exponents that control the line shape $S^{zz}(k, \omega) \propto (\omega - \omega_n^{+-}(k))^{\zeta_n^{zz}(k)}$ in the k intervals near the lower thresholds of the $n = 1$ and $n = 2$ continua marked in the spectra (right.) In the k intervals of such exponents $S^{zz}(k, \omega)$ displays sharp peaks.

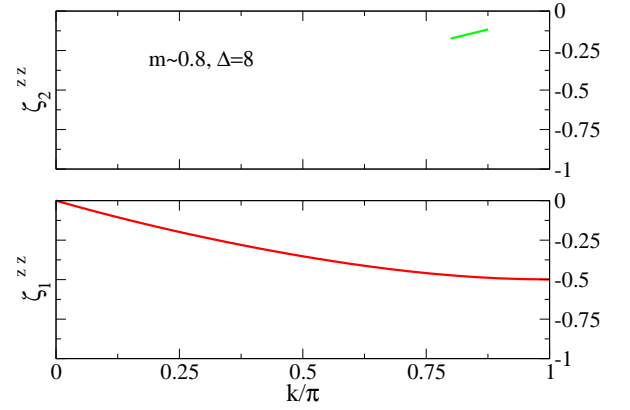
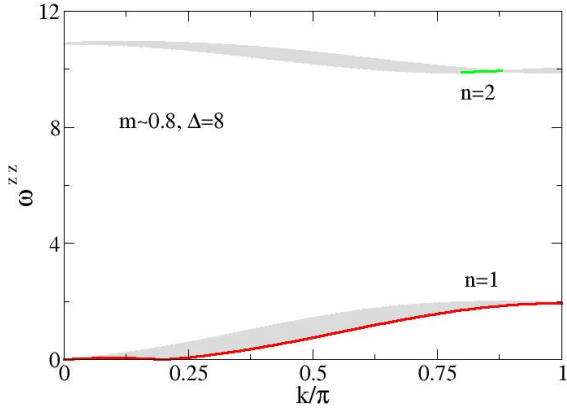
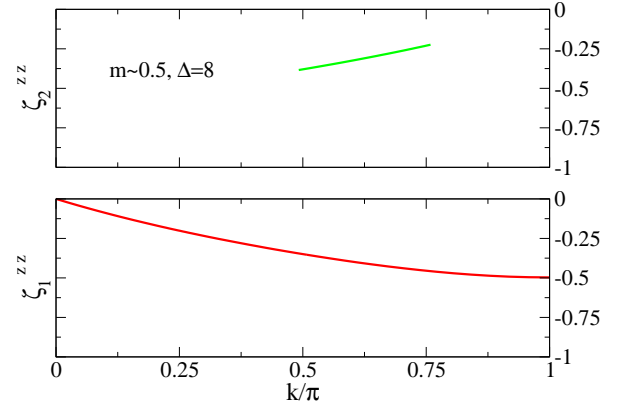
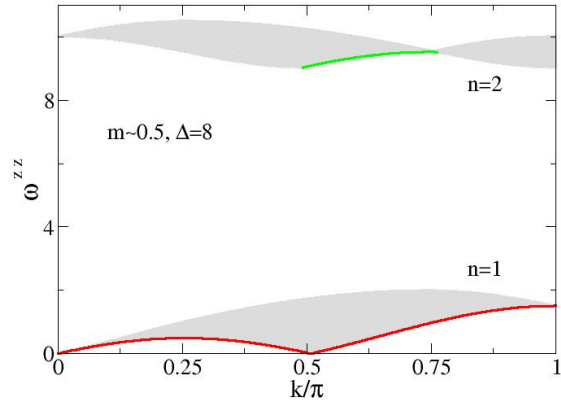
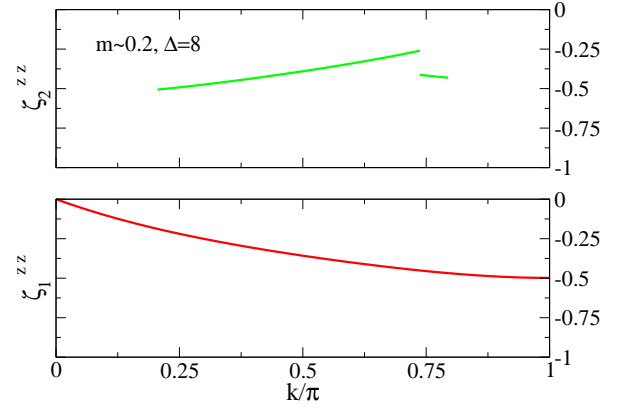
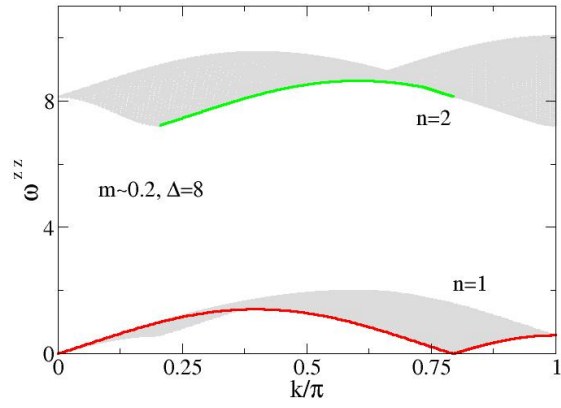


Figure 9: The same as in Fig. 8 for spin densities $m = 0.2056 \approx 0.2$, $m = 0.4918 \approx 0.5$, and $m = 0.7997 \approx 0.8$ and anisotropy $\Delta = 8$.

expressions provided in Eqs. (D27)-(D30) of Appendix D refer to $\bar{\omega}_3^{zz}(k)$ whose (k, ω) -plane $n = 3$ continuum does not contain sharp peaks and thus has no significant amount of spectral weight over it.)

As justified in Appendix C in terms of the matrix elements square $|\langle \nu | \hat{S}_k^a | GS \rangle|^2$ in Eq. (1), the line shape of the spin dynamical structure factor components $S^{ab}(k, \omega)$ where $ab = +-, -+, zz$ at and just above the (k, ω) -plane $n = 1, 2, 3$ continua lower thresholds k intervals under consideration at which there are sharp peaks has in the thermodynamic limit the following general power-law form,

$$S^{ab}(k, \omega) = C_{ab}^n(k) \left(\frac{\omega - \bar{\omega}_n^{ab}(k)}{4\pi B_1^{ab} v_1} \right)^{\zeta_n^{ab}(k)} \quad \text{for } (\omega - \bar{\omega}_n^{ab}(k)) \geq 0 \quad \text{where } ab = +-, -+, zz. \quad (42)$$

This expression is valid for small values of the energy deviation $(\omega - \bar{\omega}_n^{ab}(k)) > 0$ at fixed excitation momentum k . In it $v_1 = v_1(k_{F\downarrow})$ where $v_1(q)$ is the 1-band group velocity, Eq. (B25) of Appendix B for $n = 1$ and B_1^{ab} is a η and m dependent constant such that $0 < B_1^{ab} \leq 1$. The exponent in Eq. (42) has the following general expression,

$$\zeta_n^{ab}(k) = -1 + \sum_{\iota=\pm 1} \Phi_\iota^2(k), \quad (43)$$

where $\Phi_\iota(k)$ is the corresponding functional in Eq. (38) for $n = 1$ and in Eq. (40) for $n = 2, 3$ and the index $n = 1, 2, 3$ refers to one of the continua shown in Figs. 4,5,6,7,8,9. The multiplicative factor function $C_{ab}^n(k)$ in Eq. (42) also involves the functional $\Phi_\iota(k)$. It is found in Appendix C to have the following general form,

$$C_{ab}^n(k) = \frac{1}{|\zeta_n^{ab}(k)|} \prod_{\iota=\pm 1} \frac{e^{-f_0^{ab} + f_2^{ab}(2\Phi_\iota)^2 - f_4^{ab}(2\Phi_\iota)^4}}{\Gamma(\Phi_\iota^2(q))}. \quad (44)$$

As given in Eq. (C5) of Appendix C, here $\tilde{\Phi}_\iota = \Phi_\iota - \iota \delta N_{1,\iota}^F$ is the scattering part of the general functional, Eq. (37), *i. e.* $\tilde{\Phi}_\iota = -\frac{i}{2\pi} \ln S_1(\iota k_{F\downarrow})$. The $C_{ab}^n(k)$ expression also involves $1/|\zeta_n^{ab}(k)|$ and three η dependent constants $0 < f_l^{ab} < 1$ where $l = 0, 2, 4$. Both B_1^{ab} in Eq. (42) and these three constants stem from the general expression of the matrix elements square, Eq. (C6) of Appendix C. Their precise values and η dependences for each dynamical structure factor component are difficult to access.

As discussed in that Appendix, the $S^{ab}(k, \omega)$ expression, Eq. (42), is valid both for exponent values $-1 < \zeta_n^{ab}(k) < 0$ and $0 < \zeta_n^{ab}(k) < 1$, provided there is no spectral weight or very little such a weight below the corresponding branch line. Our study though focus on the case when $-1 < \zeta_n^{ab}(k) < 0$ whose corresponding power-law line shape refers to a sharp-peak singularity. However, the $S^{ab}(k, \omega)$ expression, Eq. (42), is not valid when $\zeta_n^{ab}(k) = 0$. Then the line shape near the sharp peak is rather logarithmic. Its corresponding general expression is provided in Eq. (C12) of Appendix C.

The one-parametric spectrum of a branch line that for small spin densities coincides with the $n = 1$ lower threshold of $S^{+-}(k, \omega)$ for $k \in [2k_{F\downarrow}, \pi]$ and for intermediate and large spin densities does not coincide with it, is marked in Figs. 4,5. We denote that one-parametric spectrum by $\tilde{\omega}_1^{+-}(k)$, which is given in Eq. (D5) of Appendix D. At and just above that branch line, the spin dynamical structure factor component $S^{+-}(k, \omega)$ also has for small deviations $(\omega - \tilde{\omega}_1^{+-}(k)) \geq 0$ the form,

$$S^{+-}(k, \omega) = \tilde{C}_{+-}^1(k) \left(\frac{\omega - \tilde{\omega}_1^{+-}(k)}{4\pi \tilde{B}_1^{+-} v_1} \right)^{\tilde{\zeta}_1^{+-}(k)}. \quad (45)$$

Its exponent expression is provided in Eq. (D17) of Appendix D. (The general expression of $\tilde{C}_{+-}^1(k)$ is similar to that of $C_{ab}^n(k)$ given in Eq. (44).) This line shape applies to k interval for which there is very little spectral weight below the branch line.

The relation of the excitation momentum k to the n -band momentum q in Eqs. (38) and (40) suitable to each $n = 1, 2, 3$ lower threshold k interval of the components $S^{ab}(k, \omega)$ as well as the corresponding specific values of the deviations δN_1^F and δJ_1^F in Eq. (39) were accounted for in the exponent expressions provided in Appendix D. The expressions of the exponents $\zeta_n^{+-}(k)$ for $n = 1, 2, 3$ are given in Eqs. (D14), (D15), (D16), respectively, of that Appendix. Those of the exponents $\zeta_n^{-+}(k)$ for $n = 1, 2, 3$ are provided in Eqs. (D19), (D20), (D21), respectively, of the same Appendix. Those of the exponents $\zeta_n^{zz}(k)$ for $n = 1, 2, 3$ are given in Eqs. (D31), (D32), (D33), respectively, of Appendix D.

All such exponents as well as other exponents associated with line shapes on (k, ω) -plane continua not shown in Figs. 4,5,6,7,8,9 have been used in our search of sharp peaks located in corresponding lower thresholds. However, in these figures *only* the exponents that are negative in some k interval are plotted. The corresponding lower thresholds

intervals are marked in the spectra shown in them. The k interval of the branch line associated with the line shape in Eq. (45) in which the corresponding exponent $\tilde{\zeta}_1^{+-}(k)$ is negative is also marked in the $n = 1$ continuum of Figs. 4,5.

Specifically, the three $n = 1, 2, 3$ exponents $\zeta_n^{+-}(k)$ are plotted in Figs. 4,5 as a function of k for the k intervals for which they are negative. The exponents $\zeta_2^{+-}(k)$ and $\zeta_3^{+-}(k)$ are positive and large for all their k intervals. Therefore, in Figs. 6,7 only the exponent $\zeta_1^{+-}(k)$ is plotted. This reveals that the corresponding $n = 2, 3$ continua have nearly no spectral weight and therefore are not shown in these figures. Also the exponent $\zeta_3^{zz}(k)$ is positive and large for its k interval. This reveals again that there is no significant amount of spectral weight in the corresponding $n = 3$ continuum of $S^{zz}(k, \omega)$ that is not shown in Figs. 8,9. The exponents $\zeta_1^{zz}(k)$ and $\zeta_2^{zz}(k)$ are plotted in these figures.

In the k intervals of Figs. 4,5,6,7,8,9 for which the momentum dependent exponents are negative there are power-law sharp peaks of form, Eq. (42), in the corresponding component $S^{ab}(k, \omega)$. Such sharp peaks are located at and just above the lower thresholds of the (k, ω) -plane three $n = 1, 2, 3$ continua for $ab = +- , n = 1$ continuum for $ab = -+ ,$ and two $n = 1, 2$ continua for $ab = zz$. The sharp peaks, Eq. (45), are located in the branch line that does not coincide with the lower threshold of the $n = 1$ continuum of $S^{+-}(k, \omega)$ for intermediate and large m values.

Inspection of the spectra and exponents plotted in Figs. 4,5,6,7,8,9, reveals that the effects of increasing anisotropy from $\Delta = 4$ to $\Delta = 8$ are in the cases of $S^{+-}(k, \omega)$ and $S^{zz}(k, \omega)$ a decrease of the continua energy bandwidths and an increase of the energies of the $n = 2$ and $n = 3$ continua. The k dependent exponent values do not show significant variations upon increasing Δ from $\Delta = 4$ to $\Delta = 8$. In the case of $S^{+-}(k, \omega)$, that Δ 's increase has nearly no effect on the corresponding $n = 1$ continuum energy bandwidth.

At the isotropic point, $\Delta = 1$, there are no sharp peaks in the gapped lower threshold of the $S^{+-}(k, \omega)$'s $n = 3$ continuum [17]. This indicates that the presence of anisotropy tends to increase the spectral weight of that gapped $n = 3$ continuum associated with excited states populated by one 3-string particle.

The dynamical structure factor expression, Eq. (42), is exact at and just above the lower thresholds of the (k, ω) -plane $n = 1$ continua shown in Figs. 4,5,6,7,8,9 under which there is no spectral weight. There is no or a negligible amount of spectral weight just below the gapped lower thresholds of the (k, ω) -plane $n = 2$ continua in Figs. 4,5,8,9 and $n = 3$ continua in Figs. 4,5. This ensures that the line shape behavior in Eq. (42) is an excellent approximation for excitation energies at and just above such gapped lower thresholds in their k intervals for which $\zeta_n^{ab}(k) < 0$.

In (k, ω) -plane $n = 2, 3$ continua gapped lower thresholds k intervals for which there is a negligible amount of spectral weight just below them, the weak coupling to that weight leads to very small higher order contributions to the expression of the exponent $\zeta_n^{ab}(k)$, Eqs. (43), that can be neglected in the present thermodynamic limit.

VI. CONCLUDING REMARKS

One of the aims of this paper is the clarification of the nature in terms of physical spins 1/2 configurations of scientifically important and interesting elementary magnetic configurations. We have exactly shown that such elementary magnetic configurations, that can occur either unbound and described by $n = 1$ real single Bethe rapidities or bound and described by $n > 1$ n -strings, are singlet $S^z = S_q = 0$ pairs of physical spins 1/2. For the present $\eta > 0$ spin-1/2 XXZ chain in a longitudinal magnetic field, spin S is *not* a good quantum number, so that such physical spins pairs are labelled by q -spin S_q .

A direct consequence of the neutral q -spin nature of such $S^z = S_q = 0$ pairs of physical spins 1/2 is that the corresponding $2\Pi = N - 2S_q = \sum_{n=1}^{\infty} 2n N_n$ paired physical spins 1/2 of an energy eigenstate do not couple to a vector potential and thus do not carry spin current [38]. Only the $M = 2S_q$ unpaired physical spins 1/2 of that state carry such a current. This property can be confirmed by adding a uniform vector potential [39] to the Hamiltonian, Eq. (3), which remains solvable by the Bethe ansatz [40, 41]. It has direct consequences for the spin transport properties of the spin-1/2 XXZ chain [42–44].

The form of the one-dimensional scalar S matrices, Eqs. (36) and (37), associated with the scattering of n -particles is another consequence of the singlet $S^z = S_q = 0$ nature of these pairs in terms of physical spins 1/2 configurations. This is an important result, since such scattering controls the power-law line shape near the sharp peaks in the spin dynamical structure factor components.

We have used a dynamical theory that relies on such S matrices to derive analytical expressions valid in the thermodynamic limit for the power-law line shape of $S^{+-}(k, \omega)$, $S^{-+}(k, \omega)$, and $S^{zz}(k, \omega)$ in the vicinity of sharp peaks. Those are located in specific (k, ω) -plane momentum k intervals. Our results refer to anisotropies $\Delta > 1$. For magnetic fields in the interval $h \in [h_{c1}, h_{c2}]$, the main difference relative to the $\Delta = 1$ isotropic point [17], is that for $\Delta > 1$ excited states containing one 3-string-particle lead to a significant yet small amount of spectral weight in $S^{+-}(k, \omega)$.

The quantum problem studied in this paper is scientifically interesting in its own right. On the other hand, the elementary magnetic configurations and corresponding n -strings studied in it have been recently realized and identified in the spin chains of $\text{SrCo}_2\text{V}_2\text{O}_8$ [45, 46] and $\text{BaCo}_2\text{V}_2\text{O}_8$ [47] by experiments. Our general theoretical results refer

to lines of sharp peaks located in k intervals much beyond the few momentum values $k = 0$, $k = \pi/2$, and $k = \pi$ of the sharp modes that could be experimentally observed [45–47].

There is a unjustified belief that for the isotropic case the elementary magnetic configurations studied in this paper are spin-1 magnons [25, 26]. This though contradicts exact results that show they rather being singlet $S^z = S = 0$ pairs of physical spins 1/2 [19, 20]. Such a misleading interpretation was likely imported from the isotropic $\Delta = 1$ case by the authors of Refs. 45–47. For $\Delta > 1$ they have identified the $n > 1$ elementary magnetic configurations bound within Bethe n -strings with spin-1 magnons. Our result that they are singlet $S^z = S_q = 0$ pairs of physical spins 1/2 corrects that interpretation, which otherwise has not affected the validity of the results of Refs. 45–47.

There is full qualitative consistency and agreement between finite-size results for $\Delta = 2$ relying on the algebraic Bethe ansatz formalism [16] and those for the $\Delta = 4$ and $\Delta = 8$ anisotropy values used in the present study of the present dynamical theory, which refers to the thermodynamic limit. This concerns both the form of the energy spectra and corresponding dynamical correlation functions line shapes. As confirmed elsewhere [38], such a full consistency and agreement becomes quantitative under the use of the present dynamical theory at anisotropy $\Delta = 2$.

The general expressions of the dynamical structure factor components obtained in this paper will also be used to show that all the experimentally observed sharp peaks are particular cases of those considered in the present study [38]. This will include extracting from the line shape of general form, Eq. (42), the h dependencies in the thermodynamic limit of the energies of the experimentally observed sharp peaks, to be compared with those observed in the spin chains of $\text{SrCo}_2\text{V}_2\text{O}_8$ [45, 46]. This study will be extended to the spin chains of $\text{BaCo}_2\text{V}_2\text{O}_8$ [47] in a future publication [48]. Also the consequences to the physics of such spin chains of the found q -spin neutral nature of the elementary magnetic configurations under study in this paper will be addressed [38, 48].

CRediT authorship contribution statement

The two authors contributed equally to the formulation of the research goals and aims and to the discussion and physical interpretation of the results. J. M. P. C. extended to anisotropy larger than one results for the isotropic point concerning both the nature in terms of physical spins 1/2 of important elementary magnetic configurations and a suitable dynamical theory and prepared the original manuscript. P. D. S. has designed the computer programs to solve the integral equations that define the phase shifts and spectra of that theory and implemented them.

Declaration of competing interest

The authors declare that they have no known competing financial interests or personal relationships that could have appeared to influence the work reported in this paper.

Acknowledgments

We thank Tomaž Prosen and David K. Campbell for fruitful discussions with the authors and Tilen Čadež for useful remarks. J. M. P. C. would like to thank the Boston University's Condensed Matter Theory Visitors Program for support and Boston University for hospitality during the initial period of this research. He acknowledges the support from FCT through the Grants Grant UID/FIS/04650/2013, PTDC/FIS-MAC/29291/2017, and SFRH/BSAB/142925/2018. P. D. S. acknowledges the support from FCT through the Grant UID/CTM/04540/2019.

Appendix A: Confirmation of the η independence of the quantum numbers represented by l_r in $|l_r, S_q, S^z, \eta\rangle$

In order to relate to the notations used in Ref. 10 for Bethe-ansatz quantities of the isotropic model ($\eta = 0$), the real part of the rapidities $\varphi_{n,i}$ of Ref. 11 is replaced in this Appendix by the following related quantity,

$$\Lambda_j^n = -\frac{\varphi_{n,j}}{\eta} \in \left[-\frac{\pi}{\eta}, \frac{\pi}{\eta}\right] \quad \text{where} \quad n = 1, \dots, \infty \quad \text{and} \quad j = 1, \dots, L_n. \quad (\text{A1})$$

In the notation $|l_r, S_q, S^z, \eta\rangle$ used in this paper for the 2^N energy eigenstates, Eq. (16), all quantum numbers other than S_q , S^z , and η needed to specify such a state are represented by l_r . For each of the n -bands of a given energy eigenstate for which $N_n > 0$, this refers to one of the $\binom{L_n}{N_n}$ independent occupancy configurations of the N_n n -particles over the $j = 1, \dots, L_n$ available discrete quantum number values. Such quantum numbers I_j^n refer to the

n -band momentum values $q_j = \frac{2\pi}{L} I_j^n$ in units of $\frac{2\pi}{L}$. They are given by,

$$\begin{aligned} q_j &= \frac{2\pi}{L} I_j^n \quad \text{for } j = 1, \dots, L_n \quad \text{where} \\ I_j^n &= 0, \pm 1, \dots, I_\pm^n \quad \text{for } L_n \text{ odd} \\ &= \pm 1/2, \pm 3/2, \dots, I_\pm^n \quad \text{for } L_n \text{ even}. \end{aligned} \quad (\text{A2})$$

These quantum numbers are such that $I_j^{n+1} - I_j^n = 1$ and only admit Pauli-like occupancies one or zero.

Our goal is to show that the $n = 1, 2, \dots, \infty$ numbers L_n are independent of η . This implies that the values of the quantum numbers represented by l_r in $|l_r, S_q, S^z, \eta\rangle = \hat{U}_\eta^+ |l_r, S = S_\eta, S^z, 0\rangle$ indeed are also independent of η and thus remain invariant under the unitary operators \hat{U}_η^+ , as S_q and S^z do. The numbers L_n were called ν_m with $m = n = 1, \dots, \infty$ in Ref. 11, yet they were not derived previously for $\eta > 0$.

In the thermodynamic limit, Λ_j^n is the real part of the Bethe-ansatz complex rapidity given in Eq. (4). The set of Bethe-ansatz equations considered in Ref. 11 can be written in functional form as,

$$2 \arctan \left(\coth \left(\frac{n\eta}{2} \right) \tan \left(\frac{\eta \Lambda^n(q_j)}{2} \right) \right) = q_j + \frac{1}{L} \sum_{(n', j') \neq (n, j)} N_{n'}(q_{j'}) \Theta_{nn'}^\eta (\Lambda^n(q_j) - \Lambda^{n'}(q_{j'})), \quad (\text{A3})$$

where $n = 1, \dots, \infty$. Here the summations refer to $\sum_{n'=1}^\infty \sum_{j'=1}^{L_{n'}}$ with the restriction $(n', j') \neq (n, j)$ and the energy eigenstates distributions $N_n(q_j)$ read $N_n(q_j) = 0$ and $N_n(q_j) = 1$ for unoccupied and occupied discrete momentum values q_j , respectively. Those are given by in Eq. (A2). Their occupancy configurations generate the energy eigenstates described by the Bethe-ansatz solution. Such states refer to fixed values for the set of numbers $\{N_n\}$ of occupied q_j values in each n band. The distributions $N_n(q_j)$ then obey the sum rule,

$$\sum_{j=1}^{L_n} N_n(q_j) = N_n \quad \text{for } n = 1, \dots, \infty. \quad (\text{A4})$$

Moreover, the function $\Theta_{nn'}^\eta(x)$ in Eq. (A3) is given by,

$$\begin{aligned} \Theta_{nn'}^\eta(x) &= \delta_{n,n'} \left\{ 2 \arctan \left(\coth(n\eta) \tan \left(\frac{\eta x}{2} \right) \right) + \sum_{l=1}^{n-1} 4 \arctan \left(\coth(l\eta) \tan \left(\frac{\eta x}{2} \right) \right) \right\} \\ &+ (1 - \delta_{n,n'}) \left\{ 2 \arctan \left(\coth \left(\frac{(n+n')\eta}{2} \right) \tan \left(\frac{\eta x}{2} \right) \right) + 2 \arctan \left(\coth \left(\frac{(|n-n'|\eta)}{2} \right) \tan \left(\frac{\eta x}{2} \right) \right) \right. \\ &\left. + \sum_{l=1}^{\frac{n+n'-|n-n'|}{2}-1} 4 \arctan \left(\coth \left(\frac{(|n-n'|+2l)\eta}{2} \right) \tan \left(\frac{\eta x}{2} \right) \right) \right\}, \end{aligned} \quad (\text{A5})$$

where $n, n' = 1, \dots, \infty$ and $\delta_{n,n'}$ is the Kronecker symbol.

As given in Eq. (A1), $\Lambda_j^n \in \left[-\frac{\pi}{\eta}, \frac{\pi}{\eta} \right]$, so that the number L_n is derived here by finding, by means of the Bethe-ansatz equations, Eq. (A3), the two limiting momentum values $q_j = \frac{2\pi}{L} I_\pm^n = q_n^\pm$ that correspond to $\Lambda_j^n = \pm \frac{\pi}{\eta}$. The numbers L_n are then given by,

$$L_n = \frac{(q_n^+ - q_n^-)}{(2\pi/L)} + 1 \quad \text{for } n = 1, \dots, \infty. \quad (\text{A6})$$

One then finds,

$$q_n^\pm = \frac{\pi}{L} \left\{ \pm N - \frac{1}{\pi} \sum_{(n', j') \neq (n, j)} N_{n'}(q_{j'}) \Theta_{nn'}^\eta \left(\pm \frac{\pi}{2} - \Lambda^{n'}(q_{j'}) \right) \right\}. \quad (\text{A7})$$

After some algebra, one achieves the following general expression,

$$q_n^\pm = \pm \frac{\pi}{L} \left\{ L_n - 1 \mp \delta L_n^\eta \right\}, \quad (\text{A8})$$

where L_n and δL_n^η are given in Eqs. (5) and (12), respectively.

While L_n is independent of η , the term δL_n^η depends on that parameter, its limiting values being,

$$\begin{aligned}\delta L_n^\eta &= n\eta \sum_{n'=1}^{\infty} \sum_{j=1}^{L_{n'}} n' N_{n'}(q_j) \left(\frac{\eta \Lambda^{n'}(q_j)}{\pi} \right) \quad \text{for } \eta \ll 1 \\ \delta L_n^\eta &= \sum_{n'=1}^{\infty} \sum_{j=1}^{L_{n'}} N_{n'}(q_j) (n + n' - |n - n'| - \delta_{n',n}) \left(\frac{\eta \Lambda^{n'}(q_j)}{\pi} \right) \quad \text{for } \eta \gg 1,\end{aligned}\tag{A9}$$

where we recall that $\frac{\eta \Lambda^{n'}(q_j)}{\pi} \in [-1, 1]$ for all $\eta \geq 0$.

From the use of the first limiting expression in Eq. (A9), one finds that $\delta L_n^\eta = 0$ at $\eta = 0$, consistently with the Bethe-ansatz solution at the isotropic point [10]. For $\eta > 0$, the numbers δL_n^η vanish when all distributions $N_n(q_j)$ are symmetrical, $N_n(q_j) = N_n(-q_j)$. Such numbers are typically of order $1/L$ for excited energy eigenstates contributing to the dynamical properties studied in this paper.

Appendix B: Ground-state rapidity functions and energy dispersions for the excited states

1. Ground-state rapidity functions and energy dispersions for the excited states at general m values

Here we use the rapidity-function notation $\varphi_{n,j} = \varphi_n(q_j)$, whose relation to the notation suitable to the isotropic case, $\Lambda_j^n = \Lambda^n(q_j)$, is given in Eq. (A1) of Appendix A. For $n = 1$ and $n > 1$ the rapidity function $\varphi_n(q_j)$ is real and the real part of a complex rapidity, respectively.

Three types of excited energy eigenstates span the subspaces associated with the spectra whose $n = 1, 2, 3$ continua, respectively, are shown in Figs. 4,5,6,7,8,9. The $n = 1$ continua stem from excited energy eigenstates with $N_n = 0$ for $n > 1$. They have 1-band numbers $N_1 = N_{F\downarrow}$, $N_1^h = N_{F\uparrow} - N_{F\downarrow}$, and $L_1 = N_1 + N_1^h = N_{F\uparrow}$. Excited energy eigenstates with $N_n = 1$ for a single $n > 1$ n -band are associated with the $n = 2$ and $n = 3$ continua in Figs. 4,5,8,9. Such excited states have numbers $N_1 = N_{F\downarrow} - n$, $N_1^h = N_{F\uparrow} - N_{F\downarrow} + 2(n - 1)$, $L_1 = N_1 + N_1^h = N_{F\uparrow} + n - 2$, $N_n = 1$, $N_n^h = N_{F\uparrow} - N_{F\downarrow}$, and $L_n = N_n + N_n^h = N_{F\uparrow} - N_{F\downarrow} + 1$. In all these expressions, either $n = 2$ or $n = 3$.

As discussed in Sec. II A, in the thermodynamic limit one may use continuous momentum variables q that replace the discrete n -band momentum values q_j . The corresponding n -band intervals then read $q \in [-k_{F\uparrow}, k_{F\uparrow}]$ for the 1-band and $q \in [-(k_{F\uparrow} - k_{F\downarrow}), (k_{F\uparrow} - k_{F\downarrow})]$ for the $n = 2$ and $n = 3$ n -bands. Here $q = \pm k_{F\uparrow}$ and $q = \pm(k_{F\uparrow} - k_{F\downarrow})$ play the role of 1-band and n -band zone limits, respectively.

The ground-state $n = 1$ rapidity distribution function $\varphi_1(q)$ where $q \in [-k_{F\uparrow}, k_{F\uparrow}]$ can be defined in terms of its 1-band inverse function $q = q_1(\varphi)$ where $\varphi \in [-\pi, \pi]$. From the use of the Bethe-ansatz equation, Eq. (A3) of Appendix A for $n = 1$ with $\Lambda_j^1 = \Lambda^1(q_j) = -\varphi_1(q_j)/\eta$, one finds that for the ground state $q = q_1(\varphi)$ is defined by the equation,

$$q_1(\varphi) = 2 \arctan \left(\coth \left(\frac{\eta}{2} \right) \tan \left(\frac{\varphi}{2} \right) \right) - \frac{1}{\pi} \int_{-B}^B d\varphi' 2\pi\sigma_1(\varphi') \arctan \left(\coth(\eta) \tan \left(\frac{\varphi - \varphi'}{2} \right) \right) \quad \text{for } \varphi \in [-\pi, \pi].\tag{B1}$$

Here the parameter B and distribution $2\pi\sigma_1(\varphi)$ are defined below.

The ground-state $n > 1$ rapidity function $\varphi_n(q)$ where $q \in [-(k_{F\uparrow} - k_{F\downarrow}), (k_{F\uparrow} - k_{F\downarrow})]$ is also defined in terms of its n -band inverse function $q = q_n(\varphi)$ where $\varphi \in [-\pi, \pi]$. From the use of the Bethe-ansatz equations, Eq. (A3) of Appendix A for $n > 1$ with $\Lambda_j^n = \Lambda^n(q_j) = -\varphi_n(q_j)/\eta$, one finds that for the ground state $q_n(\varphi)$ is defined by the following equation,

$$\begin{aligned}q_n(\varphi) &= 2 \arctan \left(\coth \left(\frac{n\eta}{2} \right) \tan \left(\frac{\varphi}{2} \right) \right) \\ &- \frac{1}{\pi} \sum_{\iota=\pm 1} \int_{-B}^B d\varphi' 2\pi\sigma_1(\varphi') \arctan \left(\coth \left(\frac{(n+\iota)\eta}{2} \right) \tan \left(\frac{\varphi - \varphi'}{2} \right) \right) \quad \text{for } \varphi \in [-\pi, \pi],\end{aligned}\tag{B2}$$

where $n > 1$.

The parameter B appearing in the above equations is such that,

$$B = \varphi_1(k_{F\downarrow}) \quad \text{with} \quad \lim_{m \rightarrow 0} B = \pi \quad \text{and} \quad \lim_{m \rightarrow 1} B = 0.\tag{B3}$$

By considering that $\varphi = B$ in Eq. (B1), one finds that B can be defined by the equation,

$$k_{F\downarrow} = 2 \arctan \left(\coth \left(\frac{\eta}{2} \right) \tan \left(\frac{B}{2} \right) \right) - \frac{1}{\pi} \int_{-B}^B d\varphi' 2\pi\sigma_1(\varphi') \arctan \left(\coth(\eta) \tan \left(\frac{B - \varphi'}{2} \right) \right). \quad (\text{B4})$$

The distribution,

$$2\pi\sigma_1(\varphi) = \frac{\partial q_1(\varphi)}{\partial \varphi}, \quad (\text{B5})$$

also appearing in the above equations is the solution of the following integral equation,

$$2\pi\sigma_1(\varphi) = \frac{\sinh(\eta)}{\cosh(\eta) - \cos(\varphi)} + \int_{-B}^B d\varphi' G_1(\varphi - \varphi') 2\pi\sigma_1(\varphi'). \quad (\text{B6})$$

The kernel $G_1(\varphi)$ in this equation is given by,

$$G_1(\varphi) = -\frac{1}{2\pi} \frac{\sinh(2\eta)}{\cosh(2\eta) - \cos(\varphi)}. \quad (\text{B7})$$

The distribution $2\pi\sigma_1(\varphi)$ obeys the sum rule,

$$\int_{-B}^B d\varphi 2\pi\sigma_1(\varphi) = \int_{-B}^B d\varphi \frac{\partial q_1(\varphi)}{\partial \varphi} = 2k_{F\downarrow}. \quad (\text{B8})$$

The corresponding $n > 1$ distribution $2\pi\sigma_n(\varphi) = \partial q_n(\varphi)/\partial \varphi$ is given by,

$$2\pi\sigma_n(\varphi) = \frac{\partial q_n(\varphi)}{\partial \varphi} = \frac{\sinh(n\eta)}{\cosh(n\eta) - \cos(\varphi)} + \int_{-B}^B d\varphi' G_n(\varphi - \varphi') 2\pi\sigma_1(\varphi'), \quad (\text{B9})$$

where the $n > 1$ function $G_n(\varphi)$ reads,

$$G_n(\varphi) = -\frac{1}{2\pi} \sum_{\iota=\pm 1} \frac{\sinh((n+\iota)\eta)}{\cosh((n+\iota)\eta) - \cos(\varphi)}. \quad (\text{B10})$$

The $n > 1$ distribution $2\pi\sigma_n(\varphi)$ obeys the sum rule,

$$\int_{-\pi}^{\pi} d\varphi 2\pi\sigma_n(\varphi) = \int_{-\pi}^{\pi} d\varphi \frac{\partial q_n(\varphi)}{\partial \varphi} = 2(k_{F\uparrow} - k_{F\downarrow}). \quad (\text{B11})$$

The limiting values of the ground-state rapidity functions $\varphi_1(q)$ and $\varphi_n(q)$ for $n > 1$ are,

$$\begin{aligned} \varphi_1(0) &= 0; \quad \varphi_1(\pm k_{F\downarrow}) = \pm B \quad \text{and} \quad \varphi_1(\pm k_{F\uparrow}) = \pm \pi \\ \varphi_n(0) &= 0 \quad \text{and} \quad \varphi_n(\pm(k_{F\uparrow} - k_{F\downarrow})) = \pm \pi. \end{aligned} \quad (\text{B12})$$

The 1-particle energy dispersion $\varepsilon_1(q)$ plotted in Fig. 1 and the $n > 1$ n -string-particle energy dispersions $\varepsilon_n(q)$ plotted in Figs. 2 and 3 for $n = 2$ and $n = 3$, respectively, that appear in the excited states spectra of the dynamical structure factor components play an important role in the studies of this paper. The energy dispersion $\varepsilon_1(q)$ is defined as follows,

$$\begin{aligned} \varepsilon_1(q) &= \bar{\varepsilon}_1(\varphi_1(q)) \quad \text{for} \quad q \in [-k_{F\uparrow}, k_{F\uparrow}] \quad \text{where} \\ \bar{\varepsilon}_1(\varphi) &= \bar{\varepsilon}_1^0(\varphi) + \frac{1}{2} g\mu_B h \quad \text{for} \quad h \in [0, h_{c1}] \\ &= \bar{\varepsilon}_1^0(\varphi) - \bar{\varepsilon}_1^0(B) \quad \text{for} \quad h \in [h_{c1}, h_{c2}], \end{aligned} \quad (\text{B13})$$

and

$$\bar{\varepsilon}_1^0(\varphi) = -J \frac{\sinh^2(\eta)}{\cosh(\eta) - \cos(\varphi)} - \frac{1}{\pi} \int_{-B}^B d\varphi' 2J\gamma_1(\varphi') \arctan \left(\coth(\eta) \tan \left(\frac{\varphi - \varphi'}{2} \right) \right). \quad (\text{B14})$$

Here $\varphi \in [-\pi, \pi]$ and the distribution $2J\gamma_1(\varphi)$ is defined below. The expression of the magnetic field h and those of the critical magnetic fields h_{c1} and h_{c2} associated with quantum phase transitions appearing in Eq. (B13) are given in Eqs. (9) and (10), respectively.

The energy dispersions $\varepsilon_n(q)$ are for $n > 1$ defined as follows,

$$\begin{aligned}\varepsilon_n(q) &= \bar{\varepsilon}_n(\varphi_n(q)) \quad \text{for } q \in [-(k_{F\uparrow} - k_{F\downarrow}), (k_{F\uparrow} - k_{F\downarrow})] \quad \text{where} \\ \bar{\varepsilon}_n(\varphi) &= \bar{\varepsilon}_n^0(\varphi) + (n-1)g\mu_B h \quad \text{for } h \in [0, h_{c1}] \\ \bar{\varepsilon}_n(\varphi) &= \bar{\varepsilon}_n^0(\varphi) - n\bar{\varepsilon}_1^0(B) \quad \text{for } h \in [h_{c1}, h_{c2}],\end{aligned}\tag{B15}$$

and

$$\begin{aligned}\bar{\varepsilon}_n^0(\varphi) &= -\frac{J}{n} \left(\frac{\sinh^2(n\eta)}{\cosh(n\eta) - \cos(\varphi)} - C_n(\eta) \right) \\ &- \frac{1}{\pi} \sum_{\iota=\pm 1} \int_{-B}^B d\varphi' 2J\gamma_1(\varphi') \arctan \left(\coth \left(\frac{(n+\iota)\eta}{2} \right) \tan \left(\frac{\varphi - \varphi'}{2} \right) \right).\end{aligned}\tag{B16}$$

Here $\varphi \in [-\pi, \pi]$, the constant $C_n(\eta)$ is given in Eq. (8), and the distribution $2J\gamma_1(\varphi)$ is defined below.

The energy dispersions $\varepsilon_1(q)$ and $\varepsilon_n(q)$ for $n > 1$ that appear in the expressions of the physical excited energy eigenstates spectra and the corresponding rapidity energy dispersions $\bar{\varepsilon}_1(\varphi)$ and $\bar{\varepsilon}_n(\varphi)$, respectively, are continuous functions of the magnetic field h for the whole range $h \in [0, h_{c2}]$. The auxiliary energy dispersions though have the following discontinuities at $h = h_{c1}$,

$$\begin{aligned}\lim_{m \rightarrow 0} \varepsilon_1^0(q) &= \varepsilon_1^0(q)|_{m=0, h=h_{c1}} - \frac{1}{2} g\mu_B h_{c1} \\ \lim_{m \rightarrow 0} \bar{\varepsilon}_1^0(\varphi) &= \bar{\varepsilon}_1^0(\varphi)|_{m=0, h=h_{c1}} - \frac{1}{2} g\mu_B h_{c1} \\ \lim_{m \rightarrow 0} \varepsilon_n^0(q) &= \varepsilon_n^0(q)|_{m=0, h=h_{c1}} - g\mu_B h_{c1} \\ \lim_{m \rightarrow 0} \bar{\varepsilon}_n^0(\varphi) &= \bar{\varepsilon}_n^0(\varphi)|_{m=0, h=h_{c1}} - g\mu_B h_{c1},\end{aligned}\tag{B17}$$

where $n > 1$.

The energy dispersions $\bar{\varepsilon}_n^0(\varphi)$ defined by Eqs. (B13) and (B14) for $n = 1$ and in Eqs. (B15) and (B16) for $n > 1$ can for $n \geq 1$ be expressed as,

$$\begin{aligned}\bar{\varepsilon}_n^0(\varphi) &= \int_0^\varphi d\varphi' 2J\gamma_n(\varphi') + A_n^0 \quad \text{where} \\ A_1^0 &= -J(1 + \cosh(\eta)) + \frac{1}{\pi} \int_{-B}^B d\varphi' 2J\gamma_1(\varphi') \arctan \left(\coth(\eta) \tan \left(\frac{\varphi'}{2} \right) \right) \\ A_n^0 &= -J \frac{\sinh(\eta)}{\sinh(n\eta)} (1 + \cosh(n\eta)) \\ &+ \frac{1}{\pi} \sum_{\iota=\pm 1} \int_{-B}^B d\varphi' 2J\gamma_1(\varphi') \arctan \left(\coth \left(\frac{(n+\iota)\eta}{2} \right) \tan \left(\frac{\varphi'}{2} \right) \right) \quad \text{for } n > 1.\end{aligned}\tag{B18}$$

One has that,

$$\frac{\partial \bar{\varepsilon}_n^0(\varphi)}{\partial \varphi} = 2J\gamma_n(\varphi) \quad \text{for } n \geq 1,\tag{B19}$$

where the distribution $2J\gamma_n(\varphi)$ obeys the following equation,

$$2J\gamma_n(\varphi) = \frac{J}{n} \frac{\sinh^2(n\eta) \sin(\varphi)}{(\cosh(n\eta) - \cos(\varphi))^2} + \int_{-B}^B d\varphi' G_n(\varphi - \varphi') 2J\gamma_1(\varphi').\tag{B20}$$

Here $G_n(\varphi - \varphi')$ is given in Eqs. (B7) and (B10) for $n = 1$ and $n > 1$, respectively. For $n = 1$, Eq. (B20) is the integral equation,

$$2J\gamma_1(\varphi) = J \frac{\sinh^2(\eta) \sin(\varphi)}{(\cosh(\eta) - \cos(\varphi))^2} + \int_{-B}^B d\varphi' G_1(\varphi - \varphi') 2J\gamma_1(\varphi'),\tag{B21}$$

whose solution is the distribution $2J\gamma_1(\varphi)$ that appears in Eqs. (B13), (B15), and (B20).

The following equalities apply,

$$\begin{aligned}\varepsilon_1(0) &= \bar{\varepsilon}_1(0); & \varepsilon_1(k_{F\downarrow}) &= \bar{\varepsilon}_1(B) = 0; & \varepsilon_1(k_{F\uparrow}) &= \bar{\varepsilon}_1(\pi) \\ \varepsilon_n(0) &= \bar{\varepsilon}_n(0); & \varepsilon_n(k_{F\uparrow} - k_{F\downarrow}) &= \bar{\varepsilon}_n(\pi) & \text{for } n > 1.\end{aligned}\quad (\text{B22})$$

The n -band energy bandwidths read,

$$\begin{aligned}W_1 &= W_1^p + W_1^h \quad \text{where} \\ W_1^p &= \varepsilon_1(k_{F\downarrow}) - \varepsilon_1(0) = \bar{\varepsilon}_1(B) - \bar{\varepsilon}_1(0) \quad \text{and} \\ W_1^h &= \varepsilon_1(k_{F\uparrow}) - \varepsilon_1(k_{F\downarrow}) = \bar{\varepsilon}_1(\pi) - \bar{\varepsilon}_1(B),\end{aligned}\quad (\text{B23})$$

for $n = 1$ and,

$$W_n = W_n^h = \varepsilon_n(k_{F\uparrow} - k_{F\downarrow}) - \varepsilon_n(0) = \bar{\varepsilon}_n(\pi) - \bar{\varepsilon}_n(0), \quad (\text{B24})$$

for $n > 1$.

The n -particles n -band group velocities are given by,

$$v_n(q) = \frac{\partial \varepsilon_n(q)}{\partial q} \quad \text{for } n \geq 1, \quad (\text{B25})$$

where $\varepsilon_n(q)$ are the $n = 1$ and $n > 1$ energy dispersions defined by Eqs. (B13)-(B14) and (B15)-(B16), respectively.

2. Ground-state rapidity functions and energy dispersions for the excited states at $m = 0$

An important case is that of vanishing spin density, $m = 0$, at which $B = \pi$ and the present model is a gapped spin insulator for magnetic fields $0 \leq h < h_{c1}$. The combined use of Fourier series and the convolution theorem permits the derivation of closed-form expressions for several quantities. The expressions in Eqs. (B1) and (B2) are then found to read,

$$\begin{aligned}q_1(\varphi) &= \frac{\varphi}{2} + \sum_{l=1}^{\infty} \frac{1}{l} \frac{\sin(l\varphi)}{\cosh(l\eta)} \quad \text{for } \varphi \in [-\pi, \pi] \\ q_n(\varphi) &= 0 \quad \text{for } n > 1 \quad \text{and } \varphi \in [-\pi, \pi].\end{aligned}\quad (\text{B26})$$

After performing the infinite summation, the function $q_1(\varphi)$ is defined in terms of its inverse function, the rapidity function $\varphi_1(q)$, as follows,

$$\varphi_1(q) = \pi \frac{F(q, u_\eta)}{K(u_\eta)} \quad \text{and} \quad \text{thus} \quad \varphi = \pi \frac{F(q_1(\varphi), u_\eta)}{K(u_\eta)}. \quad (\text{B27})$$

Here $F(q, u_\eta)$ and $K(u_\eta)$ are the elliptic integral of the first kind and the complete elliptic integral of the first kind. The former is given by,

$$F(q, u_\eta) = \int_0^q d\theta \frac{1}{\sqrt{1 - u_\eta^2 \sin^2 \theta}}. \quad (\text{B28})$$

The complete elliptic integral of the first kind $K(u_\eta) = F(\pi/2, u_\eta)$ and the η dependent function u_η are defined in Eq. (11).

The function $F(q, u_\eta) = F(q_1(\varphi), u_\eta)$ is such that $F(0, u_\eta) = 0$, $F(q, 0) = q$, and $F(q, u_\eta) = q$ for $q \rightarrow 0$. This gives the correct limiting values $q_1(0) = 0$ and $q_1(\pi) = \pi/2$. The expressions in Eq. (B27) define the functions $q_1(\varphi)$ and $\varphi_1(q)$ for the intervals $q_1(\varphi) \in [0, \pi/2]$ and $\varphi_1(q) \in [0, \pi]$, respectively. That $q_1(\varphi) = -q_1(-\varphi)$ and $\varphi_1(q) = -\varphi_1(-q)$ ensures that such an equation defines these functions for their full intervals $q_1(\varphi) \in [-\pi/2, \pi/2]$ and $\varphi_1(q) \in [-\pi, \pi]$, respectively.

The functions $K(u_\eta) = F(\pi/2, u_\eta)$ and $K'(u_\eta) = K(\sqrt{1 - u_\eta^2})$ have limiting values $K(0) = K'(1) = \pi/2$ and $K(1) = K'(0) = \infty$. Related useful limiting behaviors for $\eta \ll 1$ and $\eta \gg 1$ are,

$$\begin{aligned}K(u_\eta) &= \frac{\pi^2}{2\eta}; & K'(u_\eta) &= \frac{\pi}{2}; & u_\eta &= 1 \quad \text{for } \eta \ll 1 \\ K(u_\eta) &= \frac{\pi}{2} (1 + 4e^{-\eta}); & K'(u_\eta) &= \frac{\eta}{2} (1 + 4e^{-\eta}); & u_\eta &= 4e^{-\eta/2} \quad \text{for } \eta \gg 1.\end{aligned}\quad (\text{B29})$$

The distribution $2\pi\sigma_1(\varphi)$, Eq. (B6), is at $m = 0$ also expressed as an infinite summation that can again be solved in closed form in terms of elliptic integrals of the first kind as follows,

$$2\pi\sigma_1(\varphi) = \frac{\partial q_1(\varphi)}{\partial \varphi} = \frac{1}{2} + \sum_{l=1}^{\infty} \frac{\cos(l\varphi)}{\cosh(l\eta)} = \frac{1}{\pi} K(u_\eta) \sqrt{1 - u_\eta^2 \sin^2 q_1(\varphi)}. \quad (\text{B30})$$

At $m = 0$ the 1-band energy dispersion, Eqs. (B13) and (B14), can then be expressed as,

$$\begin{aligned} \varepsilon_1(q) &= \bar{\varepsilon}_1(\varphi_1(q)) \quad \text{for } q \in [-\pi/2, \pi/2] \quad \text{where} \\ \bar{\varepsilon}_1(\varphi) &= \bar{\varepsilon}_1^0(\varphi) + \frac{1}{2} g\mu_B h \quad \text{for } h \in [0, h_{c1}], \end{aligned} \quad (\text{B31})$$

and

$$\bar{\varepsilon}_1^0(\varphi) = -J \sinh(\eta) \left(\frac{1}{2} + \sum_{l=1}^{\infty} \frac{\cos(l\varphi)}{\cosh(l\eta)} \right) = -\frac{J}{\pi} \sinh(\eta) K(u_\eta) \sqrt{1 - u_\eta^2 \sin^2 q_1(\varphi)} \quad \text{for } \varphi \in [-\pi, \pi], \quad (\text{B32})$$

where the critical magnetic field h_{c1} is defined in Eq. (10). This directly gives an explicit simple dependence of $\varepsilon_1(q)$ on the 1-band momentum q as follows,

$$\varepsilon_1(q) = -\frac{J}{\pi} \sinh(\eta) K(u_\eta) \sqrt{1 - u_\eta^2 \sin^2 q} + \frac{1}{2} g\mu_B h \quad \text{for } q \in [-\pi/2, \pi/2] \quad \text{and } h \in [0, h_{c1}]. \quad (\text{B33})$$

At $m = 0$ the n -band energy dispersion, Eqs. (B15) and (B16), is for $n > 1$ found to be given by,

$$\begin{aligned} \varepsilon_n(q) &= \bar{\varepsilon}_n(\varphi_n(q)) \quad \text{for } q \in [0^-, 0^+] \quad \text{where} \\ \bar{\varepsilon}_n(\varphi) &= \bar{\varepsilon}_n^0(\varphi) + (n-1) g\mu_B h \quad \text{for } h \in [0, h_{c1}], \end{aligned} \quad (\text{B34})$$

and

$$\bar{\varepsilon}_n^0(\varphi) = -\frac{J}{n} \left(1 - \frac{n \sinh(\eta)}{\sinh(n\eta)} \right) \left(\frac{\sinh^2(n\eta)}{\cosh(n\eta) - \cos(\varphi)} - 1 - \cosh(n\eta) \right) \quad \text{for } \varphi \in [-\pi, \pi]. \quad (\text{B35})$$

At the limiting φ values $\varphi = 0$ and $\varphi = \pm\pi$ the $n > 1$ dispersion $\bar{\varepsilon}_n^0(\varphi)$ reads,

$$\bar{\varepsilon}_n^0(0) = 0 \quad \text{and} \quad \bar{\varepsilon}_n^0(\pm\pi) = \frac{2J}{n} \left(1 - \frac{n \sinh(\eta)}{\sinh(n\eta)} \right). \quad (\text{B36})$$

At $m = 0$ one has that $W_1^h = 0$ and thus $W_1 = W_1^p$. The finite energy dispersions bandwidths read,

$$\begin{aligned} W_1^p &= \varepsilon_1(\pi/2) - \varepsilon_1(0) = \bar{\varepsilon}_1(\pi) - \bar{\varepsilon}_1(0) = \frac{J}{\pi} \sinh(\eta) K(u_\eta) \left(1 - \sqrt{1 - u_\eta^2} \right) \\ W_n^h &= \varepsilon_n(0^\pm) = \bar{\varepsilon}_n(\pm\pi) = \frac{2J}{n} \left(1 - \frac{n \sinh(\eta)}{\sinh(n\eta)} \right) \quad \text{for } n > 1. \end{aligned} \quad (\text{B37})$$

These energy bandwidths have for $n = 1$ and $n > 1$ the following limiting behaviors,

$$\begin{aligned} W_1^p &= \frac{\pi}{2} J \quad \text{and} \quad W_n^h = 0 \quad \text{for } \eta \rightarrow 0 \\ W_1^p &= 2J \quad \text{and} \quad W_n^h = \frac{2J}{n} \quad \text{for } \eta \rightarrow \infty. \end{aligned} \quad (\text{B38})$$

Those of W_1^p are obtained from the use of the corresponding behaviors $K(u_\eta) = \frac{\pi^2}{2} \frac{1}{\eta}$ and $u_\eta = 4e^{-\eta/2}$ for $\eta \gg 1$, Eq. (B29). Those of W_n^h for $n > 1$ are obtained from the use of that quantity general expression provided in Eq. (B37).

Consistently, that $K(u_\eta) = \frac{\pi^2}{2} \frac{1}{\eta}$ for $\eta \ll 1$ in Eq. (B33) gives the following correct isotropic-point expression for the 1-particle energy dispersion $\varepsilon_1(q)$ at $h = 0$ [17, 18],

$$\lim_{\eta \rightarrow 0} \varepsilon_1(q) = -J \frac{\pi}{2} \cos q \quad \text{for } h = 0. \quad (\text{B39})$$

The behaviors found for $\eta \rightarrow 0$ are indeed consistent with the corresponding known values $W_1^p = \frac{\pi}{2} J$ and $W_n^h = 0$ where $n > 0$ for the isotropic case [17, 18]. In that case, both the momentum bandwidths and energy bandwidths of the n -bands vanish for $n > 1$ in the spin density $m \rightarrow 0$ limit. For $\eta > 1$ this applies to the momentum bandwidths, yet the $n > 1$ energy bandwidths $W_n = W_n^h$ are finite in that limit, as given in Eq. (B37).

3. Ground-state rapidity functions and energy dispersions for the excited states in the $m \rightarrow 1$ limit

In the $m \rightarrow 1$ limit one has that $B = 0$ and all expressions have the same general n -dependent form for $n \geq 1$. Specifically, the expressions, Eqs. (B1) and (B2), are given by,

$$q_n(\varphi) = 2 \arctan \left(\coth \left(\frac{n\eta}{2} \right) \tan \left(\frac{\varphi}{2} \right) \right) \quad \text{for } \varphi \in [-\pi, \pi]. \quad (\text{B40})$$

Inversion of this function gives the following closed-form expression for the n -band rapidity functions,

$$\varphi_n(q) = 2 \arctan \left(\tanh \left(\frac{n\eta}{2} \right) \tan \left(\frac{q}{2} \right) \right) \quad \text{for } q \in [-\pi, \pi]. \quad (\text{B41})$$

The distributions, Eqs. (B6) and (B9), read,

$$2\pi\sigma_n(\varphi) = \frac{\sinh(n\eta)}{\cosh(n\eta) - \cos(\varphi)} \quad \text{for } \varphi \in [-\pi, \pi]. \quad (\text{B42})$$

The energy dispersions in Eqs. (B13) and (B15) can be written as,

$$\begin{aligned} \varepsilon_n(q) &= \bar{\varepsilon}_n(\varphi_n(q)) \quad \text{for } q \in [-\pi, \pi] \quad \text{where} \\ \bar{\varepsilon}_n(\varphi) &= \bar{\varepsilon}_n^0(\varphi) + n g \mu_B h_{c2} \\ \bar{\varepsilon}_n^0(\varphi) &= -\frac{J}{n} \left(\frac{\sinh^2(n\eta)}{\cosh(n\eta) - \cos(\varphi)} - C_n(\eta) \right). \end{aligned} \quad (\text{B43})$$

Here $C_n(\eta)$ is the constant, Eq. (8), and the critical magnetic field h_{c2} to the fully-polarized ferromagnetic quantum phase reads $J(\Delta + 1)/g\mu_B$, Eq. (10).

After some algebra, one finds that in the $m \rightarrow 1$ limit the q -dependent energy dispersions in Eqs. (B13) and (B15) have the following simple closed-form expressions,

$$\begin{aligned} \varepsilon_1(q) &= J(1 - \cos q) \quad \text{and} \\ \varepsilon_n(q) &= \frac{J}{n} \left(n^2(\Delta + 1) + C_n(\eta) - \cosh(n\eta) - \cos q \right) \quad \text{for } q \in [-\pi, \pi], \end{aligned} \quad (\text{B44})$$

respectively, where $\Delta = \cosh \eta$.

Finally, in that limit one has that the n -band energy dispersions bandwidths are given by,

$$W_n = W_n^h = \varepsilon_n(\pi) - \varepsilon_n(0) = \bar{\varepsilon}_n(\pi) - \bar{\varepsilon}_n(0) = \frac{2J}{n} \quad \text{for } n \geq 1. \quad (\text{B45})$$

Appendix C: Matrix elements that control the line shape near the sharp peaks and related phase shifts

The q -spin neutral nature found in this paper for anisotropy $\Delta > 1$ of the unbound $S^z = S_q = 0$ pairs of physical spins 1/2 described by $n = 1$ real single Bethe rapidities and the $n > 1$ bound $S^z = S_q = 0$ pairs of physical spins 1/2 described by n -strings implies that the S matrices associated with their scattering have the same form, Eqs. (36) and (37), as for the isotropic point, $\Delta = 1$. It follows that the corresponding dynamical theory has the same general structure as that used in the studies of Refs. 17, 18 for the isotropic spin-1/2 chain.

Here the relation of the line shape near the sharp peaks located in continua lower thresholds, Eq. (42), to the matrix elements in Eq. (1) is shortly addressed for $\Delta > 1$. The present analysis also applies to the line shape, Eq. (45), of a sharp peak located in a $+-$ branch line that for intermediate and large spin density values does not coincide with the $n = 1$ continuum lower threshold. The following general dynamical theory expressions are similar to those of the isotropic point, $\Delta = 1$. The difference is the dependence on anisotropy $\Delta = \cosh \eta > 1$ of some of the quantities in them.

The dynamical structure factor components are within the dynamical theory used in the studies of this paper expressed as a sum of 1-particle spectral functions $B_1(k', \omega')$ (denoted by $B_Q(k', \omega')$ in Ref. 18.) Each of them is associated with a reference energy eigenstate and corresponding compactly occupied 1-band sea. Specifically, the 1-band occupancy of such a state changes at the $\iota = +1$ right and $\iota = -1$ left *reference-state* Fermi points,

$$q_{F1,\iota} = q_{F1,\iota}^0 + \frac{\pi}{L} \delta N_{1,\iota}^F. \quad (\text{C1})$$

Here $q_{F1,\iota}^0$ stands for the initial ground-state Fermi points that in the thermodynamic limit are given by $q_{F1,\iota}^0 = \iota k_{F\downarrow}$ and $\delta N_{1,\iota}^F$ are the number deviations at the $\iota = \pm 1$ 1-band Fermi points in the functional Φ_ι expression, Eq. (37), that define the reference state.

Each 1-particle spectral function $B_1(k', \omega')$ contributing to a dynamical correlation function $S^{ab}(k, \omega)$, Eq. (42), involves sums that run over $m_\iota = 1, 2, 3, \dots$ elementary particle-hole processes of $\iota = \pm 1$ elementary momentum values $\pm \frac{2\pi}{L}$ around the corresponding reference-state Fermi points $q_{F1,\iota}^0$. Such processes generate a tower of excited states upon that reference-state. The 1-particle spectral function reads,

$$B_1(k', \omega') = \sum_{m_{+1}; m_{-1}} A^{(0,0)} a(m_{+1}, m_{-1}) \times \delta\left(\omega' - \bar{\omega}_n^{ab}(k) - \frac{2\pi}{L} v_1 \sum_{\iota=\pm 1} (m_\iota + \Phi_\iota^2/4)\right) \delta\left(k' - k - \frac{2\pi}{L} \sum_{\iota=\pm 1} \iota (m_\iota + \Phi_\iota^2/4)\right). \quad (C2)$$

Here $v_1 = v_1(k_{F\downarrow})$ where $v_1(q)$ is the 1-band group velocity, Eq. (B25) of Appendix B for $n = 1$, and $\bar{\omega}_n^{ab}(k)$ is the branch-line one-parametric spectrum in the expression of $S^{ab}(k, \omega)$, Eq. (42). It is given in Appendix D for $n = 1, 2, 3$ and $ab = +- , n = 1$ and $ab = -+ ,$ and $n = 1, 2$ and $ab = zz$.

The *lowest peak weight* $A^{(0,0)}$ and the weights $A^{(0,0)} a(m_{+1}, m_{-1})$ in Eq. (C2) refer to the matrix elements square $|\langle \nu | \hat{S}_k^a | GS \rangle|^2$ in Eq. (1) between the ground state and the $m_{+1} = m_{-1} = 0$ reference excited state and the $\iota = \pm 1$ corresponding $m_\iota > 0$ tower excited states, respectively. For the subspaces spanned by the ground states and their excited energy eigenstates that contribute to the power-law spectral weight line shape near the sharp peaks in the dynamical correlation function components $S^{ab}(k, \omega)$, Eq. (42), the $\iota = \pm 1$ functionals Φ_ι have the general expressions given in Eqs. (38) and (40). They stem from the form of the 1-*particle* S matrix $S_1(\iota k_{F\downarrow})$ in Eq. (37) specific to branch lines as defined in Ref. 18.

The relative weights $a(m_{+1}, m_{-1})$ in Eq. (C2) can be expressed in terms of the gamma function as [18],

$$a(m_{+1}, m_{-1}) = \prod_{\iota=\pm 1} a_\iota(m_\iota) \quad \text{where} \quad a_\iota(m_\iota) = \frac{\Gamma(m_\iota + \Phi_\iota^2)}{\Gamma(m_\iota + 1) \Gamma(\Phi_\iota^2)}. \quad (C3)$$

For excited states whose $\iota = \pm 1$ functional values belong to the interval $\Phi_\iota \in [-1, 1]$, the matrix-element weights have in the present thermodynamic limit the following asymptotic behavior,

$$A^{(0,0)} = \left(\frac{1}{L B_1^{ab}} \right)^{-1 + \sum_{\iota=\pm 1} \Phi_\iota^2} \prod_{\iota=\pm 1} e^{-f_0^{ab} + f_2^{ab} (2\tilde{\Phi}_\iota)^2 - f_4^{ab} (2\tilde{\Phi}_\iota)^4} \quad \text{and} \\ a(m_{+1}, m_{-1}) = \prod_{\iota=\pm 1} \frac{(m_\iota + \Phi_\iota^2/4)^{-1 + \Phi_\iota^2}}{\Gamma(\Phi_\iota^2)}. \quad (C4)$$

Here,

$$\tilde{\Phi}_\iota = \Phi_\iota - \iota \delta N_{1,\iota}^F = -\frac{i}{2\pi} \ln S_1(\iota k_{F\downarrow}), \quad (C5)$$

is the scattering part of the important general functional $\Phi_\iota = \iota \delta N_{1,\iota}^F - \frac{i}{2\pi} \ln S_1(\iota k_{F\downarrow})$, Eq. (37), whose values are real. The value of the constant $0 < B_1^{ab} \leq 1$ in Eq. (C4) depends on η and m and those of the three $l = 0, 2, 4$ constants $0 < f_l^{ab} < 1$ depend on η . Both B_1^{ab} and f_l^{ab} are independent of L . Such constants have different values for each $ab = +- , -+ , zz$ dynamical structure factor component.

In the thermodynamic limit, the matrix elements square in Eq. (1) that contribute to the line shape near a sharp

peak then read,

$$\begin{aligned}
|\langle \nu | \hat{S}_k^a | GS \rangle|^2 &= |\langle k', m_{+1}, m_{-1} | \hat{S}_k^a | GS \rangle|^2 = A^{(0,0)} \prod_{\iota=\pm 1} \frac{\Gamma(m_\iota + \Phi_\iota^2)}{\Gamma(m_\iota + 1) \Gamma(\Phi_\iota^2)} \\
&= \left(\frac{1}{L B_1^{ab}} \right)^{-1+\sum_{\iota=\pm 1} \Phi_\iota^2} \prod_{\iota=\pm 1} e^{-f_0^{ab}+f_2^{ab}(2\Phi_\iota)^2-f_4^{ab}(2\Phi_\iota)^4} \frac{\Gamma(m_\iota + \Phi_\iota^2)}{\Gamma(m_\iota + 1) \Gamma(\Phi_\iota^2)} \\
&= \left(\frac{1}{L B_1^{ab}} \right)^{-1+\sum_{\iota=\pm 1} \Phi_\iota^2} \prod_{\iota=\pm 1} \frac{e^{-f_0^{ab}+f_2^{ab}(2\Phi_\iota)^2-f_4^{ab}(2\Phi_\iota)^4}}{\Gamma(\Phi_\iota^2)} (m_\iota + \Phi_\iota^2/4)^{-1+\Phi_\iota^2} \\
&= \left(\frac{1}{L B_1^{ab}} \right)^{-1+\sum_{\iota=\pm 1} \Phi_\iota^2} \\
&\times \prod_{\iota=\pm 1} \frac{e^{-f_0^{ab}+f_2^{ab}(2\Phi_\iota)^2-f_4^{ab}(2\Phi_\iota)^4}}{\Gamma(\Phi_\iota^2)} \left(\frac{L}{4\pi v_1} (\omega' - \bar{\omega}_n^{ab}(k) + \iota v_1 (k' - k)) \right)^{-1+\Phi_\iota^2}. \tag{C6}
\end{aligned}$$

Here $|\nu\rangle = |k', m_{+1}, m_{-1}\rangle$ denotes the excited energy eigenstate generated from the reference state $|\tilde{k}, 0, 0\rangle$ by $m_{+1} = 1, 2, 3, \dots$ $m_{-1} = 1, 2, 3, \dots$ elementary particle-hole processes of momentum values $\pm \frac{2\pi}{L}$ around the two $\iota = \pm 1$ 1-band reference-state Fermi points, Eq. (C1).

The two corresponding equalities,

$$m_\iota + \Phi_\iota^2/4 = \frac{L}{4\pi v_1} (\omega' - \bar{\omega}_n^{ab}(k) + \iota v_1 (k' - k)) \quad \text{for } \iota = \pm 1, \tag{C7}$$

imposed by the two δ -functions in Eq. (C2) have been used to arrive to the fourth expression in Eq. (C6).

Such δ -functions also select the specific two m_{+1} and m_{-1} values given in Eq. (C7) within the sum $\sum_{m_{+1}, m_{-1}}$ in Eq. (C2) that correspond to the fixed k' and ω' values of the 1-particle spectral function $B_1(k', \omega')$. It follows that for the general case in which the two $\iota = \pm 1$ functionals $\Phi_\iota \in [-1, 1]$ are finite, that spectral function, Eq. (C2), can then be written as,

$$\begin{aligned}
B_1(k', \omega') &= \frac{1}{L B_1^{ab}} \prod_{\iota=\pm 1} \Theta(\omega' - \bar{\omega}_n^{ab}(k) + \iota v_1 (k' - k)) \frac{e^{-f_0^{ab}+f_2^{ab}(2\Phi_\iota)^2-f_4^{ab}(2\Phi_\iota)^4}}{\Gamma(\Phi_\iota^2)} \\
&\times \left(\frac{\omega' - \bar{\omega}_n^{ab}(k) + \iota v_1 (k' - k)}{4\pi B_1^{ab} v_1} \right)^{-1+\Phi_\iota^2}. \tag{C8}
\end{aligned}$$

To reach this expression, which in the thermodynamic limit is exact, Eqs. (C2), (C4), (C6), and (C7) were used.

Our goal is to arrive to expression, Eq. (42), for the dynamical structure factor components at a fixed excitation momentum k and excitation energy such that the deviation $(\omega - \bar{\omega}_n^{ab}(k))$ is small, for each reference energy eigenstate corresponding to a given ω' value in the argument of $B_1(k', \omega')$. To reach it one selects a suitable set of tower excited states such that in average $\sum_{\iota=\pm 1} \iota (m_\iota + \Phi_\iota^2/4) = 0$ whereas $\sum_{\iota=\pm 1} (m_\iota + \Phi_\iota^2/4)$ is finite.

One then performs a suitable summation of 1-particle spectral functions that corresponds to a summation over reference energy eigenstates with different energy ω' values. That summation is equivalent to integrate that function at $k' = k$ over the energy variable $z = (\omega' - \bar{\omega}_n^{ab}(k))/(4\pi B_1^{ab} v_1)$ in suitable intervals that are determined by values of the quantity $-1 + \sum_{\iota=\pm 1} \Phi_\iota^2$. It turns out to be the exponent $\zeta_n^{ab}(k)$, Eq.(43), being positive, negative, or vanishing, respectively.

It is then useful to express $B_1(k', \omega')|_{k'=k}$ as a function of the variable $z = (\omega' - \bar{\omega}_n^{ab}(k))/(4\pi B_1^{ab} v_1)$ by considering the related function,

$$\bar{B}_1(z) = B_1(k, \omega')|_{\omega'=4\pi B_1^{ab} v_1 z + \bar{\omega}_n^{ab}(k)} = \frac{1}{L B_1^{ab}} \frac{\Theta(z)}{z} \zeta_n^{ab}(k) \prod_{\iota=\pm 1} \frac{e^{-f_0^{ab}+f_2^{ab}(2\Phi_\iota)^2-f_4^{ab}(2\Phi_\iota)^4}}{\Gamma(\Phi_\iota^2)}. \tag{C9}$$

The above expressions are valid for $\iota = \pm 1$ functional values in the interval $\Phi_\iota \in [-1, 1]$. In the studies of this paper we are mostly interested in the (k, ω) -plane line shape near sharp peaks for which $\zeta_n^{ab}(k) < 0$ in Eq. (42). However, provided there is no spectral weight below the corresponding lower threshold continuum or there is near no such a weight below it, the dynamical correlation function expression in that equation is valid also for $0 < \zeta_n^{ab}(k) < 1$

provided that $\Phi_\iota^2 \leq 1$ for $\iota = \pm 1$. In that case the power-law line shape expression, Eq. (42), does not refer to a sharp peak.

Upon performing the reference-state summation through an integration over z , $S^{ab}(k, \omega)$ is given by the following expression,

$$S^{ab}(k, \omega) = c_* \left(\frac{L}{4\pi v_1} \times 4\pi B_1^{ab} v_1 \right) \int_{z_*}^{\frac{\omega - \bar{\omega}_n^{ab}(k)}{4\pi B_1^{ab} v_1}} dz \bar{B}_1(z) = c_* L B_1^{ab} \int_{z_*}^{\frac{\omega - \bar{\omega}_n^{ab}(k)}{4\pi B_1^{ab} v_1}} dz \bar{B}_1(z). \quad (C10)$$

The values $c_* = 1$ or $c_* = -1$ of c_* and those of the integration limit z_* specific to the three cases $0 < \zeta_n^{ab}(k) < 1$, $-1 < \zeta_n^{ab}(k) < 0$, and $\zeta_n^{ab}(k) = 0$, respectively, are given in the following.

Both for $0 < \zeta_n^{ab}(k) < 1$ and $-1 < \zeta_n^{ab}(k) < 0$ the obtained general expression for $S^{ab}(k, \omega)$ is the same. However, the limits of integration in Eq. (C10) are different. For $0 < \zeta_n^{ab}(k) < 1$, such limits are such that the integral runs in the interval $z \in [0, (\omega - \bar{\omega}_n^{ab}(k))/(4\pi B_1^{ab} v_1)]$. This corresponds to $c^* = 1$ and $z_* = 0$ in Eq. (C10). For small values of the energy deviation $(\omega - \bar{\omega}_n^{ab}(k)) > 0$, ω' runs in this case from $\omega' = \bar{\omega}_n^{ab}(k)$ to $\omega' = \omega$. This is a small interval just below ω .

Consistently with the requirement of $S^{ab}(k, \omega)$ being positive, for $-1 < \zeta_n^{ab}(k) < 0$ the integral in Eq. (C10) must run in a z interval that corresponds to ω' values near ω but just above it. This generates a singular leading order term, Eq. (42), which is that physically relevant. The second term associated with the integration limit z_* in Eq. (C10) is independent of ω and has no physical meaning. Indeed, the present method only captures the leading-order term, Eq. (42). Since for $-1 < \zeta_n^{ab}(k) < 0$ the primitive function associated with the integrand in Eq. (C10) decreases very quickly upon increasing z , the suitable integration z interval in Eq. (C10) is $z \in [(\omega - \bar{\omega}_n^{ab}(k))/(4\pi B_1^{ab} v_1), \infty]$. This corresponds to $c^* = -1$ and $z_* = \infty$ in Eq. (C10). Indeed, this choice renders the second unphysical term to be zero.

Both such state summations suitable to $0 < \zeta_n^{ab}(k) < 1$ and $-1 < \zeta_n^{ab}(k) < 0$, respectively, lead to exactly the same general expression for $S^{ab}(k, \omega)$,

$$S^{ab}(k, \omega) = \left[\frac{1}{|\zeta_n^{ab}(k)|} \prod_{\iota=\pm 1} \frac{e^{-f_0^{ab} + f_2^{ab}(2\bar{\Phi}_\iota)^2 - f_4^{ab}(2\bar{\Phi}_\iota)^4}}{\Gamma(\Phi_\iota^2)} \right] \left(\frac{\omega - \bar{\omega}_n^{ab}(k)}{4\pi B_1^{ab} v_1} \right)^{\zeta_n^{ab}(k)}. \quad (C11)$$

This is the expression given in Eq. (42) with $\zeta_n^{ab}(k)$ and $C_{ab}^n(k)$ provided in Eqs. (43) and (44), respectively. It is valid for small values of the energy deviations $(\omega - \bar{\omega}_n^{ab}(k)) > 0$. (The same applies to the expression, Eq. (45).)

Importantly, this expression is not valid when $\zeta_n^{ab}(k) = -1 + \sum_{\iota=\pm 1} \Phi_\iota^2 = 0$ and thus $\sum_{\iota=\pm 1} \Phi_\iota^2 = 1$. Again consistently with the requirement of $S^{ab}(k, \omega)$ being positive, for $\zeta_n^{ab}(k) = 0$ the integral in Eq. (C10) runs in a z interval that corresponds to ω' values near ω but just above it. Then the physically relevant leading-order term contains a logarithmic rather than power-law singularity whereas the second ω independent term has again no physical meaning. To render that term zero, the suitable integration z interval in Eq. (C10) is now $z \in [(\omega - \bar{\omega}_n^{ab}(k))/(4\pi B_1^{ab} v_1), 1]$. This corresponds to $c^* = -1$ and $z_* = 1$ in Eq. (C10) and leads to,

$$S^{ab}(k, \omega) = \left[\frac{e^{\sum_{\iota=\pm 1} (-f_0^{ab} + f_2^{ab}(2\bar{\Phi}_\iota)^2 - f_4^{ab}(2\bar{\Phi}_\iota)^4)}}{\sum_{\iota=\pm 1} \frac{\pi}{2 \sin(\pi \Phi_\iota^2(q))}} \right] \left| \ln \left(\frac{\omega - \bar{\omega}_n^{ab}(k)}{4\pi B_1^{ab} v_1} \right) \right|. \quad (C12)$$

Since $\sum_{\iota=\pm 1} \Phi_\iota^2 = 1$, here that $\Gamma(x)\Gamma(1-x) = \pi/\sin(\pi x)$ for $x \neq 0, \pm 1, \dots$ was used. This gives $\Gamma(\Phi_{+1}^2)\Gamma(\Phi_{-1}^2) = \pi/\sin(\pi \Phi_{+1}^2) = \pi/\sin(\pi \Phi_{-1}^2)$ and thus also an equivalent more symmetrical expression $\Gamma(\Phi_{+1}^2)\Gamma(\Phi_{-1}^2) = \sum_{\iota=\pm 1} \pi/[2 \sin(\pi \Phi_\iota^2)]$.

The phase shifts in the general expression given in Eq. (37) of the $\iota = \pm 1$ functionals Φ_ι appearing here in Eqs. (C2)-(C12) are associated with the S matrices, Eqs. (36) and (37). They determine the momentum dependence of the exponents, Eq. (43), through such $\iota = \pm 1$ functionals Φ_ι . Such phase shifts play an important role in the dynamical properties studied in Sec. V and are given by,

$$2\pi \Phi_{n,n'}(q, q') = 2\pi \bar{\Phi}_{n,n'}(\varphi, \varphi') \quad \text{where} \quad \varphi = \varphi_n(q) \quad \text{and} \quad \varphi' = \varphi_{n'}(q'), \quad (C13)$$

for $n \geq 1$ and $n' \geq 1$.

As justified in Sec. V, in the case of the excited energy eigenstates involved in our studies, only the phase shifts $2\pi \Phi_{1,n}(q, q')$ where $n \geq 1$ play an active role. The corresponding rapidity phase shifts $2\pi \bar{\Phi}_{1,n}(\varphi, \varphi')$ are in units of 2π defined by the following integral equations,

$$\bar{\Phi}_{1,1}(\varphi, \varphi') = \frac{1}{\pi} \arctan \left(\coth(\eta) \tan \left(\frac{\varphi - \varphi'}{2} \right) \right) + \int_{-B}^B d\varphi'' G_1(\varphi - \varphi'') \bar{\Phi}_{1,1}(\varphi'', \varphi'), \quad (C14)$$

and

$$\bar{\Phi}_{1,n}(\varphi, \varphi') = \frac{1}{\pi} \sum_{\iota=\pm 1} \arctan \left(\coth \left(\frac{(n+\iota)\eta}{2} \right) \tan \left(\frac{\varphi - \varphi'}{2} \right) \right) + \int_{-B}^B d\varphi'' G_1(\varphi - \varphi'') \bar{\Phi}_{1,n}(\varphi'', \varphi'), \quad (\text{C15})$$

for $n > 1$ where the kernel $G_1(\varphi)$ is given in Eq. (B7) of Appendix B.

The following quantities play an important role in the dynamical properties studied in Sec. V. The phase shifts in units of 2π that appear in the expressions of the momentum-dependent exponents given in Appendix D are the following,

$$\begin{aligned} \Phi_{1,1}(\iota k_{F\downarrow}, q) &= \bar{\Phi}_{1,1}(\iota B, \varphi_1(q)) \quad \text{for } \iota = \pm 1 \\ \Phi_{1,n}(\iota k_{F\downarrow}, q) &= \bar{\Phi}_{1,n}(\iota B, \varphi_n(q)) \quad \text{for } \iota = \pm 1 \text{ and } n = 2, 3. \end{aligned} \quad (\text{C16})$$

The related 1-band phase-shift parameter ξ_{11} in Eq. (39) that also appears in such exponent expressions plays an important role as well in the spin-density curve $h(m)$, Eq. (9). As in other integrable models [49], it also appears in operator descriptions of Virasoro algebras. From manipulations of the phase-shift integral equation, Eq. (C14), one finds that it can be expressed as,

$$\xi_{11} = \xi_{11}(B) \quad \text{where} \quad \xi_{11}(\varphi) = 1 + \int_{-B}^B d\varphi' G_1(\varphi - \varphi') \xi_{11}(\varphi'). \quad (\text{C17})$$

The kernel $G_1(\varphi)$ in the integral equation obeyed by the auxiliary function $\xi_{11}(\varphi)$ is defined in Eq. (B7) of Appendix B. Also the phase-shift related parameters ξ_{1n}^0 and $\xi_n^{\iota,\pm}$ where $n = 2, 3$ and $\iota = \pm 1$, Eq. (41), appear in the expressions of some momentum-dependent exponents given in Appendix D. They can be expressed in terms of the rapidity phase shifts defined by Eqs. (C14) and (C15) as $\xi_n^0 = 2\bar{\Phi}_{1,n}(B, 0)$ and $\xi_n^{\iota,\pm} = \bar{\Phi}_{1,n}(\iota B, \pm\pi)$. For $\Delta > 1$ and at $m = 0$ and at $m = 1$ the parameters ξ_{11} , ξ_{1n}^0 , and $\xi_n^{\iota,\pm}$ are given by,

$$\begin{aligned} \xi_{11} &= \frac{1}{2}; \quad \xi_{1n}^0 = 2; \quad \xi_n^{\iota,\pm} = \iota \mp \frac{1}{2} \quad \text{at } m = 0 \\ \xi_{11} &= 1; \quad \xi_{1n}^0 = 0; \quad \xi_n^{\iota,\pm} = \mp 1 \quad \text{at } m = 1. \end{aligned} \quad (\text{C18})$$

Appendix D: Lower threshold spectra and momentum-dependent exponents

The one-parametric spectra of the gapped lower thresholds of the $n = 2$ continua shown in Figs. 4,5,8,9 and of the $n = 3$ continuum shown in Figs. 4,5 have a different form for three spin density intervals, $m \in]0, \bar{m}_n]$, $m \in]\bar{m}_n, \tilde{m}_n]$, and $m \in [\tilde{m}_n, 1[$, respectively. Here \bar{m}_n and \tilde{m}_n such that $\bar{m}_n < 1/3$ and $\tilde{m}_n > \bar{m}_n$ are for $n = 2$ and $n = 3$ two η -dependent spin densities at which the following equality holds,

$$W_n^h = -\varepsilon_1(2k_{F\downarrow} - k_{F\uparrow}) \quad \text{at } m = \bar{m}_n < 1/3 \quad \text{and} \quad \text{at } m = \tilde{m}_n > \bar{m}_n \quad \text{for } n = 2, 3. \quad (\text{D1})$$

The 1-particle energy dispersion $\varepsilon_1(q)$ and the energy bandwidth $W_n = W_n^h$ for $n = 2, 3$ appearing here are defined in Eqs. (B13)-(B14) and (B24) of Appendix B, respectively. One has that $\lim_{\eta \rightarrow 0} \bar{m}_n = 0$.

Some specific excitation momentum k 's values separate momentum intervals of the lower thresholds of the $S^{+-}(k, \omega)$ $n = 2, 3$ continua in Figs. 4,5 and $S^{zz}(k, \omega)$ $n = 2$ continuum in Figs. 8,9 that refer to different types of momentum dependences. Such specific k values either equal a momentum denoted here by \tilde{k}_n or their expression involves \tilde{k}_n where $n = 2, 3$. That momentum is defined by the following relations,

$$\begin{aligned} \varepsilon_n(\tilde{k}_n) &= \varepsilon_n(0) - \varepsilon_1(k_{F\downarrow} - \tilde{k}_n) \quad \text{for } \tilde{k}_n \leq (k_{F\uparrow} - k_{F\downarrow}) \quad \text{and } m \in]0, \bar{m}_n] \\ W_n^h &= \varepsilon_1(k_{F\uparrow} - \tilde{k}_n) - \varepsilon_1(k_{F\downarrow} - \tilde{k}_n) \quad \text{for } \tilde{k}_n \geq (k_{F\uparrow} - k_{F\downarrow}) \quad \text{and } m \in [\bar{m}_n, \tilde{m}_n] \\ \varepsilon_n(\tilde{k}_n) &= \varepsilon_n(0) - \varepsilon_1(k_{F\downarrow} - \tilde{k}_n) \quad \text{for } \tilde{k}_n \leq (k_{F\uparrow} - k_{F\downarrow}) \quad \text{and } m \in [\tilde{m}_n, 1[, \end{aligned} \quad (\text{D2})$$

where the energy dispersion $\varepsilon_n(q)$ is for $n = 2, 3$ given in Eq. (B15) of Appendix B.

The momentum \tilde{k}_n reads $\tilde{k}_n = (k_{F\uparrow} - k_{F\downarrow})$ both at $m = \bar{m}_n$ and $m = \tilde{m}_n$. For $m \in [0, \bar{m}_n]$ it increases upon increasing m from $\tilde{k}_n = 0$ for $m \rightarrow 0$ to $\tilde{k}_n = (k_{F\uparrow} - k_{F\downarrow})$ at $m = \bar{m}_n$. For $m \in [\bar{m}_n, \tilde{m}_n]$ it first increases relative to $(k_{F\uparrow} - k_{F\downarrow})$ and after decreases relative to it, until being again given by $\tilde{k}_n = (k_{F\uparrow} - k_{F\downarrow})$ at $m = \tilde{m}_n$. Finally, for $m \in [\tilde{m}_n, 1[$ it decreases upon increasing m from $\tilde{k}_n = (k_{F\uparrow} - k_{F\downarrow})$ at $m = \tilde{m}_n$ to $\tilde{k}_n = 0$ for $m \rightarrow 1$.

The one-parametric spectra given in the following also involve the energy dispersions $\varepsilon_1(q)$ plotted in Fig. 1 and $\varepsilon_n(q)$ plotted in Figs. 2 and 3 for $n = 2$ and $n = 3$, respectively. Such energy dispersions are defined by Eqs. (B13)-(B18) of Appendix B. In the cases of the gapped lower thresholds of the $n = 2$ continua shown in Figs. 4,5,8,9 and of the $n = 3$ continuum shown in Figs. 4,5, the one-parametric spectra under consideration obey the following relations,

$$\begin{aligned}\bar{\omega}_n^{zz}(k) &= \bar{\omega}_n^{+-}(\pi - k) \quad \text{for } n = 2, 3 \quad \text{and } k \in [0, \pi] \\ \bar{\omega}_3^{+-}(k) &= \bar{\omega}_2^{+-}(\pi - k) \quad \text{for } k \in [0, \pi] \\ \bar{\omega}_3^{zz}(k) &= \bar{\omega}_2^{zz}(\pi - k) \quad \text{for } k \in [0, \pi].\end{aligned}\tag{D3}$$

In the following we provide the expressions of the one-parametric lower threshold spectra $\bar{\omega}_n^{ab}(k)$ of the $n = 1, 2, 3$ continua for $ab = +-$, $n = 1$ continuum for $ab = -+$, and $n = 1, 2$ continua for $ab = zz$ and corresponding momentum-dependent exponents $\zeta_n^{ab}(k)$ in Eq. (42). The branch-line spectrum $\tilde{\omega}_1^{+-}(k)$ and corresponding exponent $\tilde{\zeta}_1^{+-}(k)$ in Eq. (45) are also given.

1. Lower threshold spectra and exponents of $S^{+-}(k, \omega)$ for $m > 0$

The $n = 1$ lower threshold spectrum $\bar{\omega}_1^{+-}(k)$ in the expression of $S^{+-}(k, \omega)$, Eq. (42) for $ab = +-$ and $n = 1$, is for $m > 0$ divided into the following two branch-line intervals,

$$\begin{aligned}\bar{\omega}_1^{+-}(k) &= \varepsilon_1(k - k_{F\uparrow}) \quad \text{and } k = k_{F\uparrow} + q \quad \text{where} \\ &k \in [0, (k_{F\uparrow} - k_{F\downarrow})] \quad \text{for } q \in [-k_{F\uparrow}, -k_{F\downarrow}], \\ \bar{\omega}_1^{+-}(k) &= -\varepsilon_1(k_{F\uparrow} - k) \quad \text{and } k = k_{F\uparrow} - q \quad \text{where} \\ &k \in [(k_{F\uparrow} - k_{F\downarrow}), \pi] \quad \text{for } q \in [-k_{F\downarrow}, k_{F\downarrow}].\end{aligned}\tag{D4}$$

The spectrum $\bar{\omega}_1^{+-}(k)$ in the expression of $S^{+-}(k, \omega)$, Eq. (45), of the branch line shown in Figs. 4,5 that for small spin densities coincides with the lower threshold of that component $n = 1$ continuum for $k \in [2k_{F\downarrow}, \pi]$ and for intermediate and large spin densities does not coincide with it, is given by,

$$\tilde{\omega}_1^{+-}(k) = \varepsilon_1(k - \pi - k_{F\downarrow}) \quad \text{and } k = \pi + k_{F\downarrow} + q \quad \text{where } k \in [2k_{F\downarrow}, \pi] \quad \text{for } q \in [-k_{F\uparrow}, -k_{F\downarrow}].\tag{D5}$$

The 2-string gapped lower threshold spectrum $\bar{\omega}_2^{+-}(k)$ in the expression of $S^{+-}(k, \omega)$, Eq. (42) for $ab = +-$ and $n = 2$, is for $m > 0$ divided into the following branch-line intervals,

$$\begin{aligned}\bar{\omega}_2^{+-}(k) &= \varepsilon_2(k) \quad \text{and } k = q \quad \text{where} \\ &k \in [0, \tilde{k}_2[\quad \text{and } q \in [0, \tilde{k}_2[\quad \text{for } m \in]0, \bar{m}_2] \\ &k \in [0, (k_{F\uparrow} - k_{F\downarrow})[\quad \text{and } q \in [0, (k_{F\uparrow} - k_{F\downarrow})[\quad \text{for } m \in [\bar{m}_2, \tilde{m}_2] \\ &k \in [0, \tilde{k}_2[\quad \text{and } q \in [0, \tilde{k}_2[\quad \text{for } m \in [\tilde{m}_2, 1[, \end{aligned}\tag{D6}$$

$$\begin{aligned}\bar{\omega}_2^{+-}(k) &= \varepsilon_2(k_{F\uparrow} - k_{F\downarrow}) - \varepsilon_1(k_{F\uparrow} - k) \quad \text{and } k = k_{F\uparrow} - q \quad \text{where} \\ &k \in](k_{F\uparrow} - k_{F\downarrow}), \tilde{k}_2[\quad \text{and } q \in](k_{F\uparrow} - \tilde{k}_2), k_{F\downarrow}[\quad \text{for } m \in [\bar{m}_2, \tilde{m}_2],\end{aligned}\tag{D7}$$

$$\begin{aligned}\bar{\omega}_2^{+-}(k) &= \varepsilon_2(0) - \varepsilon_1(k_{F\downarrow} - k) \quad \text{and } k = k_{F\downarrow} - q \quad \text{where} \\ &k \in]\tilde{k}_2, 2k_{F\downarrow}[\quad \text{and } q \in]-k_{F\downarrow}, (k_{F\downarrow} - \tilde{k}_2)[\quad \text{for } m \in]0, 1[, \end{aligned}\tag{D8}$$

and

$$\begin{aligned}\bar{\omega}_2^{+-}(k) &= \varepsilon_2(k - 2k_{F\downarrow}) \quad \text{and } k = 2k_{F\downarrow} + q \quad \text{where} \\ &k \in]2k_{F\downarrow}, \pi[\quad \text{and } q \in]0, (k_{F\uparrow} - k_{F\downarrow})[\quad \text{for } m \in]0, 1[.\end{aligned}\tag{D9}$$

Finally, the 3-string gapped lower threshold spectrum $\bar{\omega}_{3,l}^{+-}(k)$ in the expression of $S^{+-}(k, \omega)$, Eq. (42) for $ab = +-$ and $n = 3$, includes for $m > 0$ the following branch-line intervals,

$$\begin{aligned}\bar{\omega}_3^{+-}(k) &= \varepsilon_3(k - (k_{F\uparrow} - k_{F\downarrow})) \quad \text{and } k = (k_{F\uparrow} - k_{F\downarrow}) + q \quad \text{where} \\ &k \in]0, (k_{F\uparrow} - k_{F\downarrow})[\quad \text{and } q \in]-(k_{F\uparrow} - k_{F\downarrow}), 0[\quad \text{for } m \in]0, 1[, \end{aligned}\tag{D10}$$

$$\begin{aligned}\bar{\omega}_3^{+-} &= \varepsilon_3(0) - \varepsilon_1(k_{F\uparrow} - k) \quad \text{and} \quad k = k_{F\uparrow} - q \quad \text{where} \\ k &\in](k_{F\uparrow} - k_{F\downarrow}), (\pi - \tilde{k}_3)[\quad \text{and} \quad q \in] - (k_{F\downarrow} - \tilde{k}_3), k_{F\downarrow}[\quad \text{for} \quad m \in]0, 1[, \end{aligned} \quad (\text{D11})$$

$$\begin{aligned}\bar{\omega}_3^{+-} &= \varepsilon_3(k_{F\uparrow} - k_{F\downarrow}) - \varepsilon_1(k_{F\downarrow} - k) \quad \text{and} \quad k = k_{F\downarrow} - q \quad \text{where} \\ k &\in](\pi - \tilde{k}_3), 2k_{F\downarrow}[\quad \text{and} \quad q \in] - k_{F\downarrow}, -(k_{F\uparrow} - \tilde{k}_3)[\quad \text{for} \quad m \in [\bar{m}_3, \tilde{m}_3], \end{aligned} \quad (\text{D12})$$

and

$$\begin{aligned}\bar{\omega}_3^{+-}(k) &= \varepsilon_3(k - \pi) \quad \text{and} \quad k = \pi + q \quad \text{where} \\ k &\in](\pi - \tilde{k}_3), \pi[\quad \text{and} \quad q \in] - \tilde{k}_3, 0[\quad \text{for} \quad m \in]0, \bar{m}_3[\\ k &\in]2k_{F\downarrow}, \pi[\quad \text{and} \quad q \in] - (k_{F\uparrow} - k_{F\downarrow}), 0[\quad \text{for} \quad m \in [\bar{m}_3, \tilde{m}_3] \\ k &\in](\pi - \tilde{k}_3), \pi[\quad \text{and} \quad q \in] - \tilde{k}_3, 0[\quad \text{for} \quad m \in [\tilde{m}_3, 1[. \end{aligned} \quad (\text{D13})$$

The corresponding k dependent exponents that appear in the expression of $S^{+-}(k, \omega)$, Eq. (42) for $ab = +-$ are given by,

$$\begin{aligned}\zeta_1^{+-}(k) &= -1 + \sum_{\iota=\pm 1} \left(-\frac{\xi_{11}}{2} + \Phi_{1,1}(\iota k_{F\downarrow}, q) \right)^2 \\ &\quad \text{for} \quad q = k - k_{F\uparrow} \quad \text{and} \quad k \in]0, (k_{F\uparrow} - k_{F\downarrow})[\\ \zeta_1^{+-}(k) &= -1 + \sum_{\iota=\pm 1} \left(\frac{\iota}{\xi_{11}} - \frac{\xi_{11}}{2} - \Phi_{1,1}(\iota k_{F\downarrow}, q) \right)^2 \\ &\quad \text{for} \quad q = k_{F\uparrow} - k \quad \text{and} \quad k \in](k_{F\uparrow} - k_{F\downarrow}), \pi[, \end{aligned} \quad (\text{D14})$$

for $n = 1$,

$$\begin{aligned}\zeta_2^{+-}(k) &= -1 + \sum_{\iota=\pm 1} \left(-\frac{\iota}{2\xi_{11}} + \Phi_{1,2}(\iota k_{F\downarrow}, q) \right)^2 \quad \text{for} \quad q = k \quad \text{where} \\ k &\in]0, \tilde{k}_2[\quad \text{for} \quad m \in]0, \bar{m}_2[\\ k &\in]0, (k_{F\uparrow} - k_{F\downarrow})[\quad \text{for} \quad m \in [\bar{m}_2, \tilde{m}_2] \quad \text{and} \\ k &\in]0, \tilde{k}_2[\quad \text{for} \quad m \in [\tilde{m}_2, 1[\\ \zeta_2^{+-}(k) &= -1 + \sum_{\iota=\pm 1} \left(\frac{\xi_{11}}{2} + \xi_2^{\iota,+} - \Phi_{1,1}(\iota k_{F\downarrow}, q) \right)^2 \quad \text{for} \quad q = k_{F\uparrow} - k \quad \text{where} \\ k &\in](k_{F\uparrow} - k_{F\downarrow}), \tilde{k}_2[\quad \text{for} \quad m \in [\bar{m}_2, \tilde{m}_2] \\ \zeta_2^{+-}(k) &= -1 + \sum_{\iota=\pm 1} \left(\iota \frac{\xi_{12}^0}{2} + \frac{\xi_{11}}{2} - \Phi_{1,1}(\iota k_{F\downarrow}, q) \right)^2 \quad \text{for} \quad q = k_{F\downarrow} - k \quad \text{where} \\ k &\in]\tilde{k}_2, 2k_{F\downarrow}[\quad \text{for} \quad m \in]0, 1[\\ \zeta_2^{+-}(k) &= -1 + \sum_{\iota=\pm 1} \left(-\frac{\iota}{2\xi_{11}} + \xi_{11} + \Phi_{1,2}(\iota k_{F\downarrow}, q) \right)^2 \quad \text{for} \quad q = k - 2k_{F\downarrow} \quad \text{where} \\ k &\in]2k_{F\downarrow}, \pi[\quad \text{for} \quad m \in]0, 1[, \end{aligned} \quad (\text{D15})$$

for $n = 2$ and,

$$\begin{aligned}
\zeta_3^{+-}(k) &= -1 + \sum_{\iota=\pm 1} \left(-\frac{\iota}{\xi_{11}} + \xi_{11} + \Phi_{1,3}(\iota k_{F\downarrow}, q) \right)^2 \quad \text{for } q = k - k_{F\uparrow} + k_{F\downarrow} \quad \text{where} \\
&\quad k \in]0, (k_{F\uparrow} - k_{F\downarrow})[\quad \text{for } m \in]0, 1[\\
\zeta_3^{+-}(k) &= -1 + \sum_{\iota=\pm 1} \left(-\frac{\iota}{2\xi_{11}} + \iota \frac{\xi_{13}^0}{2} + \frac{\xi_{11}}{2} - \Phi_{1,1}(\iota k_{F\downarrow}, q) \right)^2 \quad \text{for } q = k_{F\uparrow} - k \quad \text{where} \\
&\quad k \in](k_{F\uparrow} - k_{F\downarrow}), (\pi - \tilde{k}_3)[\quad \text{for } m \in]0, 1[\\
\zeta_3^{+-}(k) &= -1 + \sum_{\iota=\pm 1} \left(-\frac{\iota}{2\xi_{11}} + \frac{\xi_{11}}{2} + \xi_3^{\iota,+} - \Phi_{1,1}(\iota k_{F\downarrow}, q) \right)^2 \quad \text{for } q = k_{F\downarrow} - k \quad \text{where} \\
&\quad k \in](\pi - \tilde{k}_3), 2k_{F\downarrow}[\quad \text{for } m \in [\tilde{m}_3, \tilde{m}_3] \\
\zeta_3^{+-}(k) &= -1 + \sum_{\iota=\pm 1} \left(-\frac{\iota}{\xi_{11}} + \Phi_{1,3}(\iota k_{F\downarrow}, q) \right)^2 \quad \text{for } q = k - \pi \quad \text{where} \\
&\quad k \in](\pi - \tilde{k}_3), \pi[\quad \text{for } m \in]0, \tilde{m}_3[\\
&\quad k \in]2k_{F\downarrow}, \pi[\quad \text{for } m \in [\tilde{m}_3, \tilde{m}_3] \quad \text{and} \\
&\quad k \in](\pi - \tilde{k}_3), \pi[\quad \text{for } m \in [\tilde{m}_3, 1[,
\end{aligned} \tag{D16}$$

for $n = 3$.

Finally, the branch-line exponent in the expression of $S^{+-}(k, \omega)$, Eq. (45), reads,

$$\tilde{\zeta}_1^{+-}(k) = -1 + \sum_{\iota=\pm 1} \left(\frac{\xi_{11}}{2} + \Phi_{1,1}(\iota k_{F\downarrow}, q) \right)^2 \quad \text{for } q = k - \pi - k_{F\downarrow} \quad \text{and } k \in]2k_{F\downarrow}, \pi[. \tag{D17}$$

The phase shifts and the parameters ξ_{11} , ξ_{1n}^0 , $\xi_n^{\iota,\pm}$ where $n = 2, 3$ and $\iota = \pm 1$ appearing in the above expressions and in the following are defined in Eq. (41) and Eqs. (C16)-(C17) of Appendix C.

The exponents in Eqs. (D14), (D15), (D16), and (D17) are plotted as a function of k in Figs. 4,5 for the k intervals for which they are negative.

2. Lower threshold spectra and exponents of $S^{-+}(k, \omega)$ for $m > 0$

The $n = 1$ lower threshold spectrum $\bar{\omega}_1^{-+}(k)$ in the expression of $S^{-+}(k, \omega)$, Eq. (42) for $ab = -+$ and $n = 1$, reads,

$$\bar{\omega}_1^{-+}(k) = -\varepsilon_1(k_{F\uparrow} - k) \quad \text{and} \quad k = k_{F\uparrow} - q \quad \text{where } k \in [(k_{F\uparrow} - k_{F\downarrow}), \pi] \quad \text{for } q \in]-k_{F\downarrow}, k_{F\downarrow}]. \tag{D18}$$

The lower threshold spectra of the $n = 2$ and $n = 3$ continua of $S^{-+}(k, \omega)$ are similar to those of $S^{+-}(k, \omega)$ given above. However, since the corresponding exponents are positive, such continua have for $S^{-+}(k, \omega)$ nearly no spectral weight. Only the exponent $\zeta_1^{-+}(k)$ is negative.

In spite of their positivity for $n = 2, 3$, we give here the expressions of the exponents $\zeta_n^{-+}(k)$ for $n = 1, 2, 3$. They read,

$$\zeta_1^{-+}(k) = -1 + \sum_{\iota=\pm 1} \left(-\frac{\xi_{11}}{2} - \Phi_{1,1}(\iota k_{F\downarrow}, q) \right)^2 \quad \text{for } q = k_{F\uparrow} - k \quad \text{where } k \in](k_{F\uparrow} - k_{F\downarrow}), \pi[, \tag{D19}$$

for $n = 1$,

$$\begin{aligned}
\zeta_2^{-+}(k) &= -1 + \sum_{\iota=\pm 1} \left(-\frac{\iota 3}{2\xi_{11}} + \Phi_{1,2}(\iota k_{F\downarrow}, q) \right)^2 \quad \text{for } q = k \quad \text{where} \\
&\quad k \in]0, \tilde{k}_2[\quad \text{for } m \in]0, \tilde{m}_2] \\
&\quad k \in]0, (k_{F\uparrow} - k_{F\downarrow})[\quad \text{for } m \in [\tilde{m}_2, \tilde{m}_2] \quad \text{and} \\
&\quad k \in]0, \tilde{k}_2[\quad \text{for } m \in [\tilde{m}_2, 1[\\
\zeta_2^{-+}(k) &= -1 + \sum_{\iota=\pm 1} \left(-\frac{\iota}{\xi_{11}} + \frac{\xi_{11}}{2} + \xi_2^{\iota,+} - \Phi_{1,1}(\iota k_{F\downarrow}, q) \right)^2 \quad \text{for } q = k_{F\uparrow} - k \quad \text{where} \\
&\quad k \in](k_{F\uparrow} - k_{F\downarrow}), \tilde{k}_2[\quad \text{for } m \in [\tilde{m}_2, \tilde{m}_2] \\
\zeta_2^{-+}(k) &= -1 + \sum_{\iota=\pm 1} \left(-\frac{\iota}{\xi_{11}} + \iota \frac{\xi_{12}^0}{2} + \frac{\xi_{11}}{2} - \Phi_{1,1}(\iota k_{F\downarrow}, q) \right)^2 \quad \text{for } q = k_{F\downarrow} - k \quad \text{where} \\
&\quad k \in]\tilde{k}_2, 2k_{F\downarrow}[\quad \text{for } m \in]0, 1[\\
\zeta_2^{-+}(k) &= -1 + \sum_{\iota=\pm 1} \left(-\frac{\iota 3}{2\xi_{11}} + \xi_{11} + \Phi_{1,2}(\iota k_{F\downarrow}, q) \right)^2 \quad \text{for } q = k - 2k_{F\downarrow} \quad \text{where} \\
&\quad k \in]2k_{F\downarrow}, \pi[\quad \text{for } m \in]0, 1[,
\end{aligned} \tag{D20}$$

for $n = 2$ and,

$$\begin{aligned}
\zeta_3^{-+}(k) &= -1 + \sum_{\iota=\pm 1} \left(-\frac{\iota 2}{\xi_{11}} + \xi_{11} + \Phi_{1,3}(\iota k_{F\downarrow}, q) \right)^2 \quad \text{for } q = k - k_{F\uparrow} + k_{F\downarrow} \quad \text{where} \\
&\quad k \in]0, (k_{F\uparrow} - k_{F\downarrow})[\quad \text{for } m \in]0, 1[\\
\zeta_3^{-+}(k) &= -1 + \sum_{\iota=\pm 1} \left(-\frac{\iota 3}{2\xi_{11}} + \iota \frac{\xi_{13}^0}{2} + \frac{\xi_{11}}{2} - \Phi_{1,1}(\iota k_{F\downarrow}, q) \right)^2 \quad \text{for } q = k_{F\uparrow} - k \quad \text{where} \\
&\quad k \in](k_{F\uparrow} - k_{F\downarrow}), (\pi - \tilde{k}_3)[\quad \text{for } m \in]0, 1[\\
\zeta_3^{-+}(k) &= -1 + \sum_{\iota=\pm 1} \left(-\frac{\iota 3}{2\xi_{11}} + \frac{\xi_{11}}{2} + \xi_3^{\iota,+} - \Phi_{1,1}(\iota k_{F\downarrow}, q) \right)^2 \quad \text{for } q = k_{F\downarrow} - k \quad \text{where} \\
&\quad k \in](\pi - \tilde{k}_3), 2k_{F\downarrow}[\quad \text{for } m \in [\tilde{m}_3, \tilde{m}_3] \\
\zeta_3^{-+}(k) &= -1 + \sum_{\iota=\pm 1} \left(-\frac{\iota 2}{\xi_{11}} + \Phi_{1,n}(\iota k_{F\downarrow}, q) \right)^2 \quad \text{for } q = k - \pi \quad \text{where} \\
&\quad k \in](\pi - \tilde{k}_3), \pi[\quad \text{for } m \in]0, \tilde{m}_3] \\
&\quad k \in]2k_{F\downarrow}, \pi[\quad \text{for } m \in [\tilde{m}_3, \tilde{m}_3] \quad \text{and} \\
&\quad k \in](\pi - \tilde{k}_3), \pi[\quad \text{for } m \in [\tilde{m}_3, 1[.
\end{aligned} \tag{D21}$$

The exponent $\zeta_1^{-+}(k)$, Eq. (D19), is plotted as a function of k in Figs. 6,7.

3. Lower threshold spectra and exponents of $S^{zz}(k, \omega)$ for $m > 0$

Although the $n = 3$ continuum of $S^{zz}(k, \omega)$ does not contain a significant amount of spectral weight, here we provide the $n = 1$, $n = 2$, and $n = 3$ lower threshold's spectra $\bar{\omega}_n^{zz}(k)$ in the expression of that dynamical structure factor component, Eq. (42) for $ab = zz$ and $n = 1, 2, 3$. They include several branch-line parts and are given by,

$$\begin{aligned}
\bar{\omega}_1^{zz}(k) &= -\varepsilon_1(k_{F\downarrow} - k) \quad \text{and} \quad k = k_{F\downarrow} - q \quad \text{where} \\
&\quad k \in [0, 2k_{F\downarrow}] \quad \text{for } q \in [-k_{F\downarrow}, k_{F\downarrow}], \\
\bar{\omega}_1^{zz}(k) &= \varepsilon_1(k - k_{F\downarrow}) \quad \text{and} \quad k = k_{F\downarrow} + q \quad \text{where} \\
&\quad k \in [2k_{F\downarrow}, \pi] \quad \text{for } q \in [k_{F\downarrow}, k_{F\uparrow}],
\end{aligned} \tag{D22}$$

$$\begin{aligned}\bar{\omega}_2^{zz}(k) &= \varepsilon_2(k - (k_{F\uparrow} - k_{F\downarrow})) \quad \text{and} \quad k = (k_{F\uparrow} - k_{F\downarrow}) + q \quad \text{where} \\ k &\in]0, (k_{F\uparrow} - k_{F\downarrow})[\quad \text{and} \quad q \in] - (k_{F\uparrow} - k_{F\downarrow}), 0[\quad \text{for} \quad m \in]0, 1[, \end{aligned} \quad (\text{D23})$$

$$\begin{aligned}\bar{\omega}_2^{zz} &= \varepsilon_2(0) - \varepsilon_1(k_{F\uparrow} - k) \quad \text{and} \quad k = k_{F\uparrow} - q \quad \text{where} \\ k &\in](k_{F\uparrow} - k_{F\downarrow}), (\pi - \tilde{k}_2)[\quad \text{and} \quad q \in] - (k_{F\downarrow} - \tilde{k}_2), k_{F\downarrow}[\quad \text{for} \quad m \in]0, 1[, \end{aligned} \quad (\text{D24})$$

$$\begin{aligned}\bar{\omega}_2^{zz} &= \varepsilon_2(-(k_{F\uparrow} - k_{F\downarrow})) - \varepsilon_1(k_{F\downarrow} - k) \quad \text{and} \quad k = k_{F\downarrow} - q \quad \text{where} \\ k &\in](\pi - \tilde{k}_2), 2k_{F\downarrow}[\quad \text{and} \quad q \in] - k_{F\downarrow}, -(k_{F\uparrow} - \tilde{k}_2)[\quad \text{for} \quad m \in [\tilde{m}_2, \tilde{m}_2], \end{aligned} \quad (\text{D25})$$

and

$$\begin{aligned}\bar{\omega}_2^{zz}(k) &= \varepsilon_2(k - \pi) \quad \text{and} \quad k = \pi + q \quad \text{where} \\ k &\in](\pi - \tilde{k}_2), \pi[\quad \text{and} \quad q \in] - \tilde{k}_2, 0[\quad \text{for} \quad m \in]0, \tilde{m}_2[\\ k &\in]2k_{F\downarrow}, \pi[\quad \text{and} \quad q \in] - (k_{F\uparrow} - k_{F\downarrow}), 0[\quad \text{for} \quad m \in [\tilde{m}_2, \tilde{m}_2] \\ k &\in](\pi - \tilde{k}_2), \pi[\quad \text{and} \quad q \in] - \tilde{k}_2, 0[\quad \text{for} \quad m \in [\tilde{m}_2, 1[, \end{aligned} \quad (\text{D26})$$

$$\begin{aligned}\bar{\omega}_3^z(k) &= \varepsilon_3(k) \quad \text{and} \quad k = q \quad \text{where} \\ k &\in [0, \tilde{k}_3[\quad \text{and} \quad q \in [0, \tilde{k}_3[\quad \text{for} \quad m \in]0, \tilde{m}_3[\\ k &\in [0, (k_{F\uparrow} - k_{F\downarrow})[\quad \text{and} \quad q \in [0, (k_{F\uparrow} - k_{F\downarrow})[\quad \text{for} \quad m \in [\tilde{m}_3, \tilde{m}_3] \\ k &\in [0, \tilde{k}_3[\quad \text{and} \quad q \in [0, \tilde{k}_3[\quad \text{for} \quad m \in [\tilde{m}_3, 1[, \end{aligned} \quad (\text{D27})$$

$$\begin{aligned}\bar{\omega}_3^z(k) &= \varepsilon_3(k_{F\uparrow} - k_{F\downarrow}) - \varepsilon_1(k_{F\uparrow} - k) \quad \text{and} \quad k = k_{F\uparrow} - q \quad \text{where} \\ k &\in](k_{F\uparrow} - k_{F\downarrow}), \tilde{k}_3[\quad \text{and} \quad q \in](k_{F\uparrow} - \tilde{k}_3), k_{F\downarrow}[\quad \text{for} \quad m \in [\tilde{m}_3, \tilde{m}_3], \end{aligned} \quad (\text{D28})$$

$$\begin{aligned}\bar{\omega}_3^z(k) &= \varepsilon_3(0) - \varepsilon_1(k_{F\downarrow} - k) \quad \text{and} \quad k = k_{F\downarrow} - q \quad \text{where} \\ k &\in]\tilde{k}_3, 2k_{F\downarrow}[\quad \text{and} \quad q \in] - k_{F\downarrow}, (k_{F\downarrow} - \tilde{k}_3)[\quad \text{for} \quad m \in]0, 1[, \end{aligned} \quad (\text{D29})$$

$$\begin{aligned}\bar{\omega}_3^z(k) &= \varepsilon_3(k - 2k_{F\downarrow}) \quad \text{and} \quad k = 2k_{F\downarrow} + q \quad \text{where} \\ k &\in]2k_{F\downarrow}, \pi[\quad \text{and} \quad q \in]0, (k_{F\uparrow} - k_{F\downarrow})[\quad \text{for} \quad m \in]0, 1[. \end{aligned} \quad (\text{D30})$$

In spite of the corresponding k dependent exponent $\zeta_3^{zz}(k)$ being positive for its whole k interval and the exponent $\zeta_2^{zz}(k)$ becoming positive upon increasing m and h , we provide in the following the expressions of the exponents $\zeta_n^{zz}(k)$ in the expression of $S^{zz}(k, \omega)$, Eq. (42) for $ab = zz$ and $n = 1, 2, 3$, independently of their values. They are found to read,

$$\begin{aligned}\zeta_1^{zz}(k) &= -1 + \sum_{\iota=\pm 1} \left(\frac{\iota}{2\xi_{11}} + \frac{\xi_{11}}{2} - \Phi_{1,1}(\iota k_{F\downarrow}, q) \right)^2 \quad \text{for} \quad q = k_{F\downarrow} - k \quad \text{where} \\ k &\in]0, 2k_{F\downarrow}[\\ \zeta_1^{zz}(k) &= -1 + \sum_{\iota=\pm 1} \left(-\frac{\iota}{2\xi_{11}} + \frac{\xi_{11}}{2} + \Phi_{1,1}(\iota k_{F\downarrow}, q) \right)^2 \quad \text{for} \quad q = k - k_{F\downarrow} \quad \text{where} \\ k &\in]2k_{F\downarrow}, \pi[, \end{aligned} \quad (\text{D31})$$

for $n = 1$,

$$\begin{aligned}
\zeta_2^{zz}(k) &= -1 + \sum_{\iota=\pm 1} \left(-\frac{\iota}{\xi_{11}} - \xi_{11} + \Phi_{1,2}(\iota k_{F\downarrow}, q) \right)^2 \quad \text{for } q = k - k_{F\uparrow} + k_{F\downarrow} \quad \text{where} \\
&\quad k \in]0, (k_{F\uparrow} - k_{F\downarrow})[\quad \text{for } m \in]0, 1[\\
\zeta_2^{zz}(k) &= -1 + \sum_{\iota=\pm 1} \left(-\frac{\iota}{2\xi_{11}} + \iota \frac{\xi_{12}^0}{2} - \frac{\xi_{11}}{2} - \Phi_{1,1}(\iota k_{F\downarrow}, q) \right)^2 \quad \text{for } q = k_{F\uparrow} - k \quad \text{where} \\
&\quad k \in](k_{F\uparrow} - k_{F\downarrow}), (\pi - \tilde{k}_2)[\quad \text{for } m \in]0, 1[\\
\zeta_2^{zz}(k) &= -1 + \sum_{\iota=\pm 1} \left(-\frac{\iota}{2\xi_{11}} - \frac{\xi_{11}}{2} + \xi_2^{\iota,-} - \Phi_{1,1}(\iota k_{F\downarrow}, q) \right)^2 \quad \text{for } q = k_{F\downarrow} - k \quad \text{where} \\
&\quad k \in](\pi - \tilde{k}_2), 2k_{F\downarrow}[\quad \text{for } m \in [\tilde{m}_2, \tilde{m}_2] \\
\zeta_2^{zz}(k) &= -1 + \sum_{\iota=\pm 1} \left(-\frac{\iota}{\xi_{11}} + \Phi_{1,2}(\iota k_{F\downarrow}, q) \right)^2 \quad \text{for } q = k - \pi \quad \text{where} \\
&\quad k \in](\pi - \tilde{k}_2), \pi[\quad \text{for } m \in]0, \tilde{m}_2[\\
&\quad k \in]2k_{F\downarrow}, \pi[\quad \text{for } m \in [\tilde{m}_2, \tilde{m}_2] \quad \text{and} \\
&\quad k \in](\pi - \tilde{k}_2), \pi[\quad \text{for } m \in [\tilde{m}_2, 1[, \tag{D32}
\end{aligned}$$

for $n = 2$ and,

$$\begin{aligned}
\zeta_3^{zz}(k) &= -1 + \sum_{\iota=\pm 1} \left(-\frac{\iota 3}{2\xi_{11}} + \Phi_{1,3}(\iota k_{F\downarrow}, q) \right)^2 \quad \text{for } q = k \quad \text{where} \\
&\quad k \in]0, \tilde{k}_3[\quad \text{for } m \in]0, \tilde{m}_3[\\
&\quad k \in]0, (k_{F\uparrow} - k_{F\downarrow})[\quad \text{for } m \in [\tilde{m}_3, \tilde{m}_3] \quad \text{and} \\
&\quad k \in]0, \tilde{k}_3[\quad \text{for } m \in [\tilde{m}_3, 1[\\
\zeta_3^{zz}(k) &= -1 - \sum_{\iota=\pm 1} \left(\frac{\iota}{\xi_{11}} + \frac{\xi_{11}}{2} + \xi_3^{\iota,+} - \Phi_{1,1}(\iota k_{F\downarrow}, q) \right)^2 \quad \text{for } q = k_{F\uparrow} - k \quad \text{where} \\
&\quad k \in](k_{F\uparrow} - k_{F\downarrow}), \tilde{k}_3[\quad \text{for } m \in [\tilde{m}_3, \tilde{m}_3] \\
\zeta_3^{zz}(k) &= -1 + \sum_{\iota=\pm 1} \left(-\frac{\iota}{\xi_{11}} + \iota \frac{\xi_{13}^0}{2} - \frac{\xi_{11}}{2} - \Phi_{1,1}(\iota k_{F\downarrow}, q) \right)^2 \quad \text{for } q = k_{F\downarrow} - k \quad \text{where} \\
&\quad k \in]\tilde{k}_3, 2k_{F\downarrow}[\quad \text{for } m \in]0, 1[\\
\zeta_3^{zz}(k) &= -1 + \sum_{\iota=\pm 1} \left(-\frac{\iota 3}{2\xi_{11}} - \xi_{11} + \Phi_{1,3}(\iota k_{F\downarrow}, q) \right)^2 \quad \text{for } q = k - 2k_{F\downarrow} \quad \text{where} \\
&\quad k \in]2k_{F\downarrow}, \pi[\quad \text{for } m \in]0, 1[, \tag{D33}
\end{aligned}$$

for $n = 3$.

The exponent $\zeta_1^{zz}(k)$ in Eq. (D31) and $\zeta_2^{zz}(k)$ in Eq. (D32) are plotted as a function of k in Figs. 8,9 for the k intervals for which they are negative.

-
- [1] R. Orbach, Phys. Rev. 112 (1958) 309.
 - [2] J. des Cloizeaux, M. Gaudin, J. Math. Phys. 7 (1966) 1384.
 - [3] C.N. Yang and C.P. Yang Phys. Rev. 150 (1966) 321 ; 150 (1966) 327; 151 (1966) 258.
 - [4] J.-S. Caux, J. M. Maillet, Phys. Rev. Lett. 95 (2005) 077201.
 - [5] R. G. Pereira, J. Sirker, J.-S. Caux, R. Hagemans, J. M. Maillet, S. R. White, I. Affleck Phys. Rev. Lett. 96 (2006) 272202.
 - [6] R. G. Pereira, J. Sirker, J.-S. Caux, R. Hagemans, J. M. Maillet, S. R. White, I. Affleck J. Stat. Mech. (2007) P08022.
 - [7] R. G. Pereira, S. R. White, I. Affleck, Phys. Rev. Lett. 100 (2008) 027206.
 - [8] J.-S. Caux, H. Konno, M. Sorrell, R. Weston, Phys. Rev. Lett. 106 (2011) 217203.

- [9] J.-S. Caux, H. Konno, M. Sorrell, R. Weston, *J. Stat. Mech.* (2012) P01007.
- [10] M. Takahashi, *Progr. Theor. Phys.* 46 (1971) 401.
- [11] M. Gaudin, *Phys. Rev. Lett.* 26 (1971) 1301.
- [12] M. Takahashi, M. Suzuki, *Progr. Theor. Phys.* 48 (1972) 2187.
- [13] M. Takahashi, *Thermodynamics of one-dimensional solvable models*, Cambridge University Press, 2019.
- [14] M. Gaudin, *The Bethe wavefunction*, Cambridge University Press, 2014.
- [15] J.-S. Caux, J. Mossel, I. P. Castillo, *J. Stat. Mech.* (2008) P08006.
- [16] W. Yang, J. Wu, S. Xu, Z. Wang, C. Wu *Phys. Rev. B* 100 (2019) 184406.
- [17] J. M. P. Carmelo, T. Čadež, P. D. Sacramento, *Nucl. Phys. B* 960 (2020) 115175.
- [18] J. M. P. Carmelo, P. D. Sacramento, J. D. P. Machado, D. K. Campbell, *J. Phys.: Condens. Matter* 27 (2015) 406001; *J. Phys.: Condens. Matter* 33 (2021) 069501 (Corrigendum).
- [19] J. M. P. Carmelo, T. Prosen, *Nucl. Phys. B* 914 (2017) 62.
- [20] J. M. P. Carmelo, T. Prosen, D. K. Campbell, *Phys. Rev. B* 92 (2015) 165133.
- [21] V. Pasquier, H. Saleur, *Nucl. Phys. B* 330 (1990) 523.
- [22] T. Prosen, E. Ilievski, *Phys. Rev. Lett.* 111 (2013) 057203.
- [23] L. D. Faddeev, L. A. Takhtajan, *Phys. Lett.* 85A (1981) 375.
- [24] J.-S. Caux, R. Hagemans, *J. Stat. Mech.* (2006) P12013.
- [25] M. Karbach, D. Biegel, G. Müller G, *Phys. Rev. B* 66 (2002) 054405.
- [26] M. Karbach, G. Müller, *Phys. Rev. B* 62 (2000) 14871.
- [27] T. Fujita, T. Kobayashi, H. Takahashi, *J. Phys. A* 36 (2003) 1553.
- [28] H. V. Kruis, I. P. McCulloch, Z. Nussinov, J. Zaanen, *Phys. Rev. B* 70 (2004) 075109.
- [29] J. M. P. Carmelo, K. Penc, D. Bozi, *Nucl. Phys. B* 725 (2005) 421; 737 (2006) 351 (E).
- [30] K. Penc, K. Hallberg, F. Mila, H. Shiba, *Phys. Rev. Lett.* 77 (1996) 1390.
- [31] K. Penc, K. Hallberg, F. Mila, H. Shiba, *Phys. Rev. B* 55 (1997) 15 475.
- [32] S. Sorella, A. Parola, *Phys. Rev. Lett.* 76 (1996) 4604.
- [33] S. Sorella, A. Parola, *Phys. Rev. B* 57 (1998) 6444 (1998).
- [34] J. M. P. Carmelo, P. D. Sacramento, *Phys. Reports* 749 (2018) 1.
- [35] A. Imambekov, L. I. Glazman, *Science* 323 (2009) 228.
- [36] A. Imambekov, T. L. Schmidt, L. I. Glazman, *Rev. Mod. Phys.* 84 (2012) 1253.
- [37] J. M. P. Carmelo, P. D. Sacramento, *Ann. Phys.* 369 (2016) 102.
- [38] J. M. P. Carmelo, P. D. Sacramento, D. K. Campbell, in preparation.
- [39] B. S. Shastri, B. Sutherland, *Phys. Rev. Lett.* 65 (1990) 243.
- [40] X. Zotos, *Phys. Rev. Lett.* 82 (1999) 1764.
- [41] J. Herbrych, P. Prelovšek, X. Zotos, *Phys. Rev. B* 84 (2011) 155125 (2011).
- [42] P. N. Jepsen, J. Amato-Grill, I. Dimitrova, W. W. Ho, E. Demler, W. Ketterle, *Nature* 588 (2020) 403.
- [43] R. Steinigeweg, W. Brenig, *Phys. Rev. Lett.* 107 (2011) 250602
- [44] M. Žnidarič, *Phys. Rev. Lett.* 106 (2011) 220601
- [45] A. K. Bera, J. Wu, W. Yang, R. Bewley, M. Boehm, J. Xu, M. Bartkowiak, O. Prokhnenko, B. Klemke, A. T. M. N. Islam, J. M. Law, Z. Wang, B. Lake, *Nature Phys.* 16 (2020) 625.
- [46] Z. Wang, J. Wu, W. Yang, A. K. Bera, D. Kamenskyi, A. T. M. N. Islam, S. Xu, J. M. Law, B. Lake, C. Wu, A. Loidl, *Nature* 554 (2018) 219.
- [47] Z. Wang, M. Schmidt, A. Loidl, J. Wu, H. Zou, W. Yang, C. Dong, Y. Kohama, K. Kindo, D. I. Gorbunov, S. Niesen, O. Breunig, J. Engelmayer, T. Lorenz, *Phys. Rev. Lett.* 123 (2019) 257201.
- [48] J. M. P. Carmelo, P. D. Sacramento, in preparation.
- [49] J. M. P. Carmelo, A. H. Castro Neto, D. K. Campbell, *Phys. Rev. B* 50 (1994) 3683.